NASA Technical Paper 1636

Measurement of the Handling Characteristics of Two Light Airplanes

Staff of the Flight Dynamics Branch

JUNE 1980

NASA

NASA Technical Paper 1636

Measurement of the Handling Characteristics of Two Light Airplanes

Staff of the Flight Dynamics Branch
Langley Research Center
Hampton, Virginia

National Aeronautics
and Space Administration

**Scientific and Technical
Information Office**

1980

SUMMARY

A flight investigation of the handling characteristics of two single-engine general aviation airplanes, one a high-wing and the other a low-wing, has been conducted by NASA at the Langley Research Center. The investigation included a variety of measurements of different characteristics of the two airplanes. The characteristics measured included those of the control systems, performance, static and dynamic longitudinal and lateral responses, and stall motions.

INTRODUCTION

A study was undertaken by the National Aeronautics and Space Administration to document typical landing practices of general aviation pilots as reported in reference 1. The study involved measurements of the pilot-control inputs and aircraft motions with ground-based and airborne instruments using two different popular light airplanes which are shown in figure 1. One airplane was low winged and the other was high winged, and both had a single engine, tractor propellers, and a fixed tricycle landing gear. In support of this study, the pilot handling characteristics of the two airplanes were measured using special flight instrumentation installed in each airplane. These particular flight tests were performed by research pilots using flight maneuvers intended to identify the static, dynamic, and control characteristics both longitudinally and laterally. These tests also included some performance measurements and a few stall maneuvers.

The purpose of this paper is to document, in a strictly quantitative manner, the handling characteristics of these two airplanes. The data have been presented in a side-by-side manner so as to illustrate the similarities and differences that exist in the handling characteristics of these two particular airplanes. These measured characteristics, however, are not considered to be necessarily representative of actual similarities and differences between all light airplanes of the two generic configurations.

Although the airplanes were somewhat similar in size and weight, they differed in the power of the engine. Consequently, there are expected differences in the flight characteristics directly related to engine power, such as cruise and maximum speeds, rate of climb, and take-off distances. However, these performance differences were considered to have no significant influence on the other handling characteristics of the airplane which were the primary subject of this study.

The airplanes were operated in the normally prescribed manner for the categories in which they had been originally certified under the Federal Air Regulations, Part 23 (ref. 2). The present study did not include a qualitative or pilot rating evaluation or an attempt to correlate such an evaluation with the measured characteristics.

The conduct of the flight tests for both airplanes, the reduction and analyses of the data, and the preparation of this report have extended over a period of several years; but because of the press of other research efforts and other factors, the work was not published until now. As a result, major contributions to this study have been made by several members or former members of the Flight Dynamics Branch of the Flight Dynamics and Control Division at the Langley Research Center. These contributions were made by Eric C. Stewart, Thomas M. Moul, Thomas C. O'Bryan, Randall L. Harris (transferred), Robert L. Cannaday (resigned), Maxwell W. Goode (deceased), and Marna H. Mayo.

SYMBOLS

All quantities were measured with respect to the set of orthogonal body reference axes (X, Y, and Z in fig. 2) which originated at the center of gravity of the aircraft and were aligned with the reference axes defined by the manufacturer of each airplane. The definitions and sign convention of some of the measurements are illustrated in figure 2.

Values are given in both SI and U.S. Customary Units. Measurements and calculations were made in U.S. Customary Units.

A_x acceleration along airplane X-axis, g units

$\left.\begin{matrix}\hat{a},\hat{b},\hat{c},\hat{d},\\ \hat{e}_1,\hat{e}_2,\hat{e}_3,\hat{f}\end{matrix}\right\}$ constants in least-squares equations for static longitudinal characteristics

b wing span, m (ft)

$C_{h,e}$ elevator (stabilator) hinge-moment coefficient, $\dfrac{H_e}{q_o S_e c_e}$

C_L' lift coefficient, $\dfrac{\text{Airplane weight}}{q_o S}$

C_{L_α}' trimmed lift-curve slope, per deg

C_l rolling-moment coefficient

$C_{l_p} = \dfrac{\partial C_l}{\partial \dfrac{pb}{2V}}$

$\bar{c}$ mean aerodynamic chord, m (ft)

c_e elevator chord, m (ft)

F_a lateral (aileron) wheel force at radius of 18 cm (7 in.), positive when pilot pulls clockwise, N (lb)

F_e longitudinal (elevator) column force, positive when pilot pulls, N (lb)

F_r pedal (rudder) force, positive when pilot pushes on right pedal, N (lb)

G elevator-to-wheel (stabilator) gearing ratio, rad/m

H_e hinge moment about elevator hinge line or stabilator rotational axis, positive when tending to force trailing edge down, N-m (ft-lb)

I_{xx} airplane moment of inertia about X-axis, kg-m^2 (slug-ft^2)

K_1 upwash correction factor for angle of attack

K_2 correction to angle of attack due to misalignment of vane relative to longitudinal reference axis, deg

L rolling moment, N-m (ft-lb)

L_p $= \frac{\partial L}{\partial p}$

p,q,r roll, pitch, and yaw angular velocities, deg/sec

p_{max} maximum roll rate, deg/sec

q_o free-stream dynamic pressure, Pa (psi)

S wing area, m^2 (ft^2)

S_e elevator area, m^2 (ft^2)

u,v,w velocity components along airplane X-, Y-, and Z-axes, knots (mph)

V true velocity, knots (mph)

V_c calibrated airspeed, knots (mph)

V_i indicated airspeed, instrumented system, knots (mph)

$V_{i,p}$ indicated airspeed, pilot system, knots (mph)

X,Y,Z airplane body axes, origin at center of gravity

X_e, Y_e, Z_e	Earth-fixed reference axes, Z_e-axis vertical, with direction of X_e- and Y_e-axes arbitrary
α	angle of attack, deg
α_c	angle of attack calibrated for upwash and alignment, deg
α_i	indicated angle of attack, deg
β	angle of sideslip, deg
δ_a	total aileron deflection, positive with right aileron down, $\delta_{a,r} - \delta_{a,l}$, deg
$\delta_{a,l}$	left aileron deflection, positive with trailing edge down, deg
$\delta_{a,max}$	maximum aileron deflection, deg
$\delta_{a,r}$	right aileron deflection, positive with trailing edge down, deg
δ_e	elevator or stabilator deflection, positive for trailing edge down, deg
δ_r	rudder deflection, positive with trailing edge left, deg
δ_{tab}	elevator-trim-tab deflection, positive with trailing edge down, deg
δ_c	linear displacement of pilot-control column for deflecting the elevator, positive for displacements aft of instrument panel, cm (in.)
δ_p	linear displacement of pilot right rudder pedal, positive for forward displacements with zero at neutral point, cm (in.)
δ_w	angular displacement of pilot-control wheel for deflecting the ailerons, positive for rotations in a clockwise sense as viewed by pilot, deg
θ	pitch attitude, deg
ρ	air density, kg/m^3 ($slugs/ft^3$)
τ_r	roll-mode time constant, sec
ϕ	roll attitude, deg

Abbreviations:

PLF	power for level flight
N.P.	neutral point

APPARATUS AND TEST PROCEDURE

Test Airplanes

The two test vehicles shown in figure 1 were selected as being representative of the standard production types of airplanes employed in the major segment of general aviation. The airplanes were leased from a fixed-base operator. Both airplanes were four-passenger types with fixed tricycle landing gear and had single engines with fixed-pitch propellers. The low-wing airplane was equipped with a 134-kW (180-hp) engine and the high-wing, a 112-kW (150-hp) engine. The pertinent physical characteristics of the airplanes are given in tables I and II. Except for the wing-tip mounted booms described later, the only modifications to the airplanes were on the airplanes' interiors for the test instrumentation.

Both airplanes were operated for all tests under the conditions of the normal category for airworthiness certification, according to the respective manufacturer's handbooks. Flight tests to determine the longitudinal characteristics of the airplanes were performed for three different center-of-gravity (c.g.) locations which were established by varying the loading. For most tests a project engineer was carried to serve as test observer. The loading envelopes, in terms of c.g. locations and total mass, were based on the manufacturer's handbook information and are given in figure 3. The solid symbols in the figures represent measured c.g. locations and masses at which the airplane was tested, while the open symbols represent calculated c.g. locations and masses using the manufacturer's handbook procedure.

Various normal operating conditions of the two airplanes are indicated in table III and are based on calibrated airspeeds given in the airplane operating handbooks. The table also lists the lift coefficients computed from these airspeeds for the airplane gross mass and the wing areas given in tables I and II. The two airplanes differ primarily in cruise and stall velocities. The low-wing airplane both cruises and stalls at higher velocities than the high-wing airplane. These differences are probably due to the different engine power and wing design.

Test Instrumentation Systems

Test instrumentation systems mounted on removable pallets were installed in the rear of the cabins of the airplanes. A list of the sensors, recorded test parameters, and associated ranges of the instrument system are given in table IV. The estimated accuracy of each of these measurements after processing is considered to be within 2 to 3 percent of full scale. In the case of the low-wing airplane, the system was placed in the baggage compartment and the rear seat was available for passenger accommodations. In the high-wing airplane, the rear seat was removed to accommodate the pallet so that a passenger could be carried only in one of the front seats.

Both pallets had masses of 68 kg (4.7 slugs) each and contained a seven-track multiplexed magnetic tape recorder, various signal conditioning units, and power supplies as well as accelerometers, attitude gyros, and rate gyros.

Elevator and aileron forces were measured by strain gauges on a special control wheel installed in place of the manufacturer's control wheel. As with the wheel, rudder forces were measured using special rudder-force pedals which contained strain gauges. The sensors were connected electrically to the instrumentation system through shielded cables. A small control panel which included a switch and an indicator light was installed on the airplane instrument panel so that the pilot could record data for specific test intervals.

Control-surface positions on the low-wing airplane were recorded during flight by transducers attached to the control cables in the vicinity of the cockpit. During the early testing of the high-wing airplane its control-position transducers were also attached to the control cables near the cockpit. Later, however, the transducers were moved to the control surfaces.

Before the transducers were moved on the high-wing airplane, a few crude measurements were made to determine the impact of measuring control position with transducers attached to the cables. These measurements were made on the ground with the aerodynamic-control surfaces mechanically fixed so they could not move. A force was applied to the pilot controls and the change in indicated surface position (based on the no-load calibration used in flight) was recorded from the transducer outputs. The results of these measurements are summarized in the following table which shows substantial changes in the indicated surface positions even though the actual positions were constant:

Control	Force, N (lb)	Change in indicated surface position, deg
Elevator	130 (30)	2.5
Aileron	40 (10)	10.0
Rudder	180 (40)	4.0

These indications of control-system flexibility really include only about one-half of the total flexibility between the pilot controls and the aerodynamic surfaces because the transducers were located about in the middle of the cables. An indication of the total elevator-control-system flexibility for the high-wing airplane was obtained in later flight tests with the transducer located at the surface. That is, the longitudinal column was pulled to its stop (which was coincident with the elevator stop under no load) with a force of about 200 N (45 lb) but the elevator was 8^{o} from its stop.

These measurements indicate that there can be a significant difference between the indicated control position (based on a no-load calibration) and the actual control position depending on the load and the transducer location. This difference applies to both the aerodynamic-control-surface positions (δ_e, δ_a, and δ_r) and the pilot-control positions (δ_c, δ_w, and δ_p), although the relative differences may not be the same. The data which follow are not corrected for these differences because it was assumed that the control systems were perfectly rigid. Only the aerodynamic-control-surface positions for the high-wing airplane for about one-half the data including that for the static

longitudinal characteristics were considered to be relatively free of this effect. On the other hand, the pilot-control positions for these same data for the high-wing airplane probably have the maximum error. All other data for both the low-wing and high-wing airplanes probably have errors consistent with the ground measurements on the high-wing airplane quoted above.

A boom containing a pitot static head and a set of angle-of-attack and angle-of-sideslip vanes was attached to the left wing tip and extended approximately 3/4-local-chord distance ahead of the leading edge. The boom was aligned with the longitudinal reference axis for each of the airplanes and the angle-of-attack and angle-of-sideslip vanes rotated about axes perpendicular to the airplane's Y- and Z-axes, respectively. Thus, the angle-of-attack vane measured an angle proportional to $\tan^{-1}\frac{w}{u}$, and the angle-of-sideslip vane measured an angle proportional to $\tan^{-1}\frac{v}{u}$. The angle for the angle-of-attack vane is equal to the customary definition of angle of attack; but the angle for the angle-of-sideslip vane differs from customary definition of angle of sideslip, $\sin^{-1}\frac{v}{V}$. For small angles of sideslip and angles of attack the difference in these two quantities is insignificant. Therefore, no corrections were made herein to the measurements from the angle-of-sideslip vane. The pitot static head was independent of the airplane's normal static and total pressure systems.

For some of the flight tests for the high-wing airplane, the measured or uncorrected angle of attack and angle of sideslip were displayed to the pilot; otherwise, none of the test measurements were displayed to the pilots.

Measurements

Most of the test data were obtained using standard flight-testing techniques such as those described in reference 3.

Performance.- Data for the rate of climb of the low-wing airplane were obtained from power-on and power-off tests in which the time to change altitude by 305 m (1000 ft) as indicated by the pilot altimeter was measured by means of a stopwatch. Data for the high-wing airplane were obtained directly from the test instrument system. In both cases, the airspeeds and rates of climb or descent were stabilized before beginning the test period. No corrections to the rate-of-climb data were made to account for nonstandard conditions such as airplane mass and atmospheric air density.

Longitudinal.- The control-system characteristics were obtained from ground tests at zero velocity in which control positions and forces as well as the control-surface deflections were recorded as the controls were cycled through their full ranges of travel. Positions of the pilot controls and the control surfaces were measured during the ground test by use of a tape measure, protractor scales, and inclinometers.

The static longitudinal stability characteristics were obtained by use of the slow acceleration-deceleration technique in which the data were recorded continuously as the speed of the airplane was slowly increased and decreased from an initial trimmed condition without changing throttle and flap settings.

The long-period (phugoid) motions were measured by first stabilizing the airplane and trimming the elevator-control forces to zero at the desired flight condition. The airspeed was then either increased or decreased by about 10 to 20 knots using the elevator control. At this point, the control was smoothly moved to the new zero-force position and released. The resulting motion was permitted to persist for at least three cycles. The short-period motions were generated by the "doublet-pulse" technique in which the elevator control was rapidly stroked through a one-cycle oscillation and then released with the control at the zero-force position.

Longitudinal maneuvering stability was measured in terms of the elevator position and the elevator-control forces required to sustain different load-factor levels generated using the "wind-up turn" technique. In this technique a coordinated turn with a gradually increasing roll attitude and normal acceleration is flown at constant airspeed, throttle, and flap settings. The maneuver was started from a trimmed level-flight condition, and the recording system operated continuously throughout the maneuver.

Lateral.- Steady-heading sideslips to the left and right were performed at different airspeeds, power settings, and flap positions to measure the combined lateral-directional static control characteristics. In these tests, the rudder position was gradually changed from neutral to one extreme and then back to the other extreme while the ailerons were used to maintain a constant heading. This use of crossed controls generated a continuous variation of sideslip which was recorded. Throttle was held constant but the elevator was deflected so as to maintain nearly constant airspeed throughout the maneuver.

Spiral stability characteristics were obtained by establishing steady level flight and momentarily pulsing the rudder while holding the ailerons fixed in their level-flight, trimmed position. The ensuing motion was recorded for about 30 to 40 sec. These tests were repeated in the opposite direction and with the controls free.

The Dutch-roll motion characteristics were obtained with controls both fixed and free by using the rudders to excite the motions and then either releasing the controls or fixing them at their normal level-flight, trimmed positions.

Roll-control responses of the airplanes were obtained by establishing 45° banked turns in one direction and recording the results of rapid aileron deflections in the opposite direction.

Stalls.- The motions of each airplane during stalls were measured with flaps up and down. The stall was approached by slowly decreasing the airspeed at a rate of about 1 knot per second from trimmed speeds of about 1.3 times the nominal stall speed. The pilot attempted to maintain coordinated entry conditions ("ball" centered) in all the stalls. Initiation of recovery control

inputs was purposely delayed beyond the break in some cases to establish clearly the nature of the stalled motions without control inputs. Stalls were performed from a wing-level attitude with maximum throttle, minimum throttle, and with throttle required for level flight at an airspeed 1.3 times the stall speed.

Data Handling Procedure

Most of the direct-current (dc) data signals were recorded continuously after conversion to frequency-modulated (FM) form. The remaining data signals were sampled at 20 samples per second using a commutator. The output of the commutation was then converted to FM and recorded. The postflight data processing involved converting the FM signals back to dc, filtering, and digitizing at 10 samples per second. Calibration factors were then applied to the data to convert to engineering units.

Airspeed.- The calculations of all aerodynamic parameters for both airplanes were based on the airspeed measurements obtained with the boom-mounted pitot static system. These measurements were corrected for position error on the basis of flight tests made with the trailing anemometer system discussed in reference 4. The pilot airspeed system for the low-wing airplane consisted of a small mast, with a rectangular cross section and a beveled end, protruding into the airstream under the left wing from about the midchord and mid-semispan wing position. This mast sensed both the total and static pressures at this location. The pilot airspeed system for the high-wing airplane utilized a single static port located on the fuselage just forward of the left cabin door and a short total-head tube extending slightly below and forward of the wing leading edge just outboard of the wing support strut. The comparisons of the indicated airspeed of the test system and the pilot airspeed system for each airplane with the calibrated airspeed obtained from the true airspeed measured with the anemometer system are shown in figure 4.

Angle of attack.- Corrections to angle-of-attack measurements were applied to account for the effects of upwash due to the flow around the wing. The upwash effects on angle of attack were measured during carefully trimmed, unaccelerated flight at constant altitude for several airspeeds. Angle-of-attack correction factors were determined as follows:

$$\alpha_c \equiv \sin^{-1} A_x = K_1 \alpha_i + K_2$$

where α_c is the corrected angle of attack (defined as the inverse sine of the longitudinal acceleration) and α_i is the indicated value from the vane. Values of K_1 (upwash factor) and K_2 (alignment error of the vane relative to the longitudinal reference axis) were found to be

Correction	Airplane	
	Low-wing	High-wing
K_1	0.75	0.82
K_2, deg	0	-.55

There was no measurable effect of flap deflection or throttle setting on these values. In dynamic maneuvers, after the upwash correction was applied α_i was corrected for the induced linear velocities at the remote vane location due to pitch, roll, and yaw motions.

Lift coefficient.- The lift coefficient is referred to in several instances in this report in terms of C_L' which is defined here as airplane weight divided by the dynamic pressure and wing area. This term is obtained directly from the flight-test measurements and is essentially equal to the lift coefficient for unaccelerated flight conditions. The exact values for lift coefficient were impossible to obtain because of the lack of a suitable method for obtaining thrust measurements which, along with the weight, must be known to calculate lift.

Static longitudinal characteristics.- The longitudinal wheel force was converted to elevator hinge moment using the relationship

$$H_e = F_e/G$$

where G is the elevator-to-wheel gearing ratio. The hinge moment was then nondimensionalized as follows:

$$C_{h,e} = \frac{H_e}{q_o S_e c_e}$$

In order to calculate the stick-free neutral point (N.P.) a second-order equation of the form

$$C_{h,e} = \hat{a} + \hat{b}C_L' + \hat{c}C_L'^2$$

was fit (in a least-squares sense) to the data for each longitudinal stability flight maneuver. Once the equation was determined, the derivative of hinge-moment coefficient with respect to lift coefficient was taken and evaluated at different lift coefficients. These derivatives or slopes were then used to determine the stick-free neutral point as described in reference 3.

A similar procedure was used to determine the stick-fixed neutral point except that advantage was taken of the fact that the trim-tab position (which varied from maneuver to maneuver) had a negligible effect on elevator position. That is, the coefficients for the equations

$$\delta_{e,1} = \hat{d} + \hat{e}_1 C_L' + \hat{f}C_L'^2$$

$$\delta_{e,2} = \hat{d} + \hat{e}_2 C_L' + \hat{f}C_L'^2$$

$$\delta_{e,3} = \hat{d} + \hat{e}_3 C_L' + \hat{f} C_L'^2$$

were determined simultaneously for all three values of c.g. where the numbered subscripts correspond to different c.g. positions. These equations were then used to determine the stick-fixed neutral point as described above.

RESULTS AND DISCUSSION

The results of several different tests conducted with each airplane are presented and discussed with respect to the control-system characteristics, general performance characteristics, longitudinal and lateral stability and control characteristics, and the stall behavior.

At completion of the planned flight-test programs and preliminary analysis of the test data, all test equipment was removed from the low-wing airplane for use in another test, and the airplane was returned to the fixed-base operator from whom it was leased. However, the high-wing airplane was retained in flight-test status. Consequently, this airplane was available for further testing when more complete analysis of the original data revealed the need for more information. Therefore, the test results for the high-wing airplane were more complete than those for the low-wing airplane.

Control-System Characteristics

The kinematic and mechanical characteristics of the control systems measured during ground calibration tests with the systems unloaded are presented in figure 5. This figure includes plots of the variations in control-surface positions and control forces as functions of pilot-control position for the longitudinal control (stabilator or elevator), the aileron, and the rudder. The plots show the results of a complete cycle of motion of the control position from one stop to the other and return. These plots reveal that there were relatively small amounts of mechanical free-play or nonlinear motions in the control systems of both airplanes. Overcoming longitudinal system friction and surface unbalance with no aerodynamic loading required a pull force of about 17 to 22 N (4 to 5 lb) for the low-wing airplane and 40 to 50 N (9 to 10 lb) for the high-wing airplane for the wheel in about the center of its travel. Returning the wheel to its original position required about 13 N (3 lb) of push force for the low-wing, and practically no force for the high-wing. The zero force occurs because the high-wing elevator-control system was not completely mass balanced and the unbalance just about cancelled the friction. Wheel forces required to deflect ailerons through their full travel under no-load conditions resulted in about a 13-N (3-lb) difference due to friction hysteresis for the low-wing airplane and about 4 to 10 N (1 to 2 lb) for the high-wing. Rudder-pedal-force hysteresis was about 90 to 180 N (20 to 40 lb) for the low-wing and 65 to 90 N (15 to 20 lb) for the high-wing.

In-flight longitudinal-control-system characteristics obtained from a longitudinal stability test for both airplanes are shown in figure 6. For the

low-wing airplane, roughly a 13-N (3-lb) difference was observed in the hysteresis loop of wheel force as a function of calibrated airspeed. About a 17-N (4-lb) difference was observed for the high-wing airplane.

Performance

To the pilot, airspeed is an important parameter by which he operates his airplane. To the engineer (especially from the standpoint of handling qualities, stability, and control), lift coefficient is frequently a more useful parameter. Consequently, as a convenience, reference will be made to both parameters. The relation of the two parameters for both airplanes operating in unaccelerated level flight is given in figure 7. The various normal operating conditions of the airplanes (taken from table III) are included on the figure for reference.

Lift characteristics.- The measured lift characteristics of both airplanes, presented in figure 8, show the variation of trimmed lift coefficient with angle of attack for flaps up and flaps down. These data indicate approximately equal trimmed lift-curve slopes C'_{L_α} for both airplanes for the flaps-up condition. Deflecting the flaps increased the lift-curve slopes for both airplanes, although this effect was more pronounced for the high-wing airplane.

Full deflection of the flaps produced C'_L increments of about 0.44 and 0.56 for the low- and high-wing airplanes, respectively, at $\alpha_c = 2^\circ$. At a constant coefficient of $C'_L = 0.8$, corresponding to a nominal approach speed for both airplanes, the angle of attack was about 4.8° and 5.6° less for flaps down than flaps up for the two respective airplanes. This effect is due to the lift generating capabilities of the flaps, and the difference in the two values reflects the simple design of the slotted flap of the low-wing and the more complex design of the Fowler flap of the high-wing.

Rate of climb.- The effects of airspeed on the rates of climb with maximum and minimum power are presented in figure 9 for the cases of flaps up and flaps down for both airplanes. The low-wing airplane had significantly higher rates of climb for both flap conditions primarily because of the higher available power. For minimum power with flaps up, the low-wing airplane also had a somewhat higher rate of descent or more negative rate of climb. This result is attributable to the lower aspect ratio of the low-wing airplane. It is pertinent to note that, in general, full deflection of the flaps has a greater negative effect on the rates of climb or descent for the high-wing than for the low-wing airplane. This result is primarily due to the difference in the design of the flaps mentioned earlier.

Longitudinal Characteristics

Static characteristics.- The static longitudinal characteristics of the two airplanes are presented in figures 10 and 11 for the two extreme c.g. locations tested (data for an intermediate c.g. position were omitted from the figures for clarity). The three c.g. positions are the ones shown in figure 3. For the flaps-up configurations both airplanes exhibit conventional character-

istics for both c.g. locations - that is, aft-stick deflections and pull forces are required to slow the airplane. The upward curvature of the elevator curves for the low-wing airplane and the downward curvature for the corresponding curves of the high-wing airplane are characteristic of the two wing positions. The curvature results from the pitching moment generated by the drag on the wing multiplied by the vertical location of the wing with respect to c.g.

For the flaps-down configuration, both airplanes have the conventional characteristics for the forward c.g. positions. However, for the aft c.g. position, the high-wing airplane required reversed control deflections for all the plotted parameters except wheel force F_e which retains the pull force to slow down. It was also impossible to trim the wheel force to zero for this configuration at this c.g. It should be pointed out that the two flaps-down configurations for the two airplanes are not really comparable. That is, although both airplanes were flown with power levels sufficient to maintain level flight, the more powerful flaps and smaller engine of the high-wing airplane necessitated a full-power setting while the low-wing airplane only required about 40 percent throttle even though the airspeed was higher. Therefore, the flaps-down configuration for the high-wing airplane was a full-power "go-around" condition while the flaps-down configuration for the low-wing airplane was more nearly like an "approach" condition. In the "go-around" condition the characteristics presented in figure 11(b) for the aft c.g. (i.e., the reversed control deflections which may be indicative of a static instability) are tolerable as discussed in reference 5 on page 51. This reversal is not considered to be important because of the short periods of time the airplane is flown in the "go-around" condition.

The least-squares calculated control derivatives $d\delta_e/dC_L'$ and $dC_{h,e}/dC_L'$ and neutral points are presented in figures 12 and 13 for different lift coefficients. All the derivatives have the conventional signs except, of course, for the flaps-down ("go-around") condition of the high-wing airplane. Likewise, the calculated neutral points are all aft of the allowable c.g. range except for the "go-around" condition of the high-wing airplane. Increasing lift coefficient moves the neutral point forward on the low-wing airplane and aft on the high-wing airplane, a result which is a consequence of the curvature in the plots shown in figures 10 and 11 and mentioned above.

Dynamic longitudinal stability.- A listing of the period and time to damp to half-amplitude for the phugoid or long-period motions of the two airplanes for various flight conditions is given in table V. The data indicate that the phugoid motions of both airplanes were lightly damped and had periods of from about 20 to 40 sec, depending upon the flight condition. The variation of period with airspeed roughly followed the trend of increasing period with increasing airspeed for both airplanes. As the c.g. for the high-wing airplane was moved rearward the period increased slightly. This trend was not discernible for the low-wing airplane. Measurements of the time to damp to half-amplitude and the corresponding damping ratio for this type of motion were difficult to obtain accurately and the values given in the tables represent only approximate estimates. Consequently, the variations in these values with the different flight conditions are not considered to be significant.

For the short period, typical time histories of the elevator deflections and the pitching velocities following a "doublet-pulse" input for both airplanes are given in figure 14. The short-period motions are shown to be very heavily damped and measurements of the period and damping could not be obtained reliably.

Longitudinal maneuvering stability.- The variations of elevator-control forces and positions with load factor, expressed in g units, are presented in figure 15 for both airplanes with different airspeeds. The longitudinal-column force gradient and the elevator-position gradient increased, as expected, for both airplanes as the c.g. was moved forward. The control-free and control-fixed maneuver points (which can be determined by inspection from fig. 15) were aft of the allowable c.g. range for both airplanes, although the high-wing airplane evidently had a much larger margin.

The absolute values of the gradients for the high-wing airplane were also much larger than those for the low-wing airplane. This difference was largely due to the use of an elevator on the high-wing airplane and a stabilator on the low-wing airplane. Another factor which tended to increase the longitudinal-column force gradient on the high-wing airplane was the "bob-weight" effect of the unbalanced control system mentioned earlier in the section entitled "Control-System Characteristics." Extending the flaps seemed to decrease the gradients slightly on the low-wing airplane, but there were no flaps-down data for the high-wing airplane.

Longitudinal trim settings.- Trim-tab settings required to trim the column forces to zero at various airspeeds with power for level flight (PLF) are shown in figure 16 for the high-wing airplane. The trim-tab position was measured relative to the plane of the chord line of the elevator. Lowering flaps required considerably more nose-down trim-tab deflection, especially at the more aft c.g. location. No data were available for the certificated aft c.g. limit, but it appears that it would not be possible to trim the forces to zero for the aft c.g., flaps down, and PLF for the higher speeds. No trim-tab measurements were made on the low-wing airplane.

Lateral-Directional Characteristics

Static characteristics.- The results of the steady-heading sideslip tests are presented in figures 17 and 18 in which the variations of aileron, rudder, and elevator deflections and control forces with sideslip angle are shown for the various test conditions. These data indicate that both airplanes possessed positive directional stability and positive effective dihedral for the conditions tested as indicated by the sign or direction of the slopes of the curves for the rudder and aileron deflections, respectively. The stability is proportional to the slopes of these curves with the constant of proportionality being the control effectiveness. Measurement of control effectiveness was not accomplished in these tests.

The effects of changing speed with PLF are shown in figure 17(a) for the low-wing airplane with flaps up. The aileron and rudder deflections are basically unaffected except for offsets because their slopes are primarily dependent

on nondimensional aerodynamic coefficients which are apparently relatively constant. The roll angle, wheel force, and pedal force, on the other hand, are reduced as the airspeed is reduced at a given angle of sideslip because of the reduction in dynamic pressure. The main effect of speed with PLF on the elevator position during the sideslips is the offset due to the change in trim at the two flight conditions. A very slight increase in up elevator is required as the sideslip is changed to either side of zero (implying a very slight nose-down pitching moment with sideslip). Most of the same basic trends are evident for the high-wing airplane for both flaps up (fig. 18(a)) and down (fig. 18(b)). However, the change in elevator with sideslip is a little more pronounced and in the opposite direction of that observed on the low-wing airplane. This implies a nose-up pitching moment with sideslip which is opposite that frequently encountered with single-engine tractor airplanes (see ref. 6, p. 21).

Data from steady-heading sideslips with flaps up and down for the low-wing airplane are presented in figure 17(b). Although the airspeeds were about the same for both flap configurations, the power setting was higher for the flaps-down case because of the increased drag. Therefore, the effects shown in figure 17(b) are for both flaps and power. In any case, the slope of the aileron-deflection/sideslip curve was decreased with flaps and power, indicating either a reduced dihedral effect or (less likely) an increased aileron effectiveness. The slope of the rudder-deflection/sideslip curve, on the other hand, showed an increase in slope indicating increased directional stability or reduced rudder effectiveness. The control forces were proportional to the control-surface deflections.

The effects of flaps can be more readily isolated for the high-wing airplane in figure 18(c) because all the data were taken with maximum power and approximately the same airspeed. In this case, flaps do not seem to affect appreciably the aileron deflections but do require increased rudder deflections for a given sideslip. The rudder-pedal forces reflect the rudder deflections in that they were increased with flap deflections.

This effect of flaps on the rudder deflections can be explained at least partially by referring to the data of figures 54 and 58 of reference 7, which presents full-scale wind-tunnel data for a high-wing airplane similar to the subject airplane. These wind-tunnel data reveal that the effect of the flaps being lowered was both to increase the directional stability and to reduce the rudder effectiveness and that this effect was most pronounced with high-thrust coefficients. Trends observed in these wind-tunnel data are the same as the trends observed in the flight-test data of figure 18(c).

The effect of power can be seen in figure 18(d) for the high-wing airplane. There seems to be no significant difference in any of the traces for maximum and minimum power, but this result may only be true for the relatively high airspeed at which these data were taken. In fact, other unpublished data for lower airspeeds (which were less complete but still contained the extreme points) did, in fact, show a decrease in required rudder deflection with power. This decrease was probably due to the increase in rudder effectiveness as a result of increased dynamic pressure at the tail from the propeller slipstream. This result of increased rudder effectiveness with power as the airspeed

decreases also has been observed in some recent tests of another low-wing light airplane as reported in reference 8.

Spiral stability.- Time histories of the airplane motion after disturbing the airplane are shown in figures 19 and 20 for the various test conditions. Only one spiral stability run was available for the low-wing airplane and is shown in figure 19. For the cruise condition, the spiral mode was excited by a rudder pulse, after which the roll attitude diverged gradually at a rate of about 1° per second. The records indicate that the controls remained stationary at their original positions throughout the run.

Several spiral stability tests were performed with the high-wing airplane at various airspeeds and are shown in figure 20. With flaps up and test airspeeds ranging from about 63 knots to about 104 knots, small rudder pulses were input to excite the spiral mode. For the higher test airspeeds and higher power levels, the high-wing airplane exhibited spiral stability in that the roll attitude slowly approached a wings-level attitude after being displaced about 10°. (See figs. 20(a) and 20(b).) At the lower airspeed and power level (fig. 20(c)) the spiral mode was slowly divergent as evidenced by the increasing roll attitude after a disturbance. Controls free or fixed had little effect on the spiral mode for the conditions tested. With flaps down and the corresponding power level required to maintain level flight (fig. 20(d)) the airplane was spirally unstable with an almost identical divergence rate to the flaps up, low-speed, low-power condition as shown in figure 20(c). Based on the steady-heading-sideslip results, deflection of the flaps and the corresponding increase in power increased directional stability so flaps and power would tend to cause the spiral mode to move toward divergence (ref. 3).

It is possible that the apparent spiral instability resulted from an out-of-roll or yaw trim condition, rather than inherent spiral instability; since, except for a bungee system in the rudder of the low-wing airplane, neither airplane had a trim capability in roll or yaw. Also, the friction in the control systems was such that the trim devices would be largely ineffective (as the bungee system was ineffective in the low-wing airplane). This friction was probably responsible for the apparent similarity of the controls-fixed and controls-free motion because the friction effectively "fixed" the controls even after they were released. The instability problem could possibly be alleviated by installation of in-flight trimming capability for all three axes and a reduction in control-system friction. In any case, these results are true indications of the apparent spiral stability and clearly represent motions which can result when the pilot is required to take his hands off the controls and direct his attention to some other task inside the cockpit.

Dutch-roll dynamics.- Experimentally determined Dutch-roll characteristics of the subject airplanes are presented in table VI for various conditions. Data were available for both free and fixed controls on the high-wing airplane, whereas only controls-free data were available on the low-wing.

The Dutch-roll mode was more highly damped for the high-wing airplane, with typical damping ratios of about 0.35 as compared to about 0.18 for the low-wing. With the flaps up the damping ratio tended to increase as the airspeed decreased for the low-wing airplane. For the high-wing airplane the

trend was not as obvious, but probably also increased despite one point to the contrary for the 70-knot, fixed-controls case. A trend with controls free and fixed was not obvious from the data.

For the flaps-up condition of both airplanes the period increased as the airspeed decreased. For the low-wing airplane, the period ranged from 2.4 sec at 92 knots to 3.7 sec for 60 knots and for the high-wing from about 2.8 sec to about 4.1 sec for airspeeds from 105 knots to 65 knots. With the extension of the flaps the periods were slightly less at corresponding airspeeds with power for level flight.

The roll-to-sideslip ratios did not show a definite trend with airspeed, but for the high-wing airplane with flaps up fixing the controls appeared to lessen the roll-to-yaw ratio slightly. The extension of flaps reduced the roll-to-yaw ratio for both airplanes.

Rolling performance.- Very limited rolling performance tests were completed for either airplane. Measured and estimated rolling mode parameters obtained from these tests are given in table VII. The aileron deflections used to excite the rolling modes were not the maximum available, but maximum roll rates were estimated based on $p_{max} = p \frac{\delta_{a,max}}{\delta_a}$. The actual measured roll rate and the estimated maximum roll rate are included in the table. It was difficult to estimate a roll-mode time constant from the flight data; therefore, the time constant was calculated using values of C_{l_p} estimated for these airplanes from flight data using the maximum-likelihood estimation technique of reference 9. Estimated values of both longitudinal and lateral parameters for the low-wing airplane were reported in reference 10. The roll-mode time constant can be shown to be

$$\tau_r = \frac{-I_{xx}}{L_p} = \frac{-I_{xx}}{\frac{1}{4}\rho V S b^2 C_{l_p}}$$

Based on this relationship and estimations of C_{l_p}, the time constants were estimated to be about 0.32 sec for the low-wing airplane and 0.13 sec for the high-wing airplane.

Lateral trim characteristics.- Neither airplane was equipped with pilot-controlled aileron or rudder trim surfaces. The low-wing airplane, however, did have a spring attached to the rudder control cables to provide hinge moments to position the rudder for trim. By measuring the rudder and aileron deflections when the airplane was stabilized at various airspeeds and power settings, changes in the rolling and yawing moments could be inferred. These data are shown in figure 21 for both airplanes.

For the low-wing airplane only data for one power setting for each flap configuration were available. These data were taken during slow acceleration-deceleration longitudinal-static-stability runs in which the pilot was flying approximately wings level with the ball centered in the slip indicator (zero lateral acceleration). The ailerons were approximately constant with airspeed (forces were near zero), and did not change with flap deflection. This result implies that the net rolling moments were approximately constant with airspeed for this airplane. Since the rudder position changed as the airspeed decreased, the rolling moments due to rudder must have been small. The change in rudder position was in a negative (right) direction as airspeed decreased, indicating a left yawing moment as airspeed decreased. There was a corresponding increase in right pedal force (the pedal forces were apparently trimmed out at about 80 knots to 90 knots). The increasing left yawing moment for slower airspeeds is to be expected with a single-engine, tractor-propeller airplane with the propeller rotating clockwise as viewed by the pilot (ref. 6).

For the high-wing airplane data are presented for maximum- and minimum-power settings with flaps up and down as a function of airspeed. In these tests the pilot used an experimental sideslip indicator to maintain zero sideslip for all airspeeds. Although this technique should produce a nonzero lateral acceleration with the wings level (ref. 6), the lateral acceleration was actually near zero throughout the speed range. Likewise, a check of sideslip angles generated in the tests described above for the low-wing airplane showed no significant sideslip developing when the pilot held the lateral acceleration near zero. This lack of significant difference between flying with zero lateral acceleration and flying with zero sideslip is probably due to the relatively low-powered engines of these airplanes compared to the airplanes discussed in reference 6.

The data show that with flaps both up and down, the aileron deflections required to stabilize the high-wing airplane were approximately constant for the various airspeeds and power settings. The rudder position required to stabilize the airplane, however, showed the expected dependence on power setting and airspeed, and was also largely independent of flap position. For the minimum-power case the rudder position was largely independent of airspeed. The maximum-power case showed about 5° more right rudder was required at low speeds than at high speeds.

The rudder-pedal forces showed an increase in right pedal force for the maximum-power condition as airspeed decreased while left pedal force was required with minimum power. Since the rudder position was negative (right) for both power levels, there was apparently a constant negative force tending to offset the rudder to the right. A postflight check verified that the return springs did tend to offset the rudder to the right. Other airplanes may be rigged differently from this test airplane, and thus the neutral position may be different. However, the trends of increased right rudder and increased right rudder-pedal force with power and decreasing airspeed should be representative of this type of airplane.

Stalls

Selected time histories of the stall dynamics of both airplanes are shown in figures 22 and 23. For all the low-wing-airplane stall tests, the pilot implemented recovery controls almost immediately after the stall break, whereas for some of the high-wing tests, the pilot held the prostall control positions for several seconds. This latter technique permitted a closer look at the stall dynamics. In either case the pilot attempted to hold the "ball" in the turn and slip indicator at a near-center position up to the time of stall.

Both airplanes had reasonably mild stall characteristics. Also, both airplanes had an occasional tendency to buck (oscillate in pitch) at the stall, providing a stall warning to the pilot; and both recovered quickly from the stalled condition when the pilot applied adequate down elevator.

The results of stall testing the low-wing airplane appeared to indicate that the flaps-up stalls (figs. 22(a), 22(b), and 22(e)) were the most docile. Even the maximum-power, flaps-up stall (fig. 22(e)) only had roll rates of about $\pm 5^{\circ}$ per second and pitch rates were of about $\pm 10^{\circ}$ per second. The extension of flaps (figs. 22(c) and 22(d)) increased the poststall gyrations somewhat with roll rates up to about 20° per second. For these tests, the stall speed for minimum power with no flap deflection was about 58 knots at a mass of 970 kg (66 slugs) ($C_L' \approx 1.2$) and with full flaps, about 52 knots at a mass of 970 kg (66 slugs) ($C_L' \approx 1.4$).

A flaps-up, minimum-power stall with immediate pilot recovery (fig. 23(a)) is compared to a similar stall with delayed recovery (fig. 23(b)). Both stalls showed a slight amount of bucking and a roll off to the right. The roll rate increased rapidly at first to about 10° per second before the pilot made the immediate recovery, but stabilized at 5° per second when the pilot delayed the recovery. The flaps up, maximum-power stall with delayed recovery (fig. 23(c)) showed very little if any bucking but a moderate wing rock. The flaps-down, minimum-power stall with delayed recovery (fig. 23(d)) showed the most bucking motion and a very slight wing rock. The flaps-down, maximum-power stall with delayed recovery (fig. 23(e)) rolled off to the left about 30° with a maximum roll rate of about 15° per second before the pilot made his recovery.

For the high-wing airplane, the stall speed was less than 50 knots at 950 kg (65 slugs) ($C_L' \approx 1.4$) with flaps up, and between 40 and 45 knots also at 950 kg (65 slugs) ($C_L' \approx 2.0$) with flaps down.

CONCLUDING REMARKS

Numerous quantitative measurements of the pilot-handling characteristics of two light airplanes, one a low-wing and the other a high-wing configuration, have been made using standard flight-test techniques. The data obtained should be especially helpful as baseline information for persons involved in the

development of general-aviation flight simulators and for others concerned with flight dynamics and control studies of this category of airplane.

Langley Research Center
National Aeronautics and Space Administration
Hampton, VA 23665
March 28, 1980

REFERENCES

1. Goode, Maxwell W.; O'Bryan, Thomas C.; Yenni, Kenneth R.; Cannaday, Robert L.; and Mayo, Marna H.: Landing Practices of General Aviation Pilots in Single-Engine Light Airplanes. NASA TN D-8283, 1976.

2. Airworthiness Standards: Normal, Utility, and Acrobatic Category Airplanes. Federal Aviation Regulation Part 23, Rules Serv. Co. (Washington, D.C.), Feb. 1, 1965.

3. Langdon, S. D.: Fixed Wing Stability and Control - Theory and Flight Test Techniques. USNTPS-FTM-No. 103, U.S. Navy, Aug. 1, 1969. (Available from DTIC as AD 703 681.)

4. Kershner, David D.: A Suspended Anemometer System for Measuring True Airspeed on Low-Speed Airplanes. NASA TN D-8523, 1977.

5. Gilruth, R. R.: Requirements for Satisfactory Flying Qualities of Airplanes. NACA Rep. 755, 1943. (Supersedes NACA ACR, Apr. 1941.)

6. Phillips, William H.: Appreciation and Prediction of Flying Qualities. NACA Rep. 927, 1949. (Supersedes NACA TN 1670.)

7. Greer, H. Douglas; Shivers, James P.; Fink, Marvin P.; and Carter, C. Robert: Wind-Tunnel Investigation of Static Longitudinal and Lateral Characteristics of a Full-Scale Mockup of a Light Single-Engine High-Wing Airplane. NASA TN D-7149, 1973.

8. O'Bryan, Thomas C.; Goode, Maxwell W.; Gregory, Frederick D.; and Mayo, Marna H.: Description of an Experimental (Hydrogen Peroxide) Rocket System and Its Use in Measuring Aileron and Rudder Effectiveness of a Light Airplane. NASA TP-1647, 1980.

9. Grove, Randall D.; Bowles, Roland L.; and Mayhew, Stanley C.: A Procedure for Estimating Stability and Control Parameters From Flight Test Data by Using Maximum Likelihood Methods Employing a Real-Time Digital System. NASA TN D-6735, 1972.

10. Cannaday, Robert L.; and Suit, William T.: Effects of Control Inputs on the Estimation of Stability and Control Parameters of a Light Airplane. NASA TP-1043, 1977.

TABLE I.- LOW-WING AIRPLANE CHARACTERISTICS OBTAINED FROM MANUFACTURER

Single engine	
Four place	
Tricycle landing gear (fixed)	
Basic metal construction	
Fixed-pitch propeller	
Slotted flap (hinged below wing)	
Longitudinal control	Stabilator with tab used for trim and anti-servo
Rectangular wing planform	
Wing area, m^2 (ft^2)	14.9 (160)
Wing span, m (ft)	9.1 (30)
Wing dihedral, deg	7
Washout, deg	2
Wing aspect ratio	5.7
Length, m (ft)	7.2 (23.5)
Height, m (ft)	2.2 (7.3)
Power, kW (hp)	134 (180)
Empty mass, kg (slugs)	591 (40)
Gross mass, kg (slugs)	1089 (75)
Maximum speed, 100 percent power, sea level, knots (mph)	132 (152)
Cruise speed, 75 percent power at 2100 m (7000 ft), knots (mph)	124 (143)
Maximum rate-of-climb speed at sea level, knots (mph)	74 (85)
Never-exceed speed, knots (mph)	149 (171)
Approach speed for -	
Flaps up, knots (mph)	74 (85)
Flaps 10°, knots (mph)	71 (82)
Flaps 25°, knots (mph)	69 (79)
Flaps 40°, knots (mph)	66 (76)
Stall speed for -	
Flaps up, gross mass, power off, knots (mph)	57 (66)
Flaps 40°, gross mass, power off, knots (mph)	50 (57)
Take-off ground run at sea level for flaps 25°, gross mass, maximum effort, m (ft)	220 (720)
Landing ground roll at sea level for gross mass, m (ft)	183 (600)
Control-surface and controller travels:	
Stabilator, deg	-18 to 2
Stabilator tab travel, deg	-3 to 12
Wheel movement, cm (in.)	21 (8.3)
Each aileron, deg	-30 to 15
Wheel rotation, deg	170
Rudder, deg	-27 to 27
Rudder pedal, cm (in.)	6.3 (2.48)
Flap travel, deg	10, 25, 40
Wheel-to-stabilator gearing ratio, rad/m (rad/ft)	1.66 (0.51)

TABLE II.- HIGH-WING AIRPLANE CHARACTERISTICS OBTAINED FROM MANUFACTURER

Single engine	
Four place	
Tricycle landing gear (fixed)	
Basic metal construction	
Fixed-pitch propeller	
Fowler flap	
Longitudinal control	Elevator
Rectangular wing planform to 0.47b/2, then taper ratio of 0.70 to wing tip	
Wing area, m^2 (ft^2)	16.2 (174)
Wing span, m (ft)	11 (36)
Wing dihedral, deg	1.733
Wing incidence at root, deg	1.5
Wing incidence at tip, deg	-1.5
Wing aspect ratio	7.5
Wing airfoil	NACA 2412
Length, m (ft)	8.2 (27)
Flap span	2.0 (6.62)
Height, m (ft)	2.7 (8.75)
Flap area (total of both), m^2 (ft^2)	1.969 (21.2)
Power, kW (hp)	112 (150)
Empty mass, kg (slugs)	592 (40)
Gross mass, kg (slugs)	1043 (71.4)
Maximum speed, 100 percent power, sea level, knots (mph)	122 (140)
Cruise speed, 75 percent power at 2700 m (9000 ft), knots (mph)	115 (132)
Best rate-of-climb speed, knots (mph)	71 (82)
Never-exceed speed, knots (mph)	151 (174)
Approach speed for -	
Flaps up, knots (mph)	65 (75)
Flaps 40°, knots (mph)	60 (69)
Stall calibrated airspeeds for -	
Flaps up, gross mass, power off, knots (mph)	50 (57)
Flaps 40°, gross mass, power off, knots (mph)	43 (49)
Take-off ground run at sea level for flaps up, gross mass, m (ft)	263.7 (865)
Landing ground roll at sea level for flaps 40°, gross mass, m (ft)	158.5 (520)
Control-surface and controller travels:	
Elevator, deg	-28 to 23
Elevator-trim-tab travel, deg	-28 to 13
Flap travel, deg	0 to 40
Wheel-to-elevator gearing ratio, rad/m (rad/ft)	5.28 (1.61)
Wheel movement, cm (in.)	18 (7.1)
Each aileron, deg	-20 to 15
Wheel rotation, deg	-130 to 130
Rudder, deg	-17.7 to 17.7
Rudder pedal, cm (in.)	6.0 (2.4)

TABLE III.- NORMAL OPERATING CONDITIONS OF THE TEST AIRPLANES

Flight phase	Low-wing airplane		High-wing airplane	
	V_C, knots (mph)	C_L'	V_C, knots (mph)	C_L'
Normal cruise at 75 percent power at sea level	115 (133)	0.33	107 (123)	0.34
Maximum rate of climb at sea level	74 (85)	0.81	71 (82)	0.76
Landing approach, flaps up	74 (85)	0.81	61 to 70 (70 to 80)	1.05 to 0.80
Landing approach, flaps down	66 (76)	1.02	57 to 65 (65 to 75)	1.22 to 0.91
Stall, flaps up	57 (66)	1.35	50 (57)	1.58
Stall, flaps down	50 (57)	1.81	43 (49)	2.14

TABLE IV.- INSTRUMENTATION RANGES

Instrument function	Low-wing airplane	High-wing airplane
Airspeed, knots (mph)	0 to 145 (0 to 167)	0 to 122 (0 to 140)
Angle of attack, deg	-7.0 to 37.5	-8.2 to 39.0
Angle of sideslip, deg	-23.0 to 22.5	-22.3 to 25.0
Altitude, m (ft)	-162 to 2888 (-531 to 9475)	-170 to 2878 (-559 to 9441)
Normal acceleration, g units	-4.0 to 0.4	-4.0 to 0.5
Longitudinal acceleration, g units	-1.0 to 1.0	-1.0 to 1.0
Lateral acceleration, g units	-1.0 to 1.0	-1.0 to 1.0
Elevator position, deg	-19.6 to 4.4	-29.7 to 25.3
Right-aileron position, deg	-27.5 to 15.5	-20.4 to 16.8
Left-aileron position, deg	-27.0 to 16.5	-23.1 to 16.6
Rudder position, deg	-21.6 to 28.0	-18.6 to 19.3
Flap position, deg	-1.7 to 45.6	-0.5 to 41.0
Throttle position, percent full throw	0 to 100	0 to 100
Lateral wheel force, N (lb)	-111 to 111 (-25 to 25)	-111 to 111 (-25 to 25)
Longitudinal wheel force, N (lb)	-334 to 334 (-75 to 75)	-334 to 334 (-75 to 75)
Rudder force, N (lb)	-467 to 467 (-105 to 105)	-445 to 445 (-100 to 100)
Engine speed, rpm	0 to 3000	0 to 2911
Pitch rate, deg/sec	-27.8 to 28.2	-31.0 to 30.9
Roll rate, deg/sec	-29.4 to 30.1	-31.0 to 31.1
Yaw rate, deg/sec	-29.4 to 30.1	-31.0 to 31.1
Pitch attitude, deg	-36.0 to 35.9	-30.5 to 30.5
Roll attitude, deg	-68.1 to 67.6	-59.2 to 59.2
Trim tab	----------	-28 to 13
Manifold pressure, kPa (psia)	----------	0 to 105 (0 to 15)

TABLE V.- MEASURED VALUE OF PHUGOID PERIOD, TIME TO DAMP TO HALF-AMPLITUDE, AND DAMPING RATIO FOR THE THREE CENTER-OF-GRAVITY LOCATIONS

Flight with PLF		Period, sec			Time to damp to half-amplitude, sec			Damping ratio		
V_c, knots (mph)	Flaps	Center-of-gravity locations								
		Fore	Mid	Aft	Fore	Mid	Aft	Fore	Mid	Aft
Low-wing airplane										
≈95 (109)	Up	32	30	32	23	36	24	0.15	0.09	0.14
≈62 (71)	Up		26	26		42	26		.07	.11
≈62 (71)	Down	23	26	22	22	24	20	.11	.12	.12
High-wing airplane										
104 (120)	Up	33	39	44	81	45	24	0.04	0.10	0.20
69 (79)	Up	20	20	21	47	37	42	.05	.06	.06
63 (72)	Down	18	19	21	37	36	19	.05	.06	.12

TABLE VI.- RANGES OF MEASURED VALUES OF DUTCH-ROLL PERIOD, TIME TO DAMP TO HALF-AMPLITUDE, DAMPING RATIO, AND ϕ/β

Flight with PLF		Controls	Period, sec	Time to damp to half-amplitude, sec	Damping ratio	ϕ/β
V_c, knots (mph)	Flaps					
Low-wing airplane; c.g. = 0.23$\bar{c}$						
92 (105)	Up	Free	2.4 to 2.5	1.6 to 1.7	0.16	0.78 to 0.89
71 (81)	Up	Free	3.1 to 3.2	1.9 to 2.2	0.16 to 0.18	0.79 to 1.02
58 to 62 (66 to 71)	Up	Free	3.1 to 3.7	1.6 to 2.0	0.20 to 0.21	0.94 to 0.98
54 to 62 (62 to 71)	Down	Free	3.0 to 3.2	1.8 to 2.3	0.15 to 0.18	0.51 to 0.64
High-wing airplane; c.g. = 0.28$\bar{c}$						
105 (120)	Up	Free	2.8 to 3.0	1.0 to 1.1	0.31 to 0.32	0.83 to 0.93
105 (120)	Up	Fixed	2.6 to 2.9	0.8 to 0.9	0.34 to 0.35	0.71 to 0.81
65 to 70 (74 to 80)	Up	Free	4.0 to 4.3	1.6 to 2.0	0.35 to 0.41	0.75 to 0.89
70 (80)	Up	Fixed	4.0	1.5	0.30	0.68
60 (69)	Down	Free	3.8 to 3.9	1.4	0.29 to 0.30	0.39
60 (69)	Down	Fixed	3.4	1.4	0.28	0.54

TABLE VII.- ROLLING PERFORMANCE OF THE TWO SUBJECT AIRPLANES

Airplane	Flaps	V, knots (mph)	ρ, kg/m^3 (slugs/ft^3)	δ_a, deg	p, deg/sec	p_{max}, deg/sec	C_{l_p}	I_{xx}, kg-m^2 (slug-ft^2)	τ_r, sec
Low-wing	Up	89 (102)	1.148 (0.0023)	-34.0	45	58	-0.233	1220 (900)	0.32
High-wing	Up	108 (124)	1.112 (.0022)	26.3	-37	53	-.440	1694 (1255)	.13

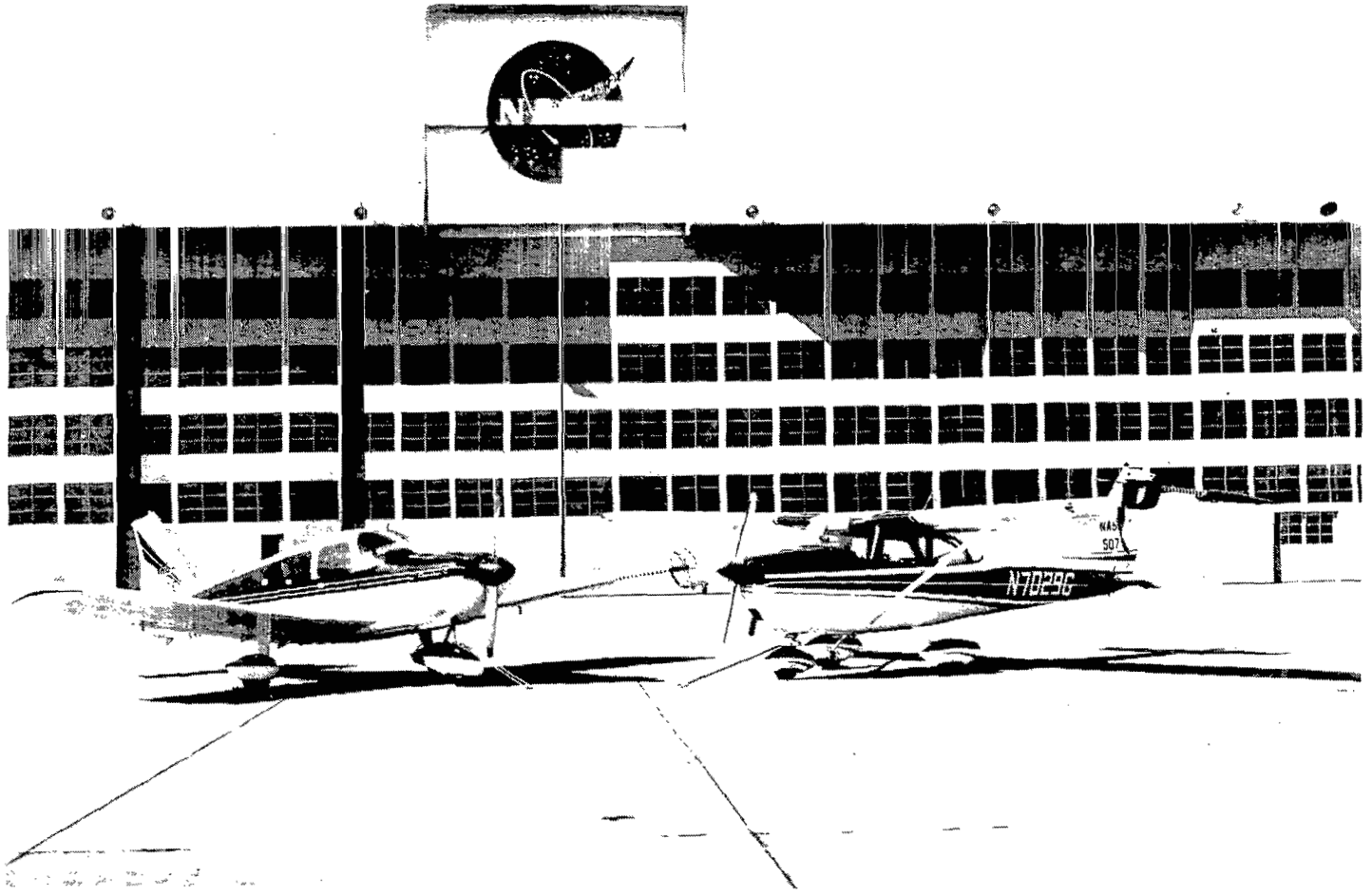

L-73-2025

Figure 1.- Test airplanes.

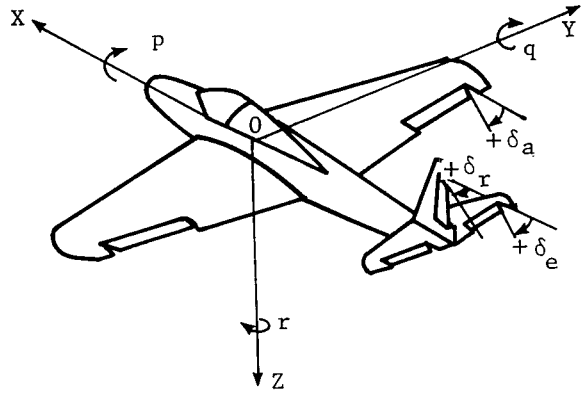

Control-surface deflections and angular rates

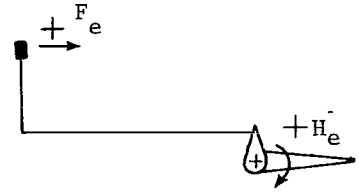

Pilot-applied elevator forces and aerodynamic-applied hinge moment

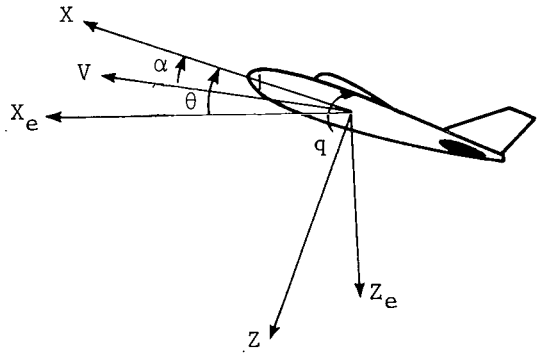

Angle of attack
(Shown with $\beta = 0^{o}$)

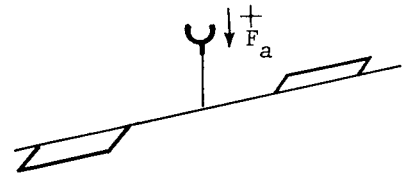

Aileron forces

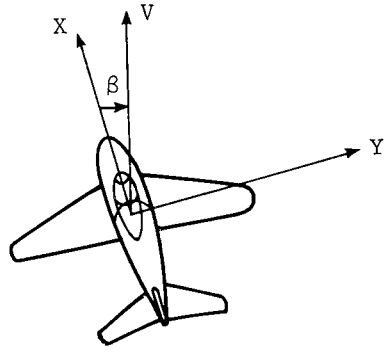

Angle of sideslip
(Shown with $\alpha = 0^{o}$)

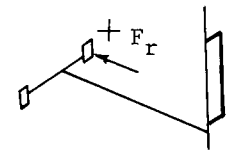

Rudder forces

Figure 2.- System of axes showing positive senses of control-surface deflections, control forces, angle of attack, and angle of sideslip.

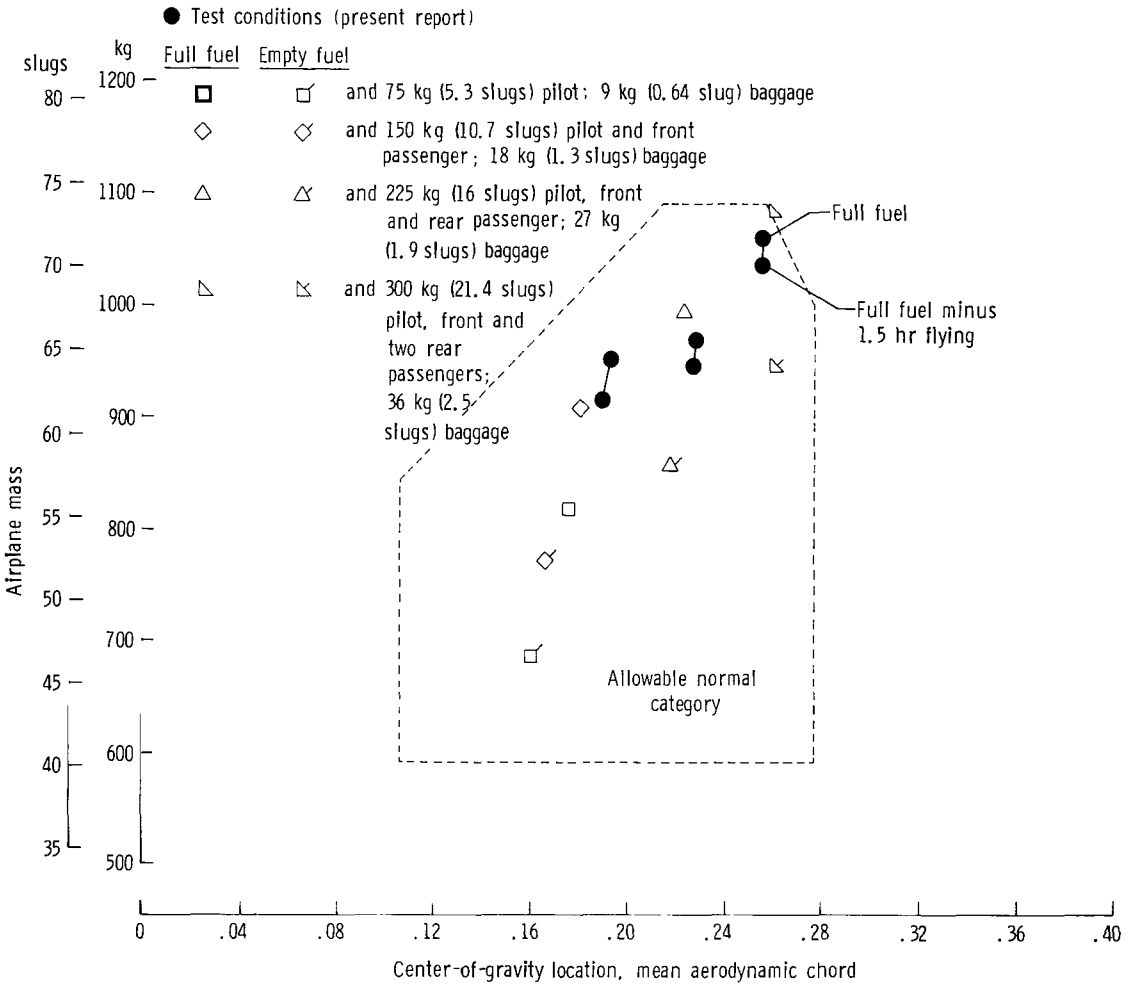

(a) Low-wing airplane.

Figure 3.- Center-of-gravity (c.g.) envelope for subject airplane showing c.g. travel for fuel usage for various loading conditions including flight-test conditions.

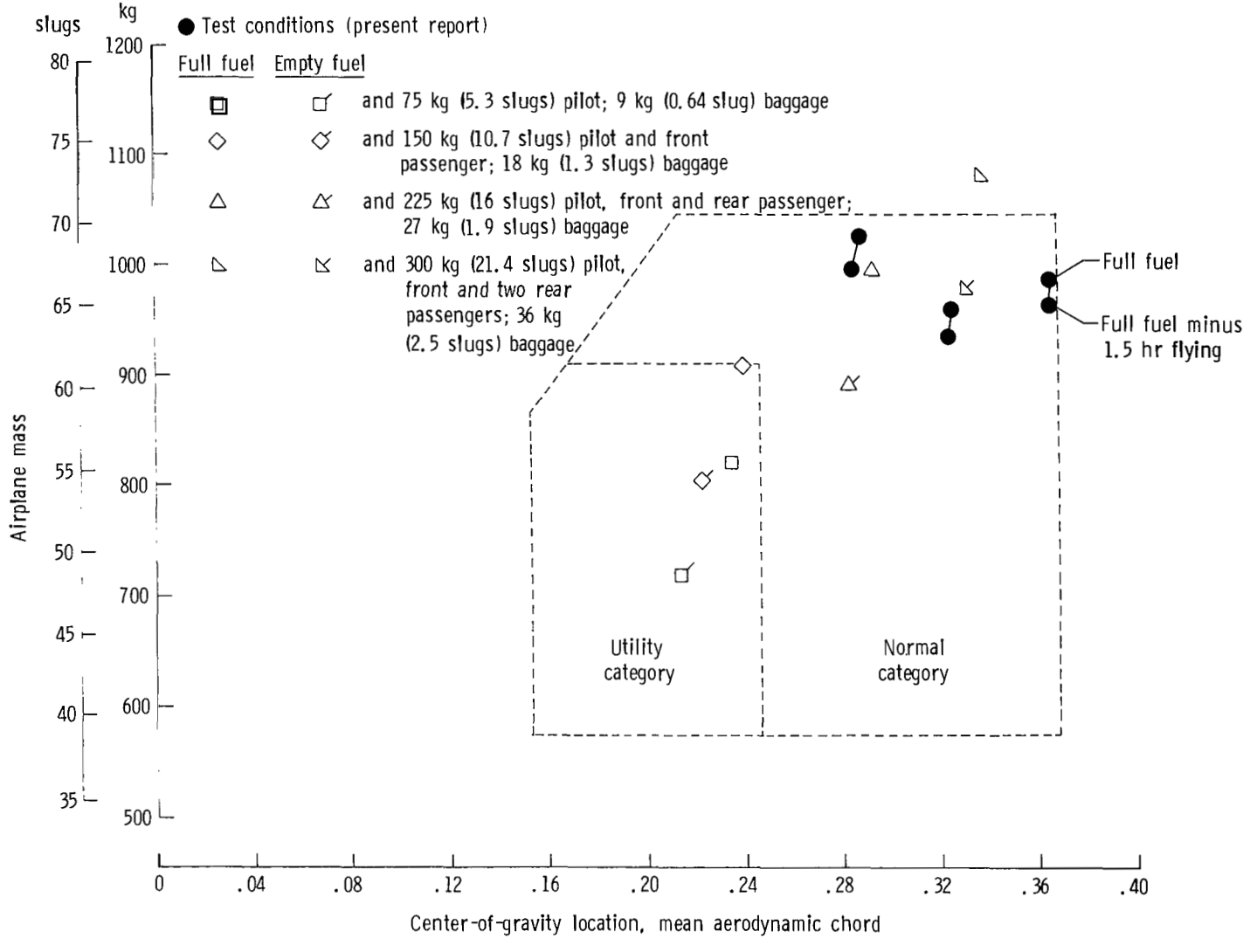

(b) High-wing airplane.

Figure 3.- Concluded.

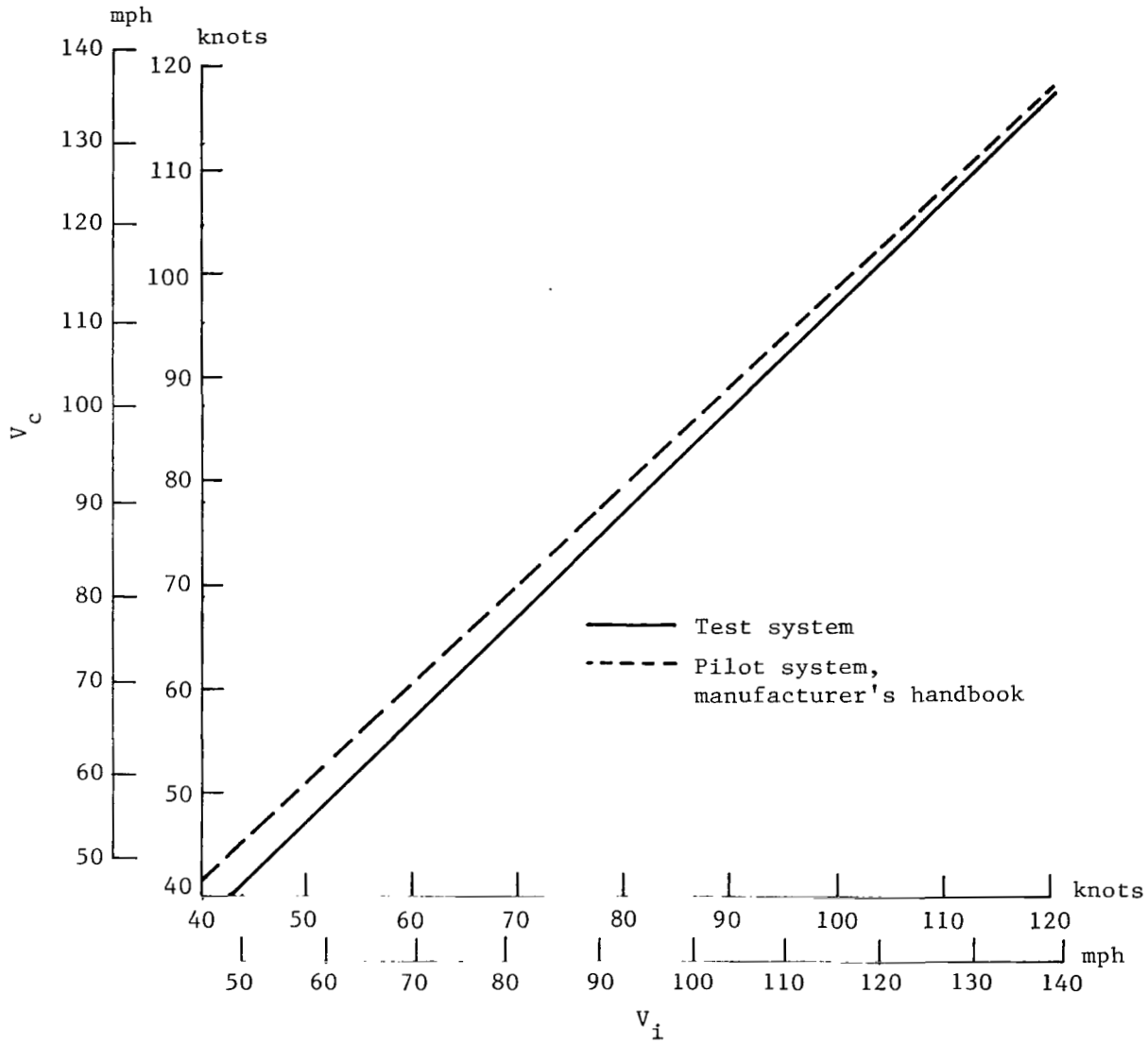

(a) Low-wing airplane.

Figure 4.- Comparison of indicated and calibrated airspeeds for pilot system and test system.

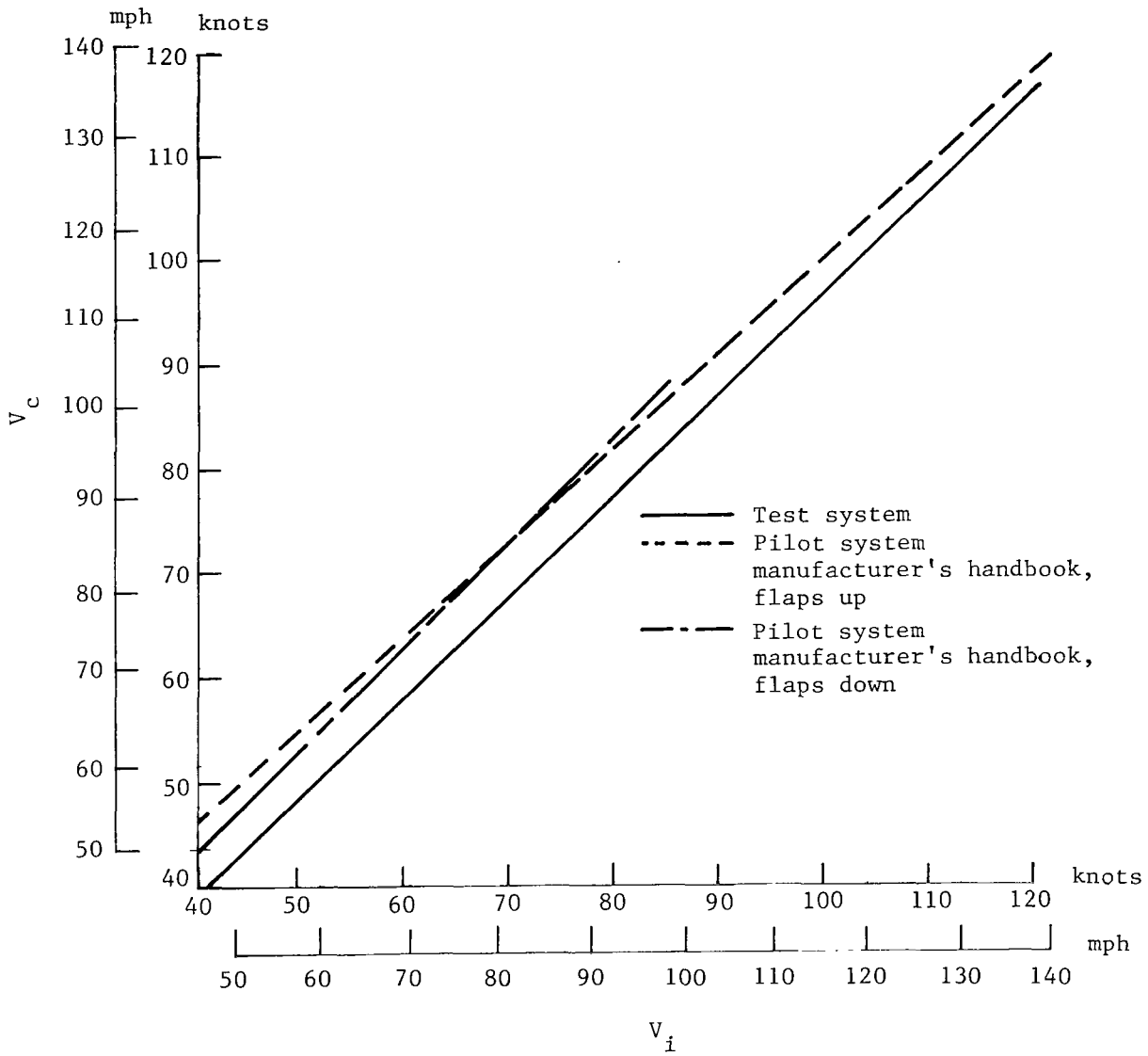

(b) High-wing airplane.

Figure 4.- Concluded.

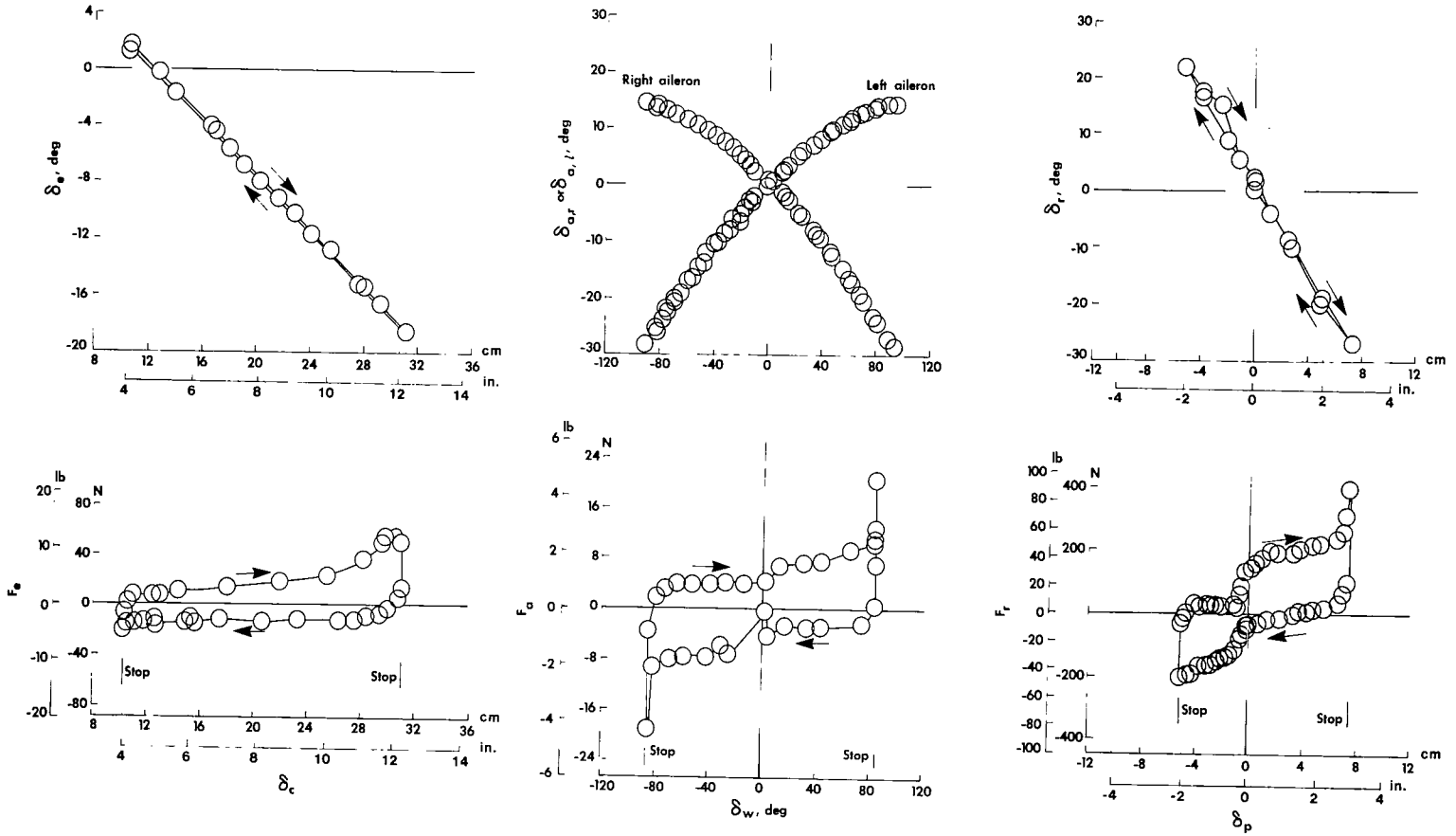

(a) Low-wing airplane.

Figure 5.- Control-system characteristics for subject airplane obtained on ground at zero velocity.

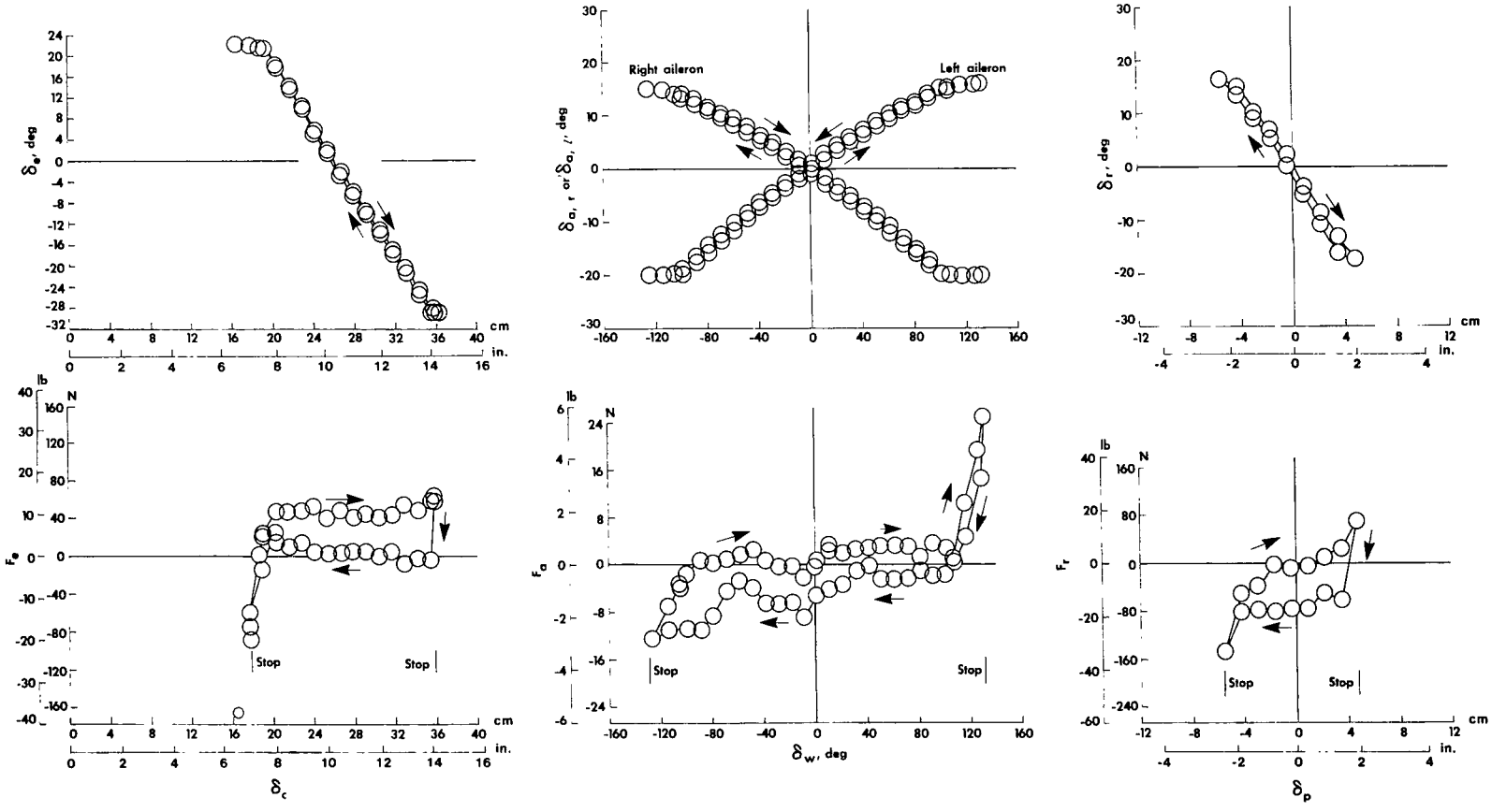

(b) High-wing airplane.

Figure 5.- Concluded.

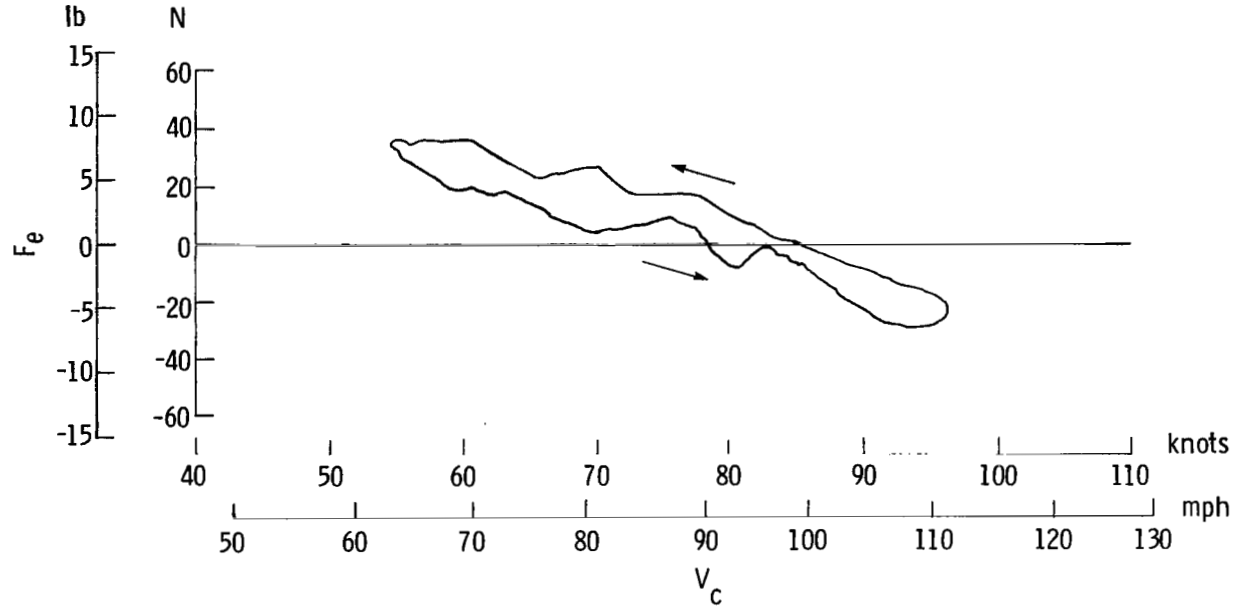

(a) Low-wing airplane.

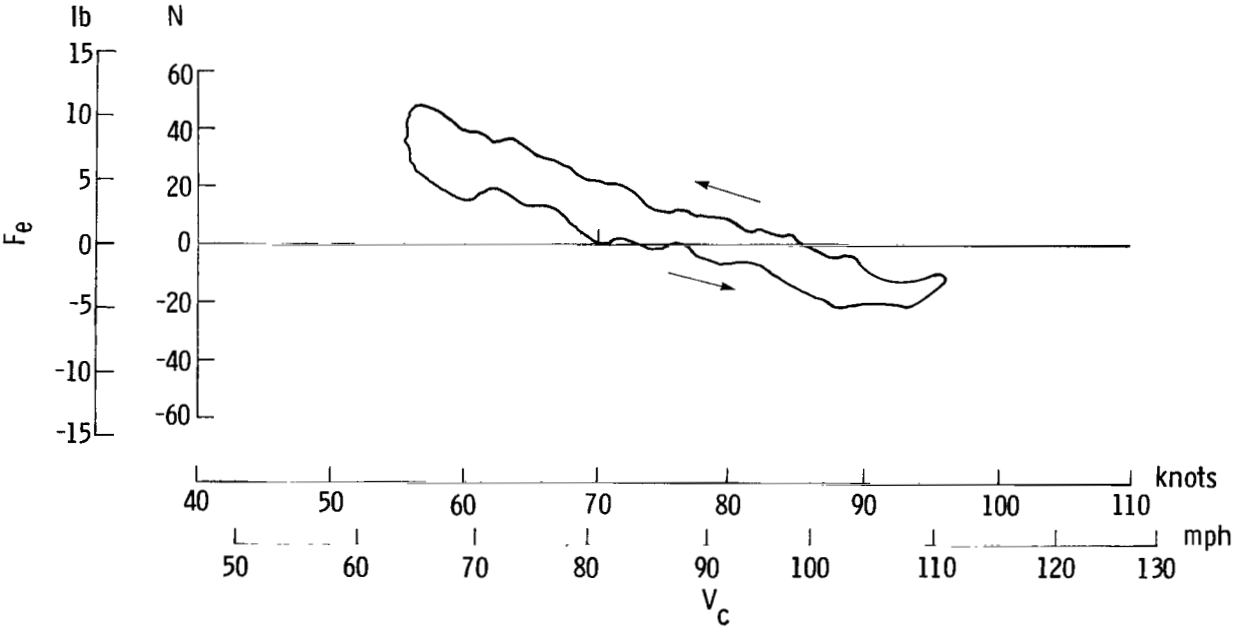

(b) High-wing airplane.

Figure 6.- In-flight longitudinal-control-system hysteresis loops for low-wing and high-wing airplanes.

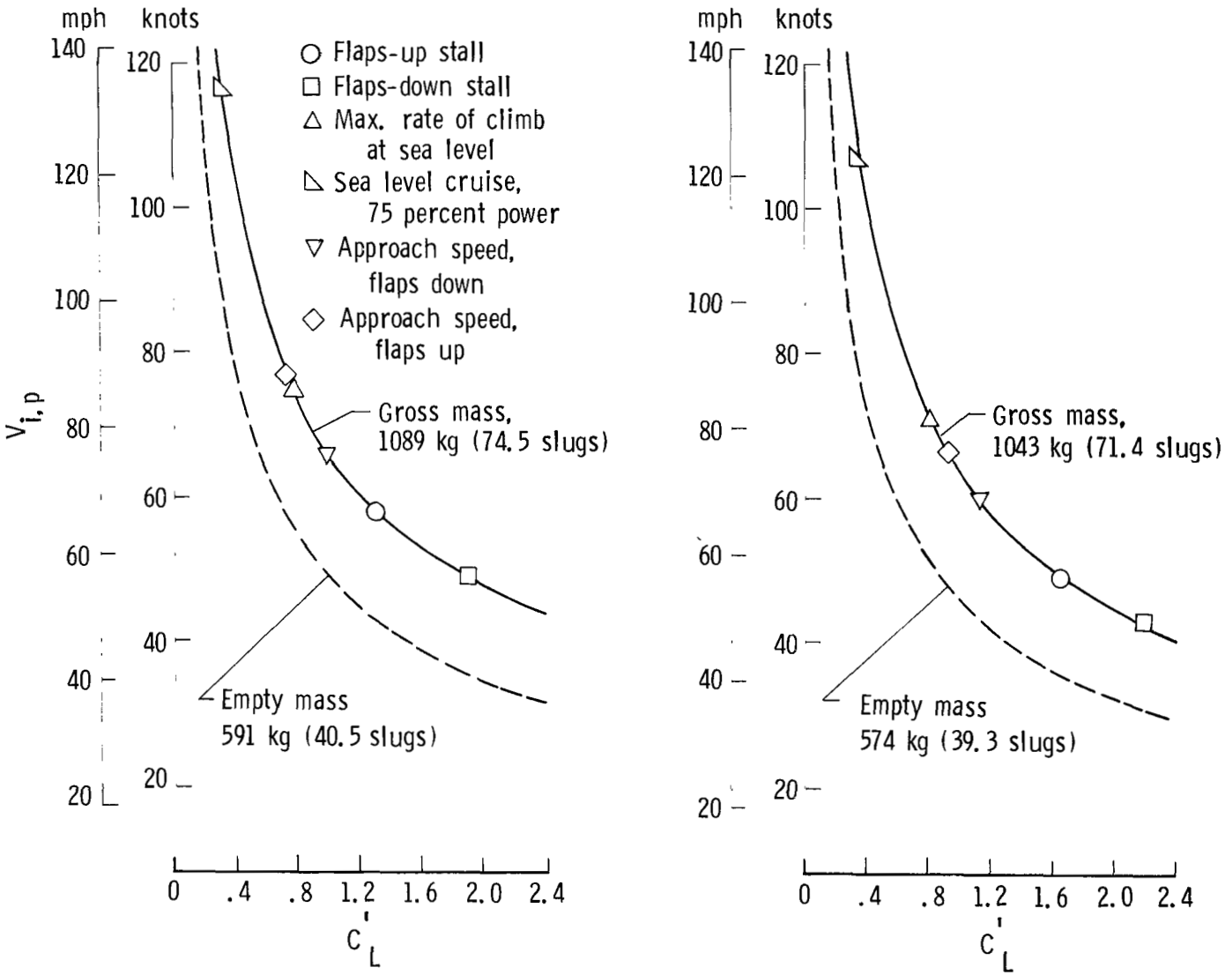

(a) Low-wing airplane.

(b) High-wing airplane.

Figure 7.- Relationships of lift coefficient and airspeed for low-wing and high-wing airplanes operating in unaccelerated level flight.

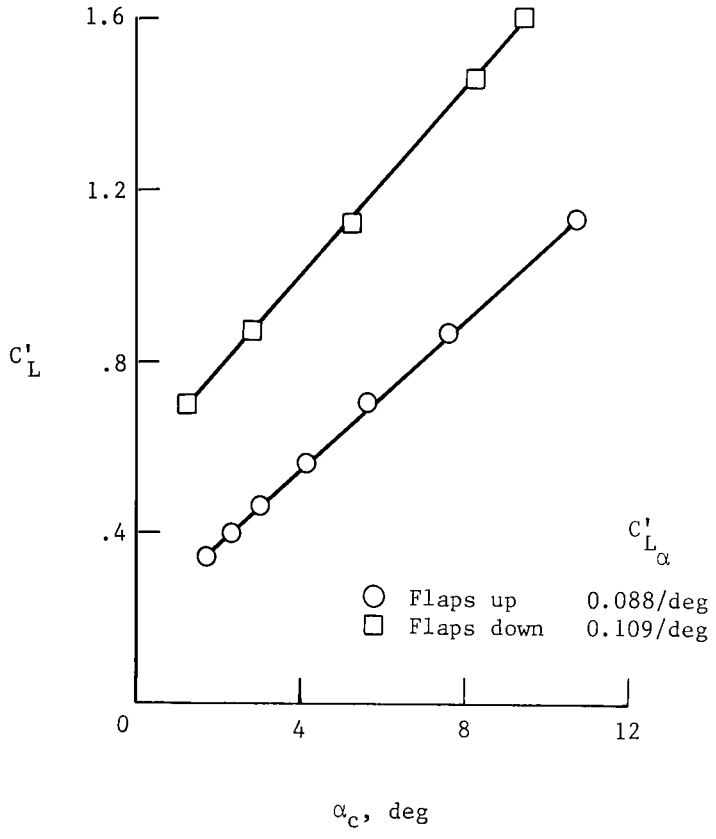

(a) Low-wing airplane.

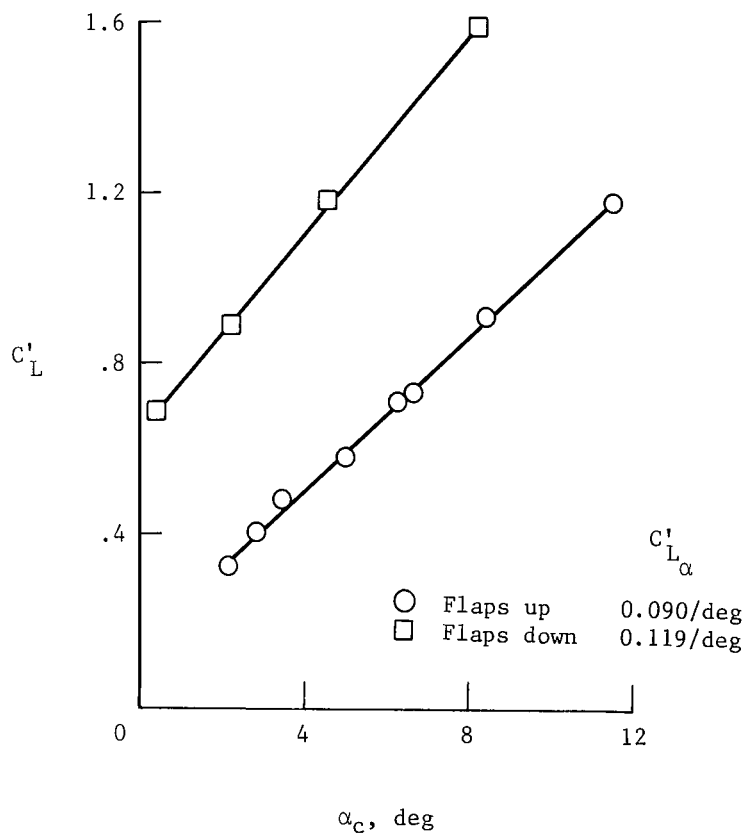

(b) High-wing airplane.

Figure 8.- Variations of angle of attack with lift coefficient in unaccelerated flight with power for level flight.

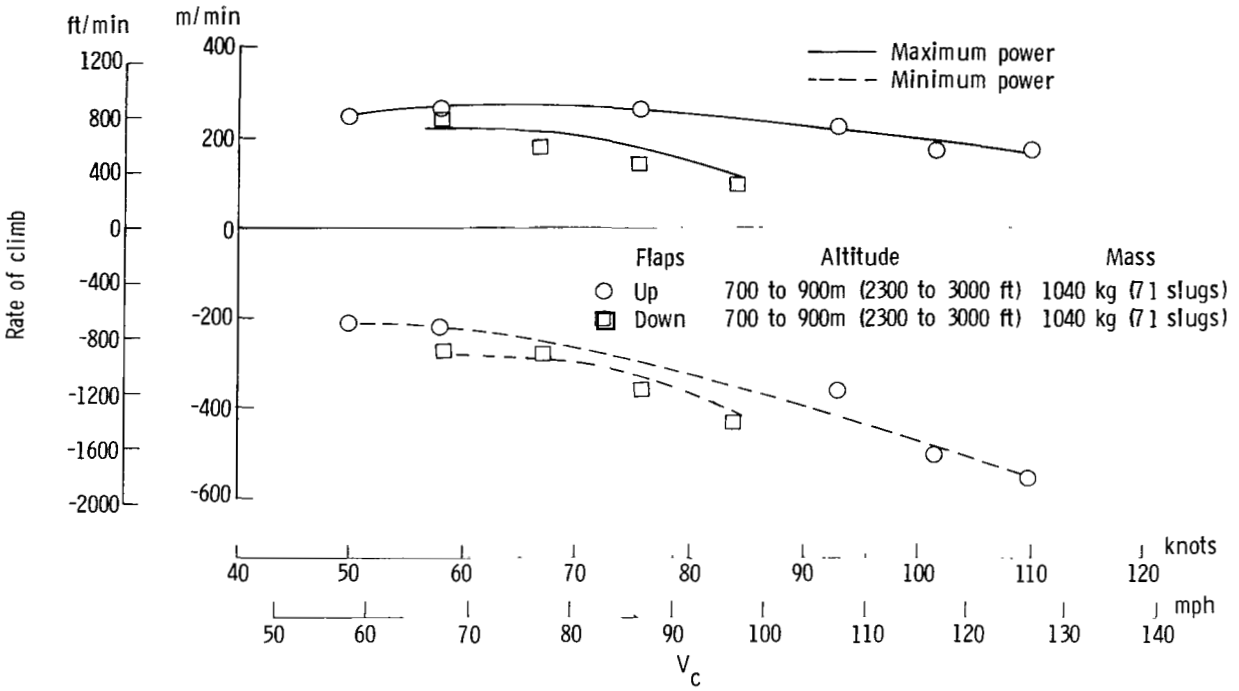

(a) Low-wing airplane.

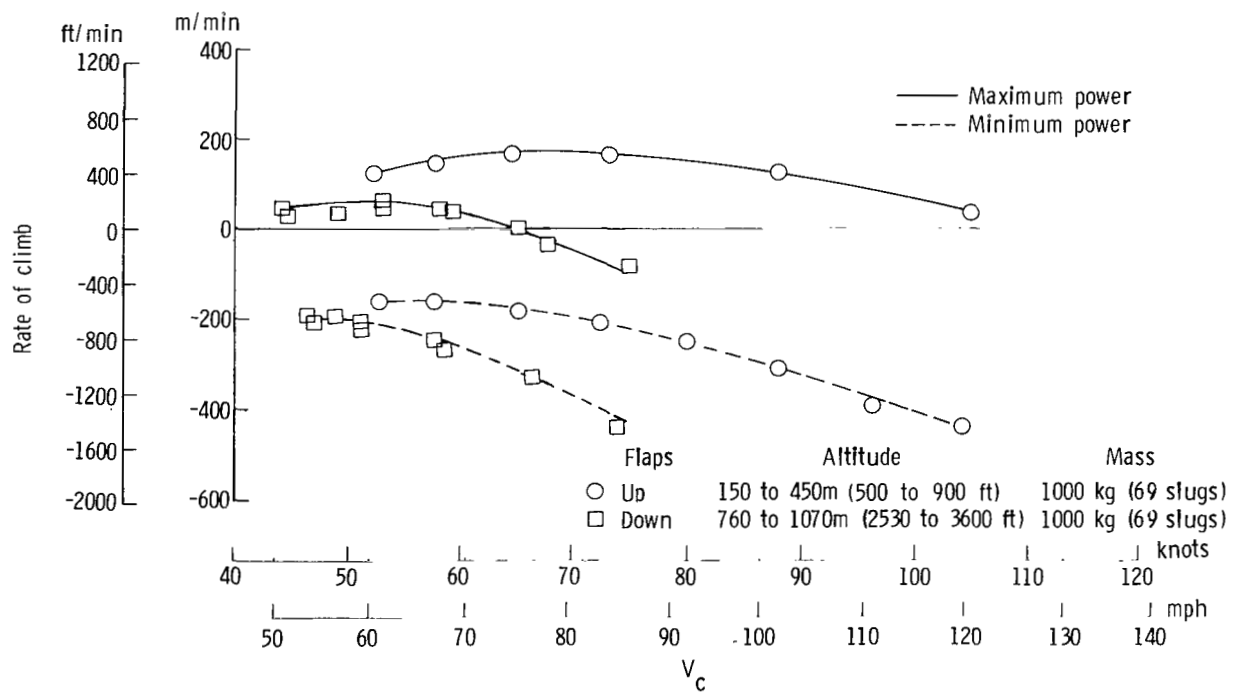

(b) High-wing airplane.

Figure 9.- Rate of climb of low-wing and high-wing airplanes.

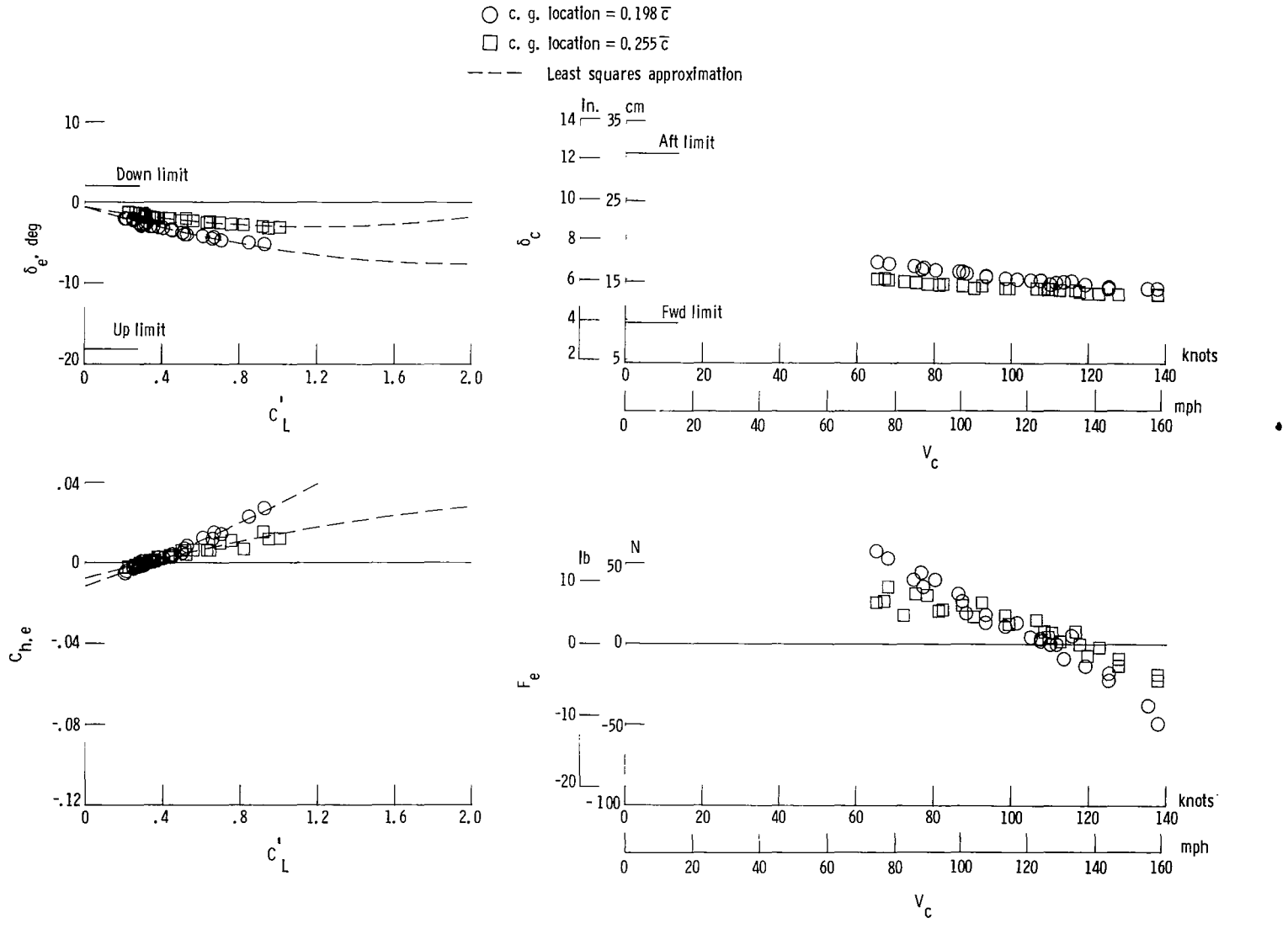

(a) Flaps up; PLF (V_c = 103 knots).

Figure 10.- Static longitudinal characteristics for low-wing airplane.

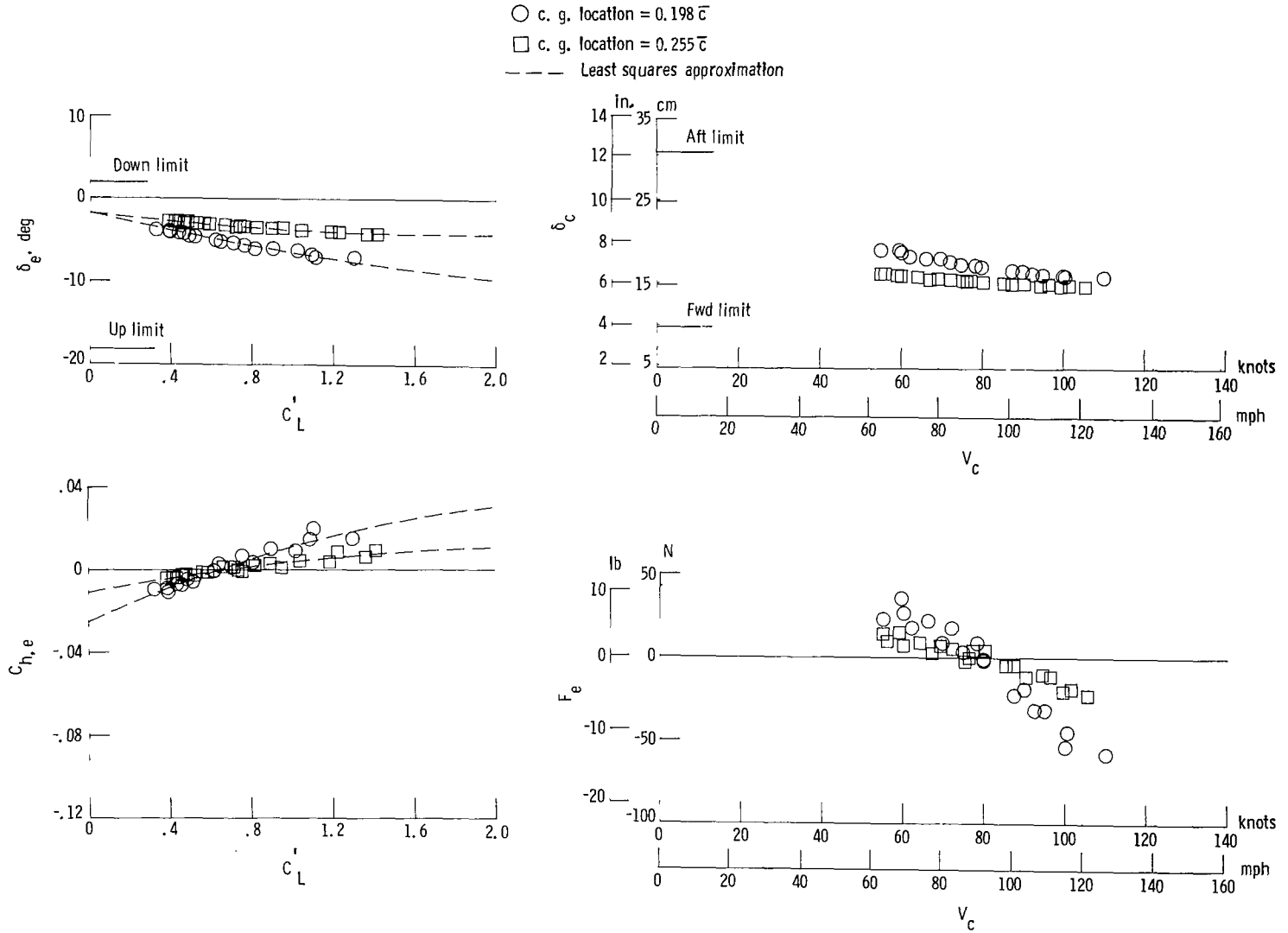

(b) Flaps down; PLF (V_c = 69 knots).

Figure 10.- Concluded.

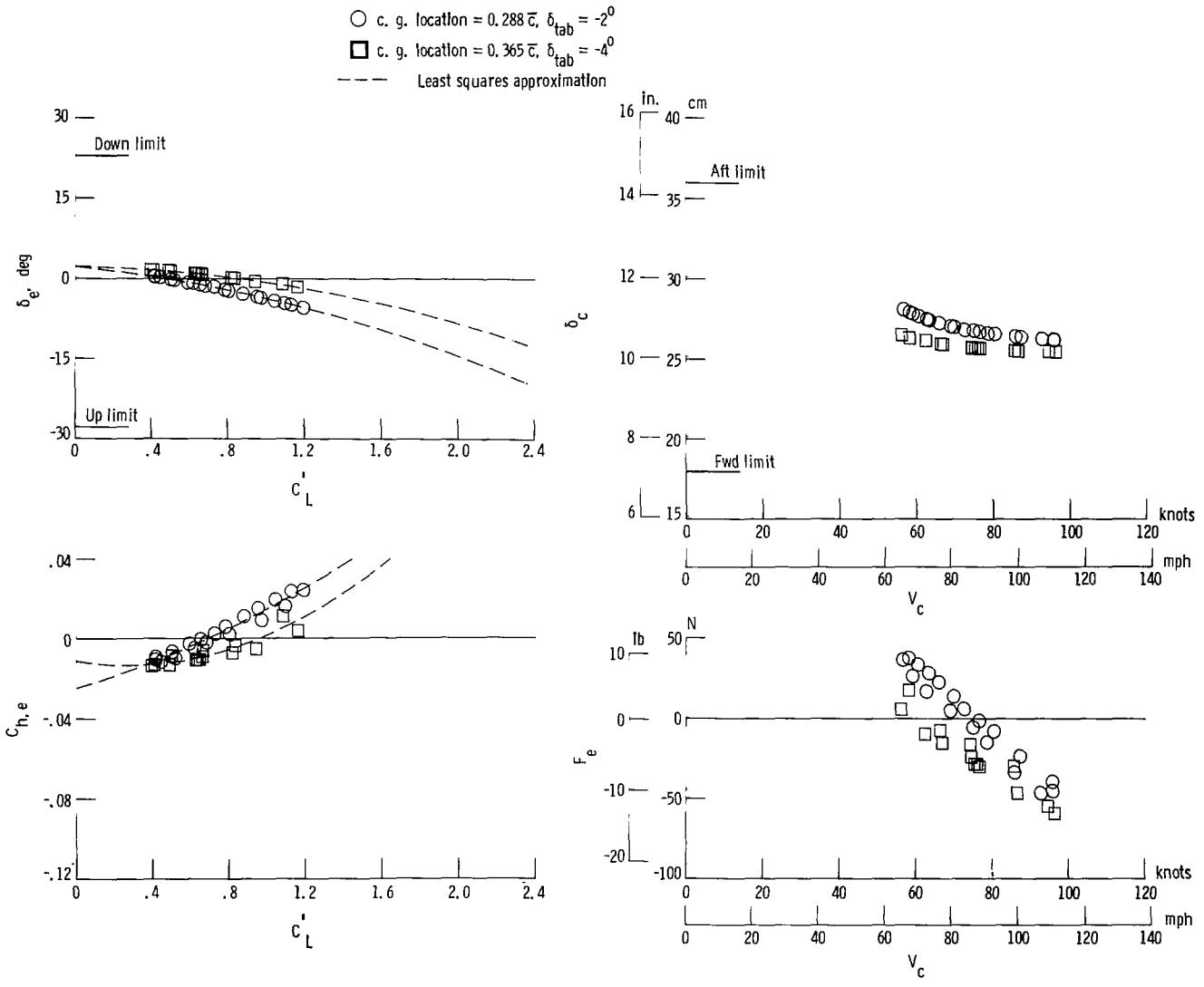

(a) Flaps up; PLF (V_c = 81 knots).

Figure 11.- Static longitudinal characteristics for high-wing airplane.

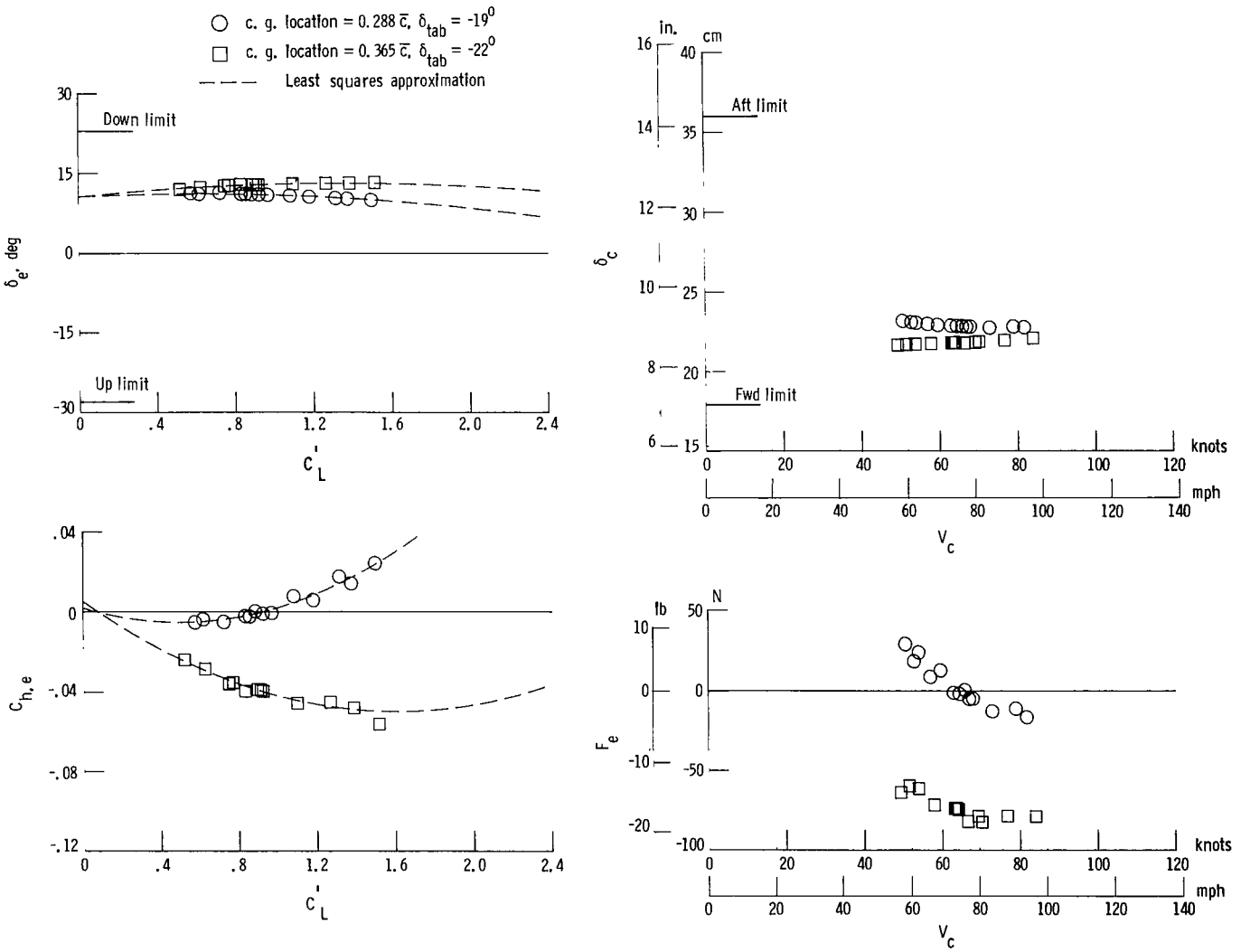

(b) Flaps down; PLF (V_c = 67 knots).

Figure 11.- Concluded.

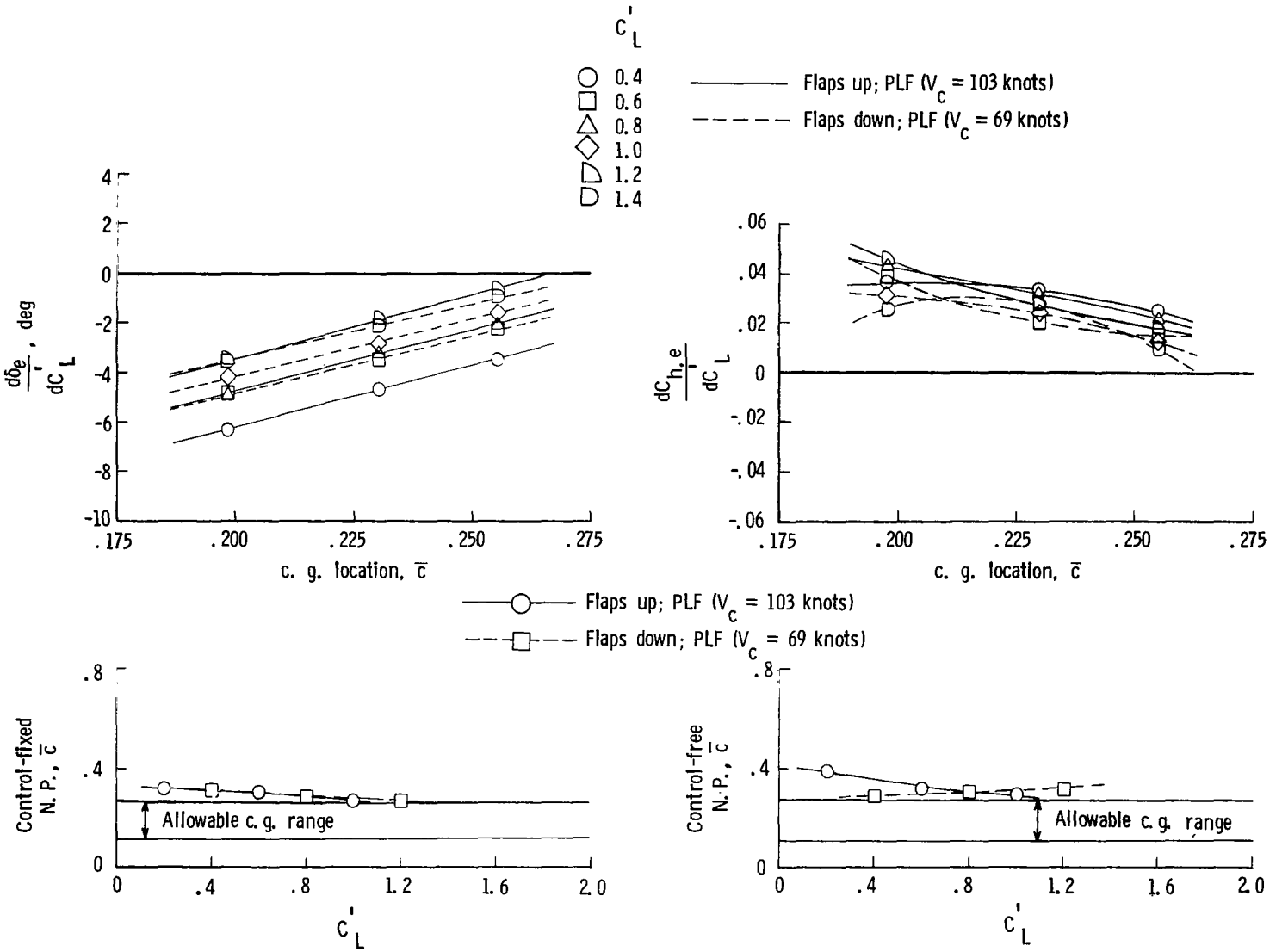

Figure 12.- Estimated static longitudinal control slopes and neutral points (N.P.) for low-wing airplane.

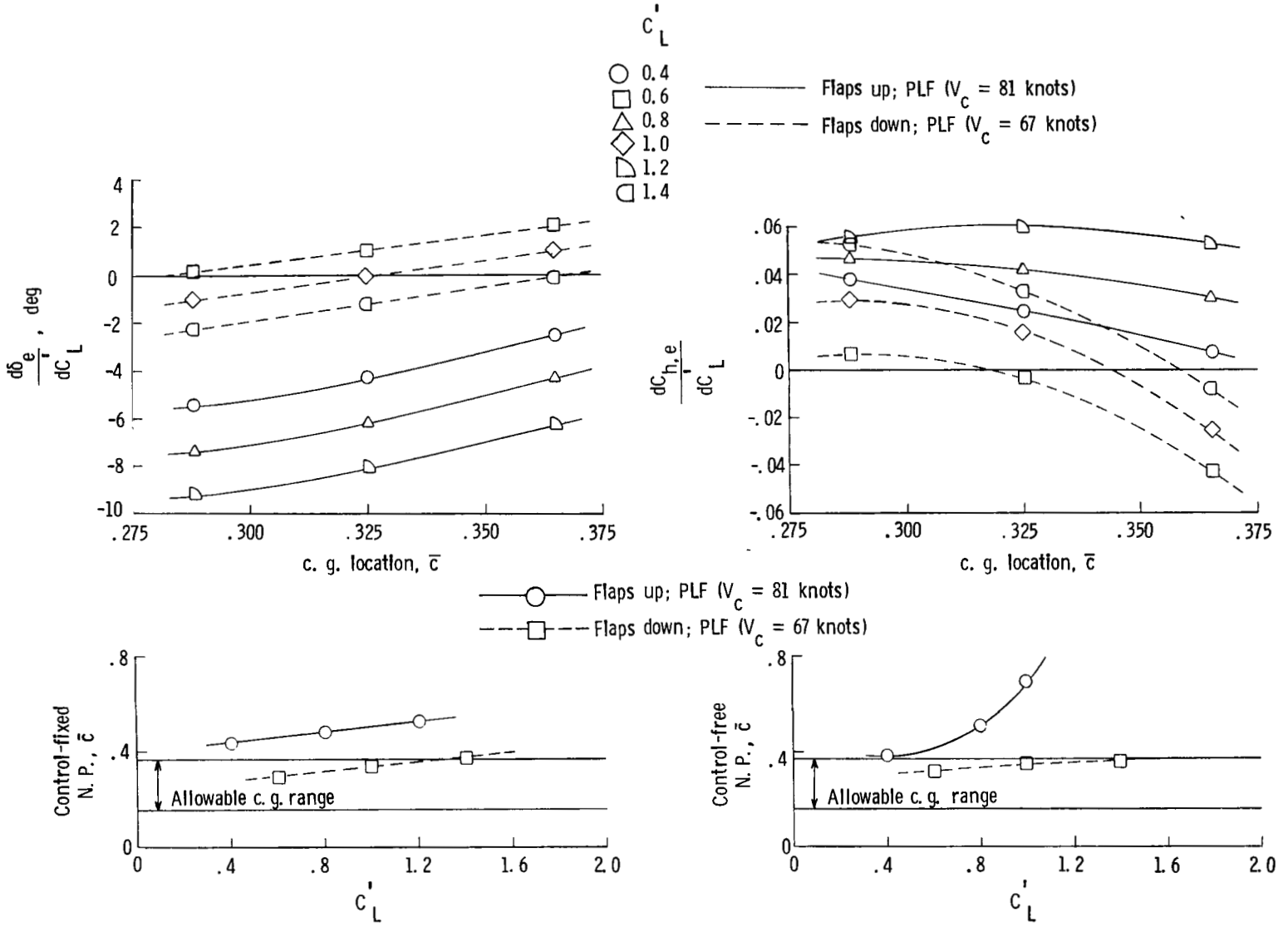

Figure 13.- Estimated static longitudinal control slopes and neutral points (N.P.) for high-wing airplane.

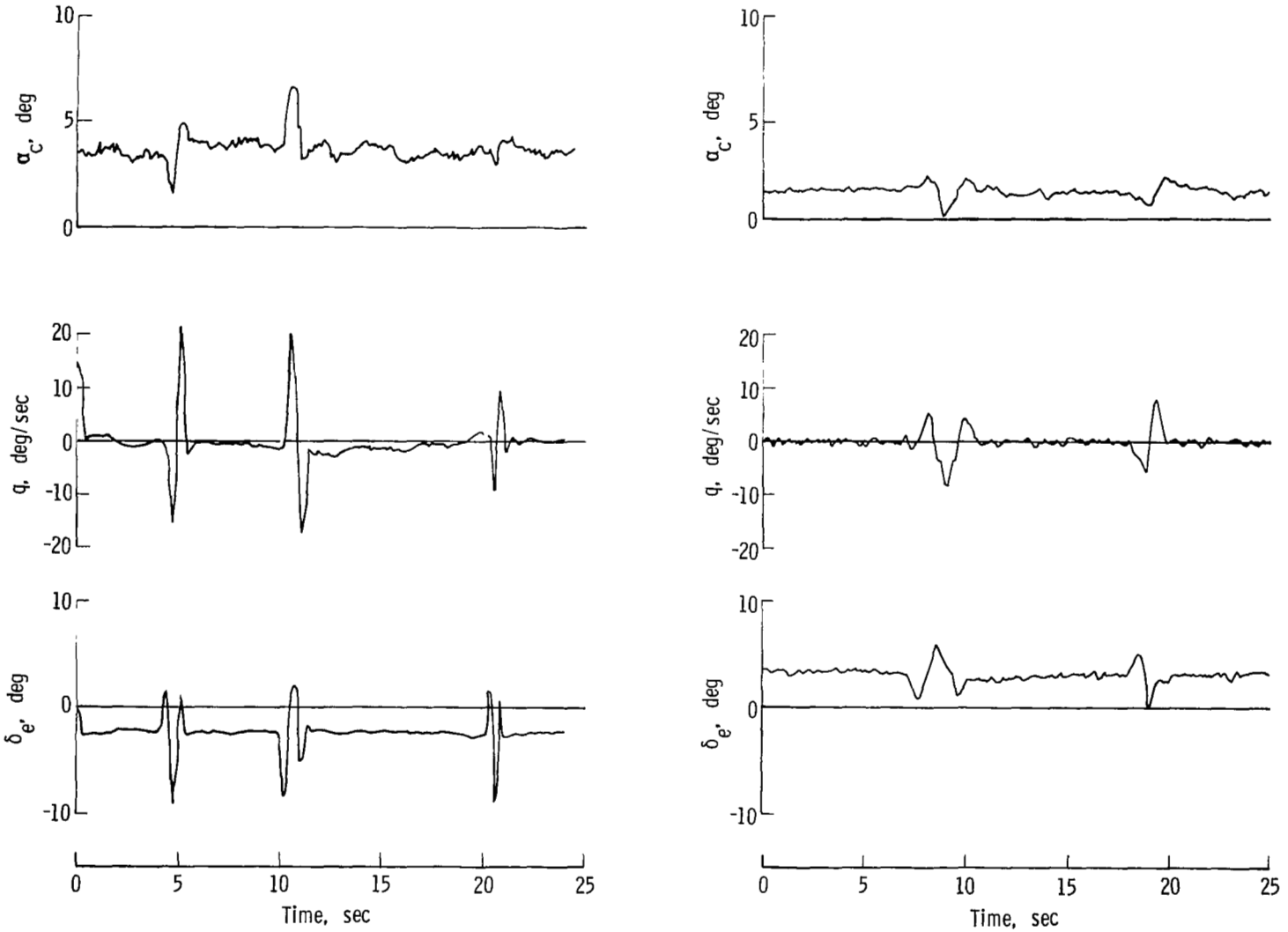

(a) Low-wing airplane.

(b) High-wing airplane.

Figure 14.- Typical time histories of short-period motions of subject airplanes.

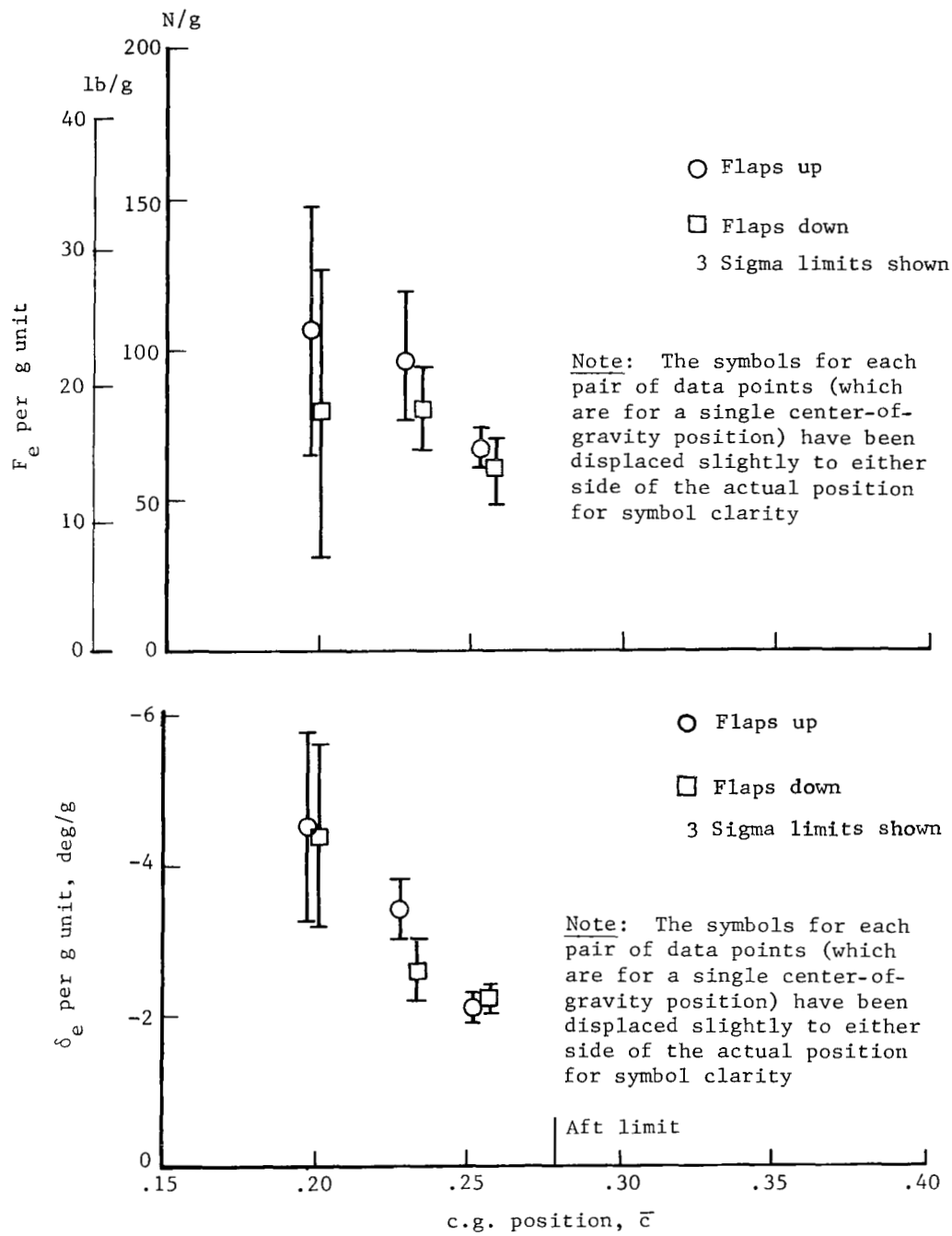

(a) Low-wing airplane.

Figure 15.- Longitudinal maneuvering stability for low-wing and high-wing airplanes.

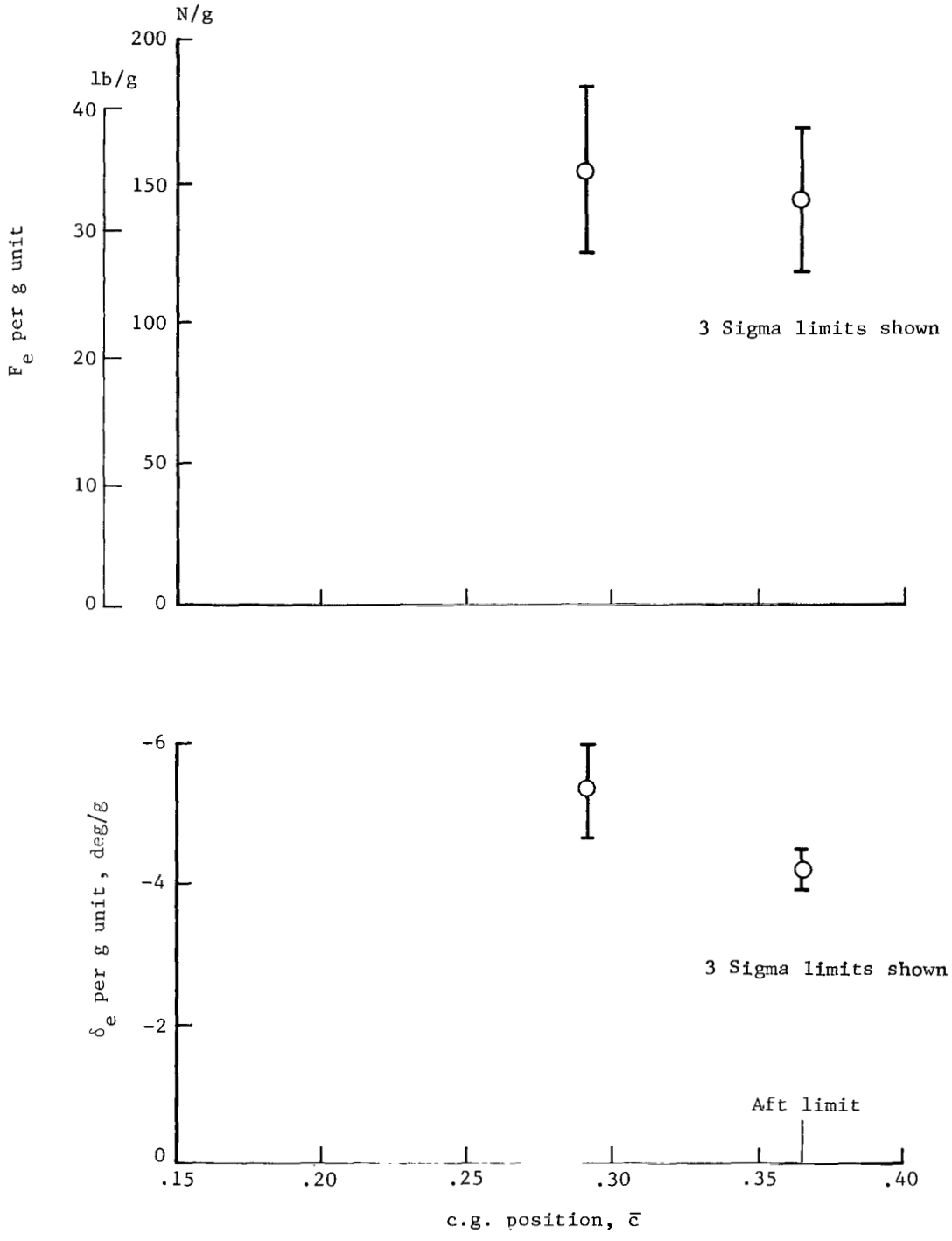

(b) High-wing airplane, flaps up.

Figure 15.- Concluded.

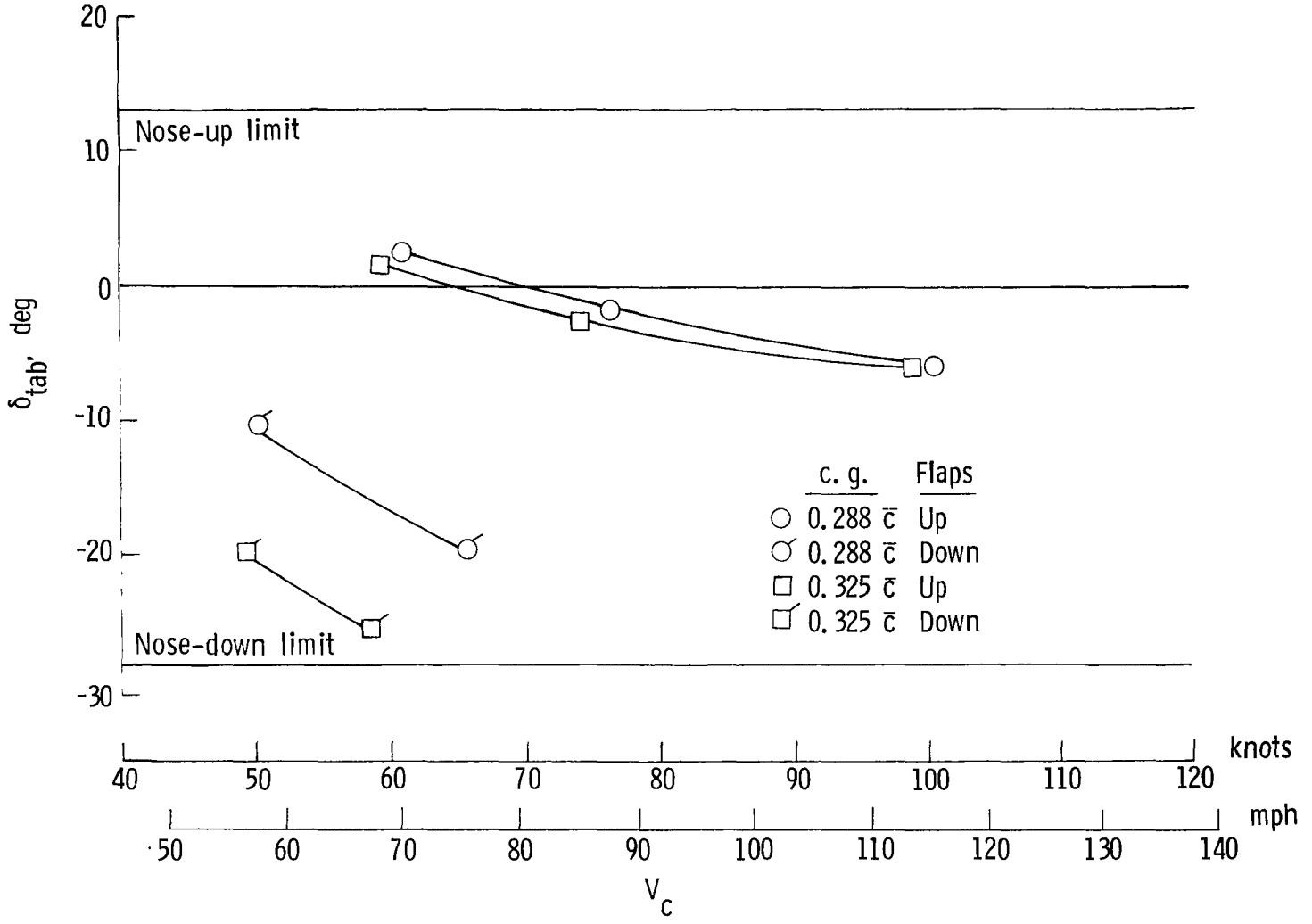

Figure 16.- Trim-tab settings required to trim longitudinal forces to zero at various airspeeds for high-wing airplane with power for level flight.

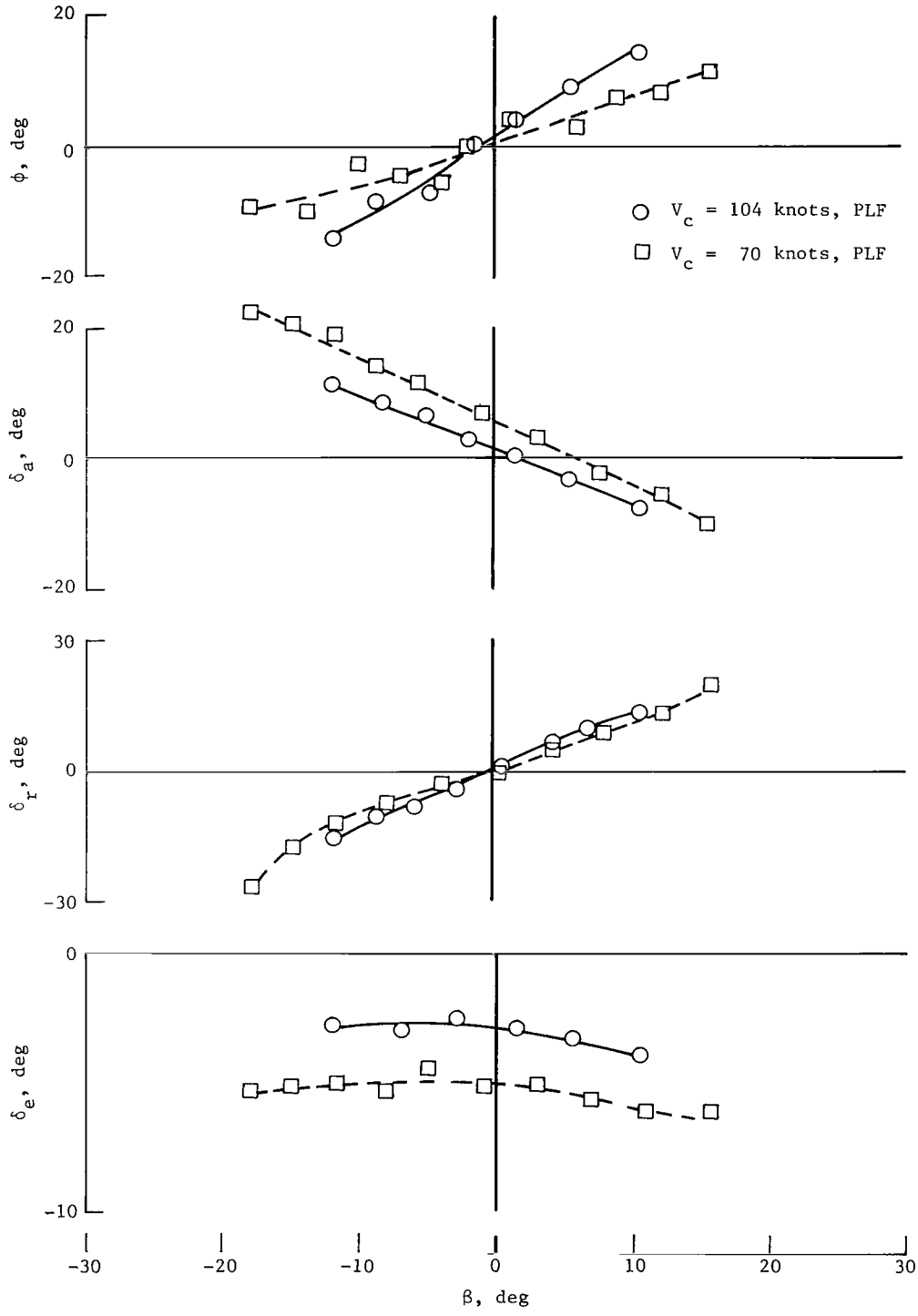

(a) Effects of speed and power with flaps up.

Figure 17.- Steady-heading sideslip data for low-wing airplane.

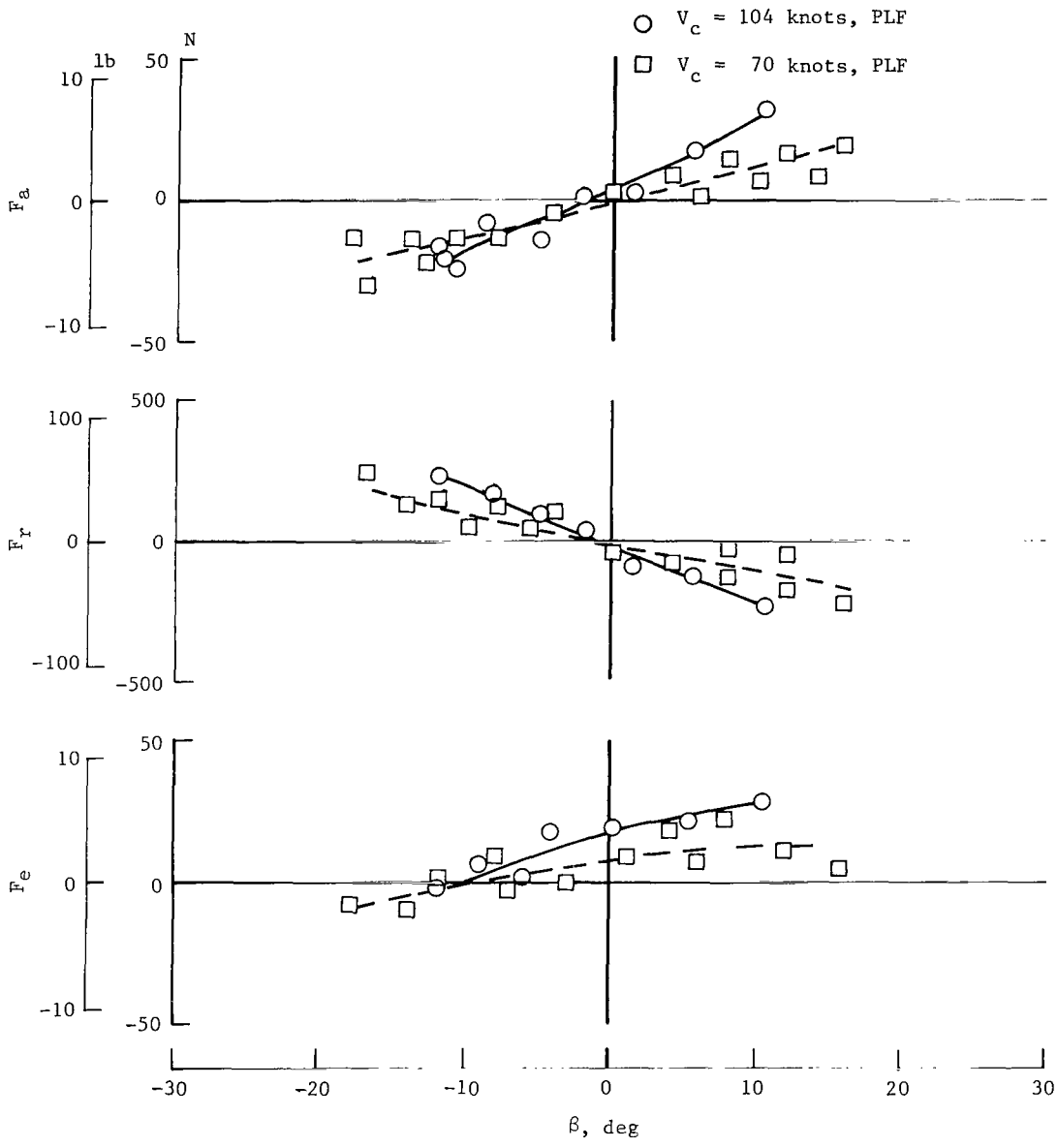

(a) Concluded.

Figure 17.- Continued.

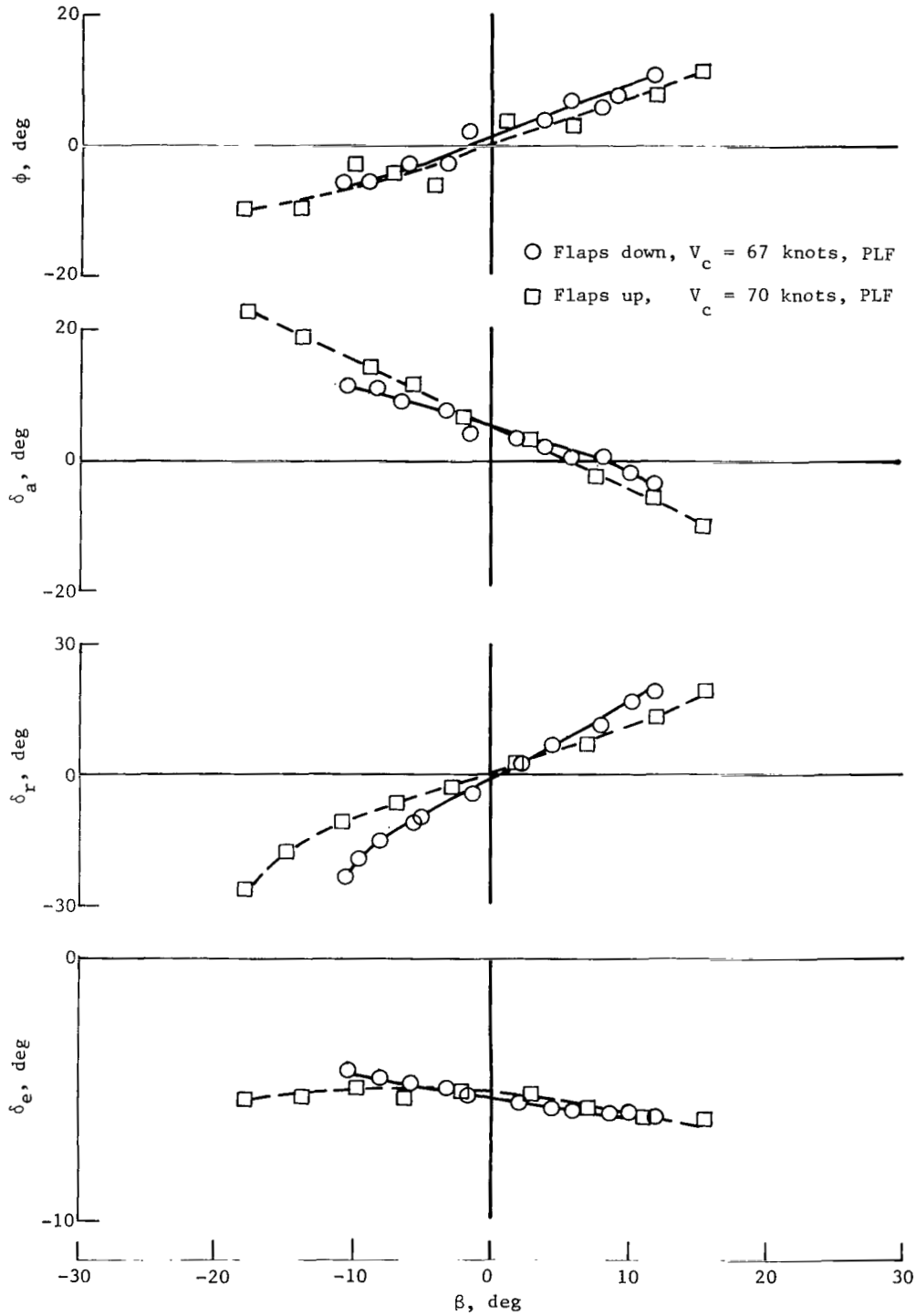

(b) Effects of flaps and power.

Figure 17.- Continued.

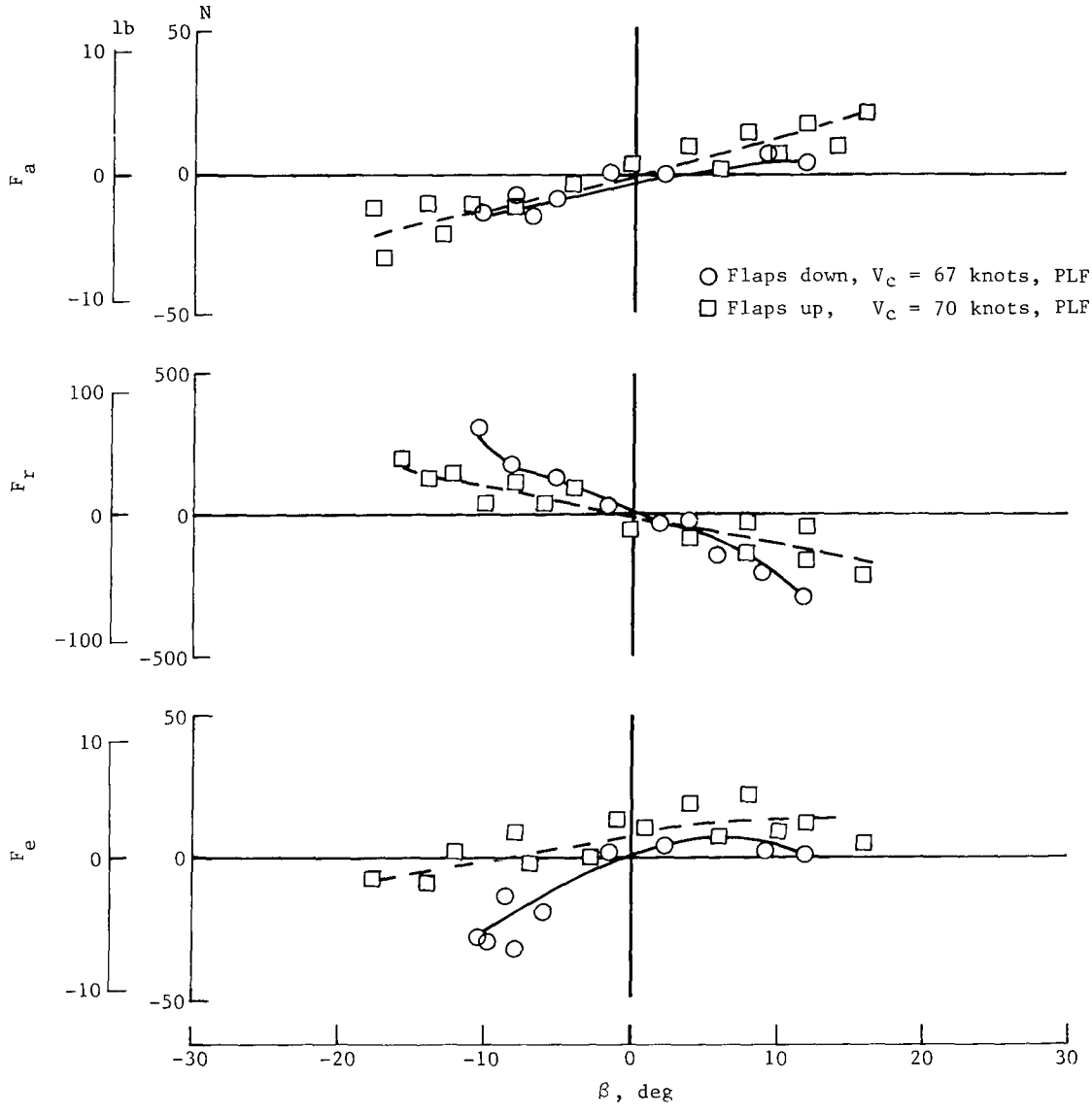

(b) Concluded.

Figure 17.- Concluded.

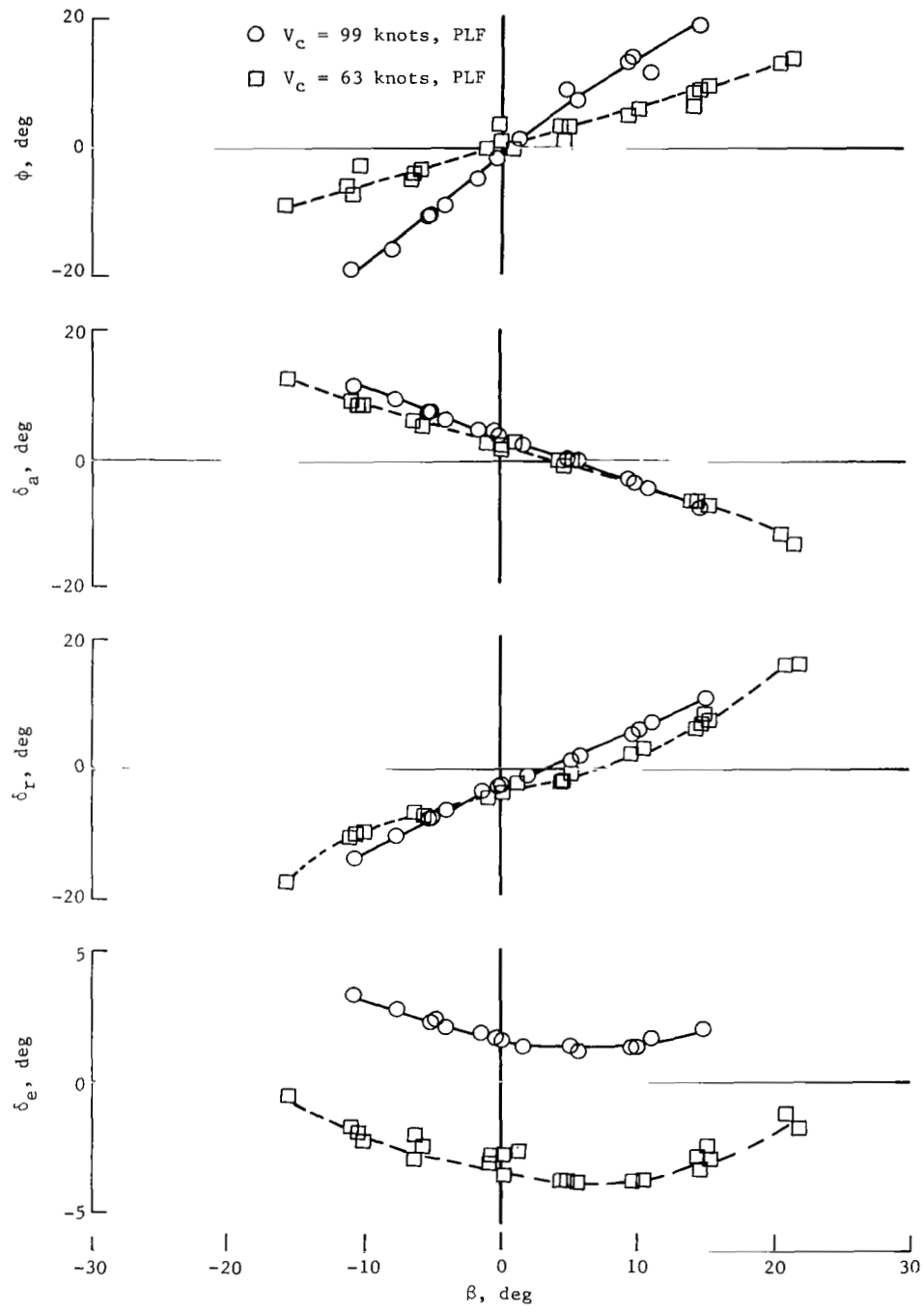

(a) Effects of speed and power with flaps up.

Figure 18.- Steady-heading sideslip data for high-wing airplane.

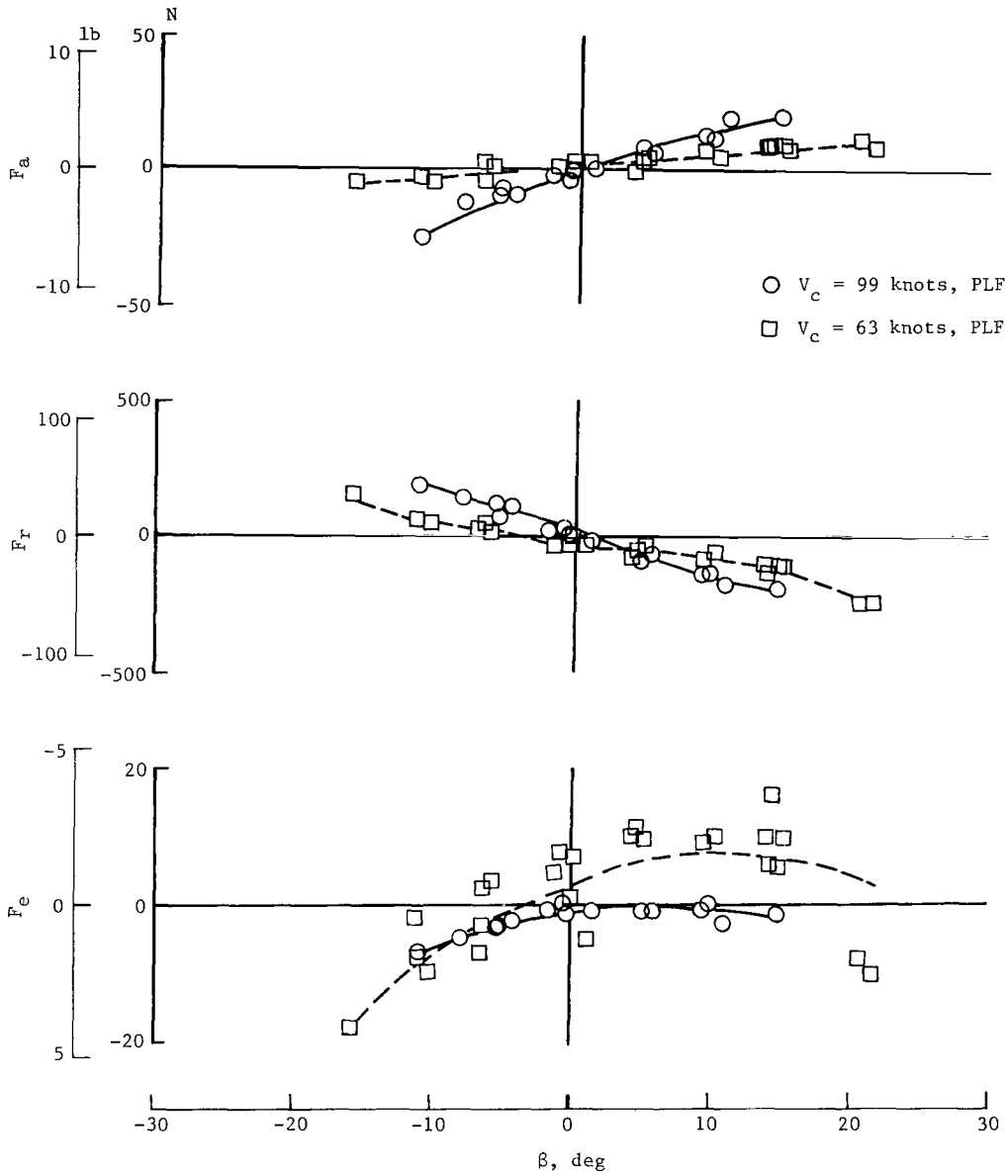

(a) Concluded.

Figure 18.- Continued.

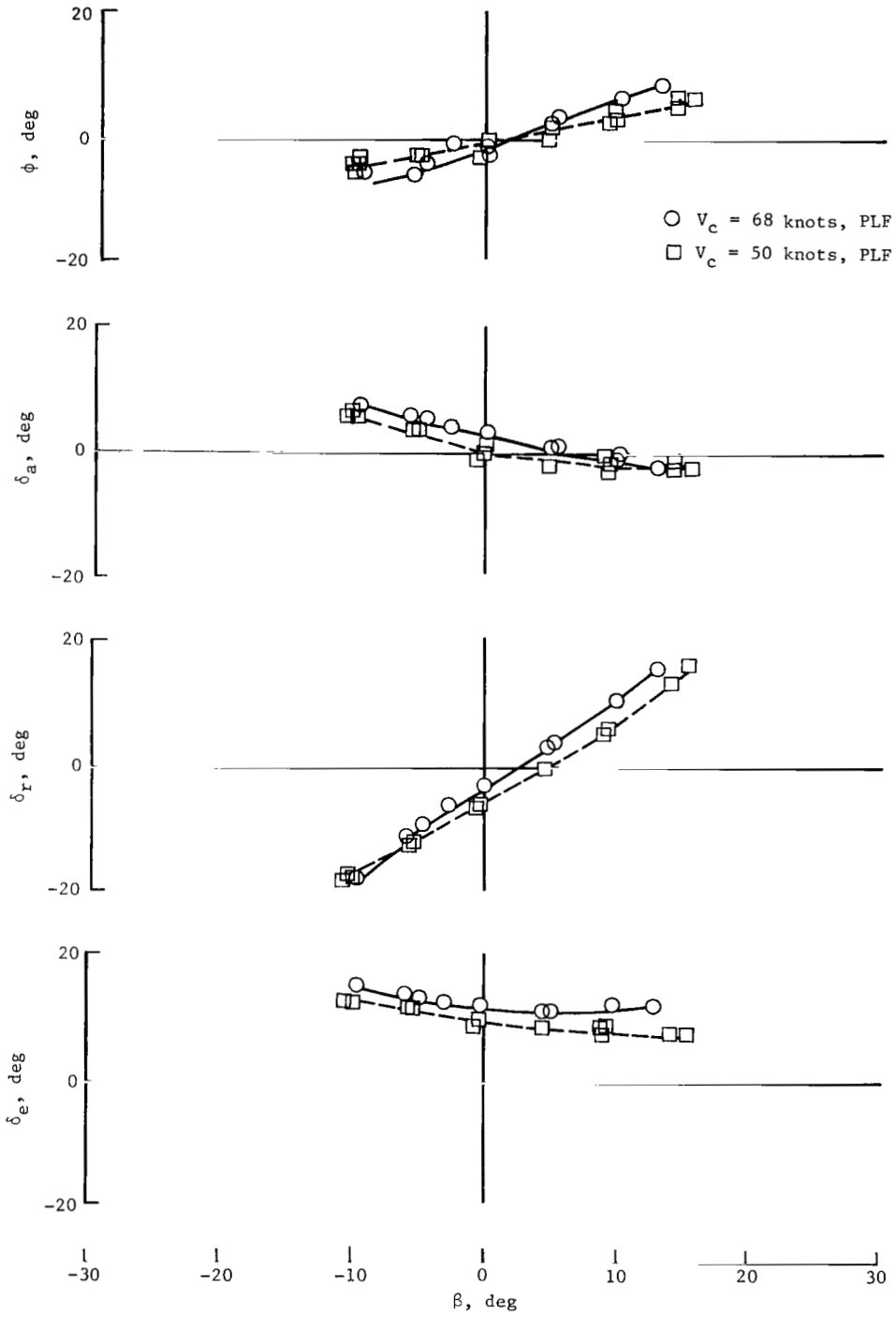

(b) Effects of speed and power with flaps down.

Figure 18.- Continued.

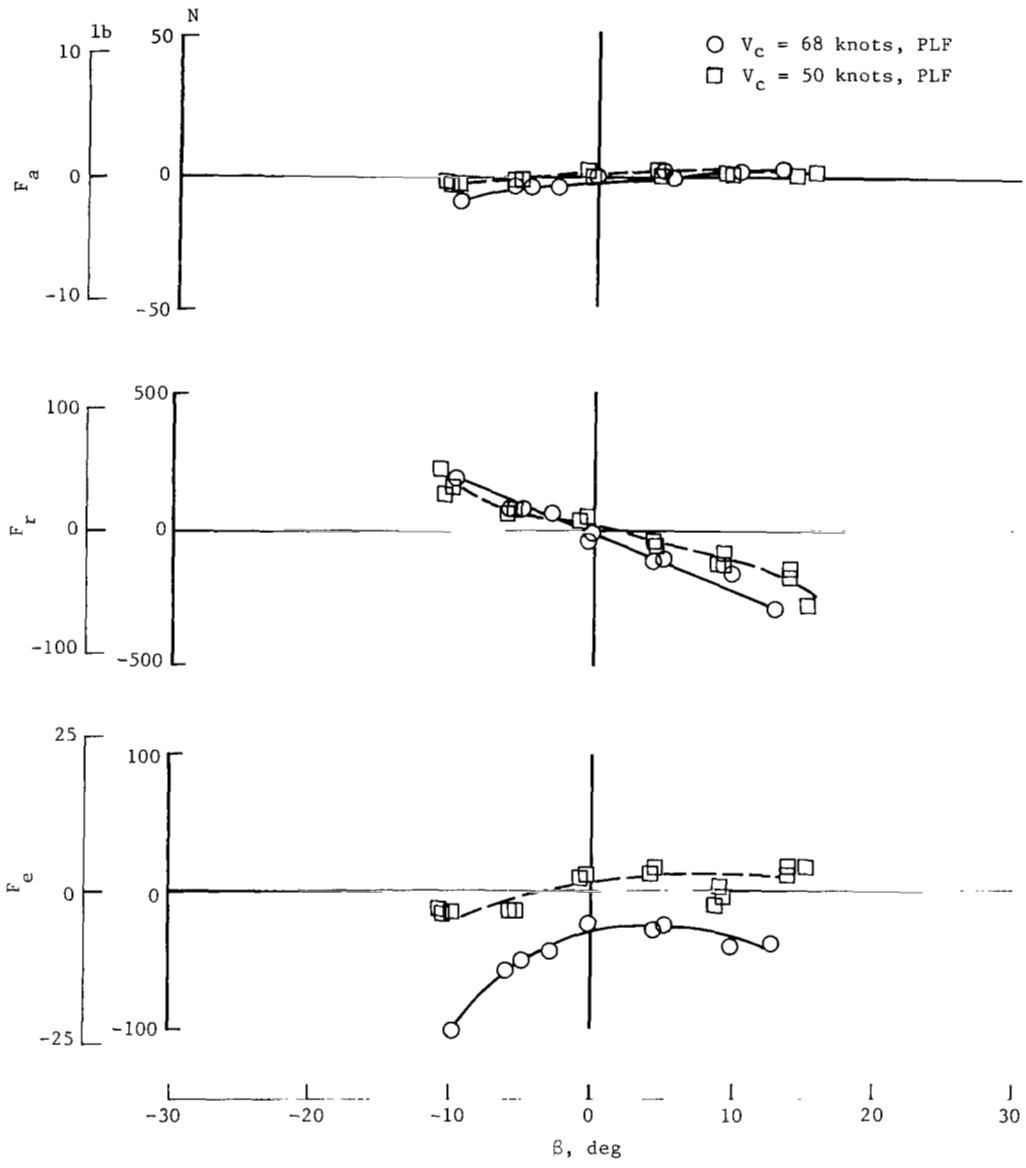

(b) Concluded.

Figure 18.- Continued.

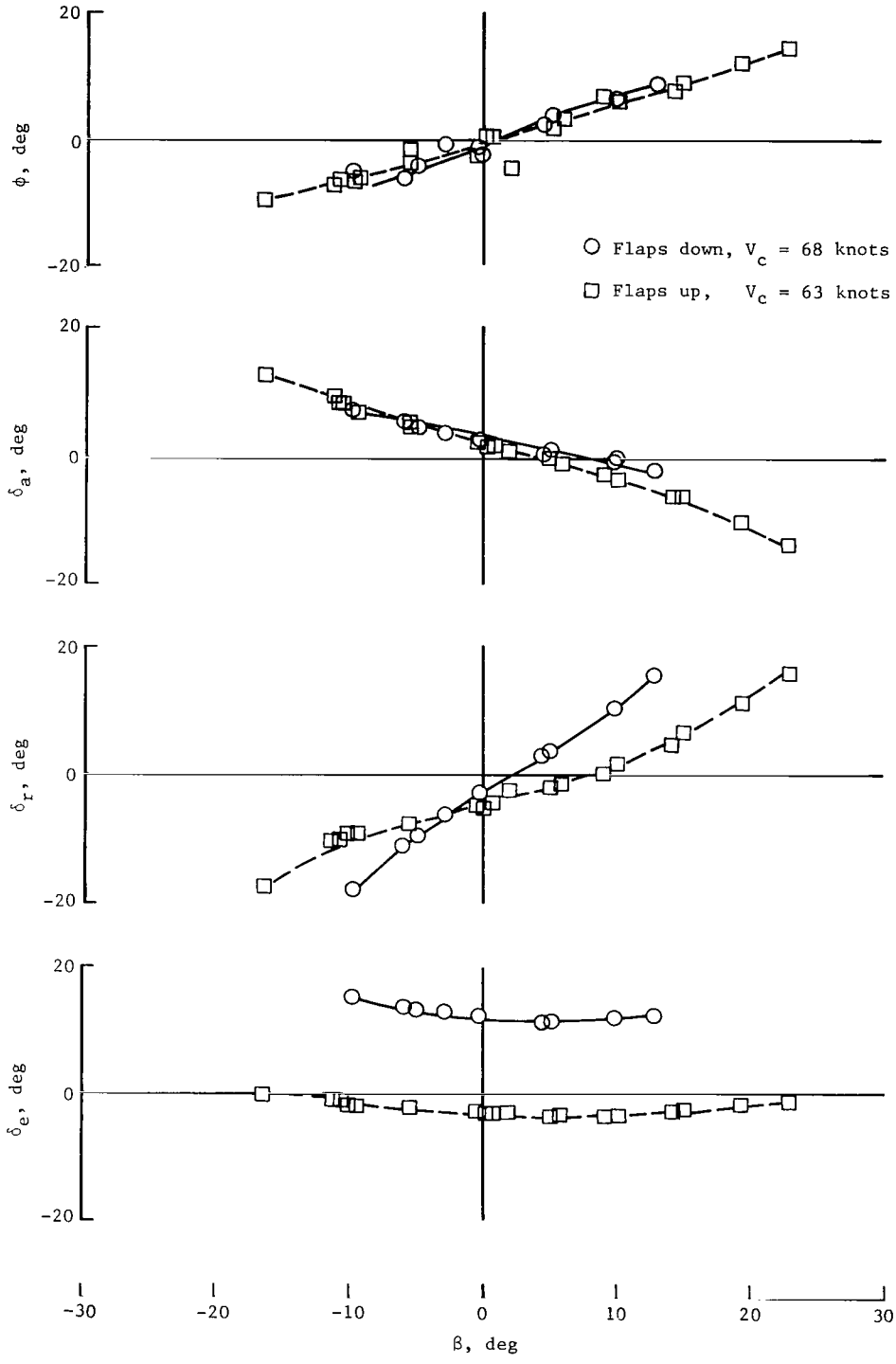

(c) Effect of flaps with maximum power.

Figure 18.- Continued.

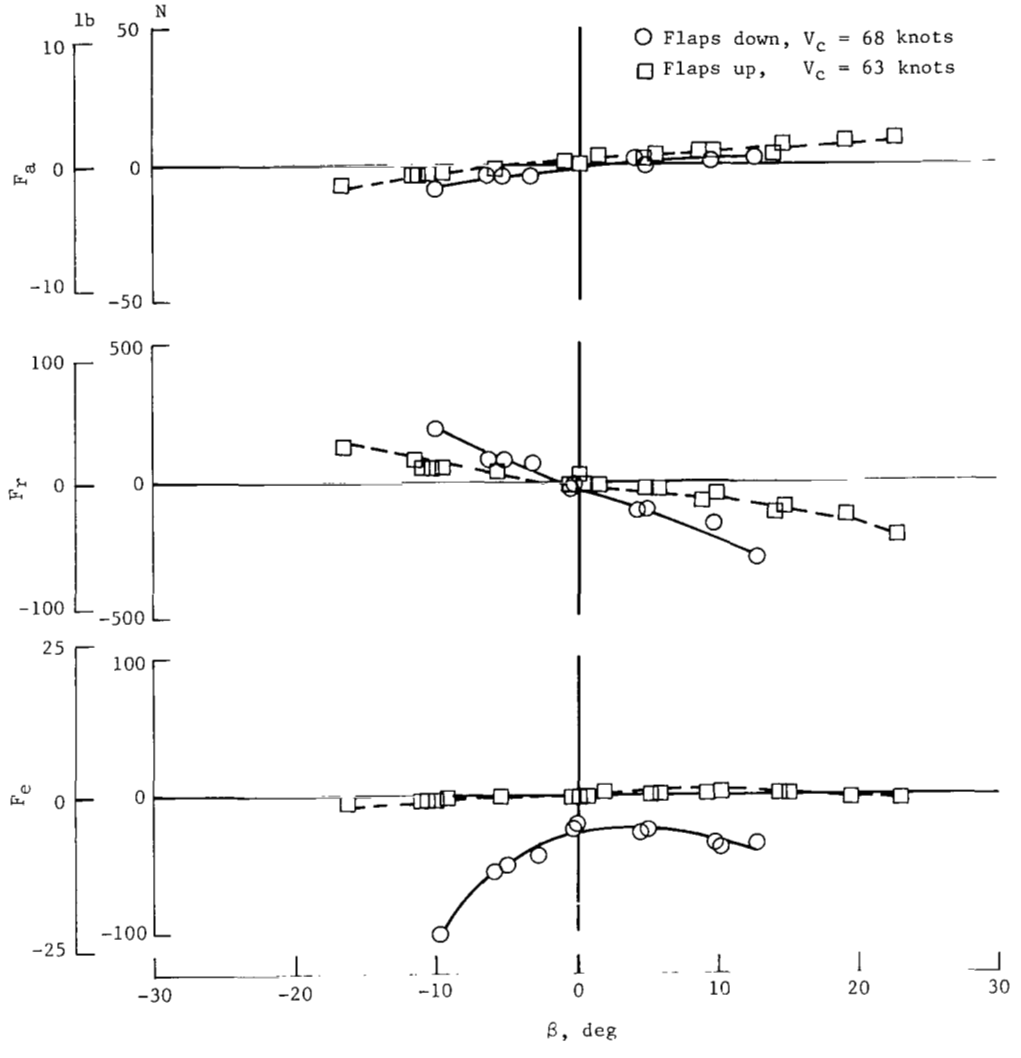

(c) Concluded.

Figure 18.- Continued.

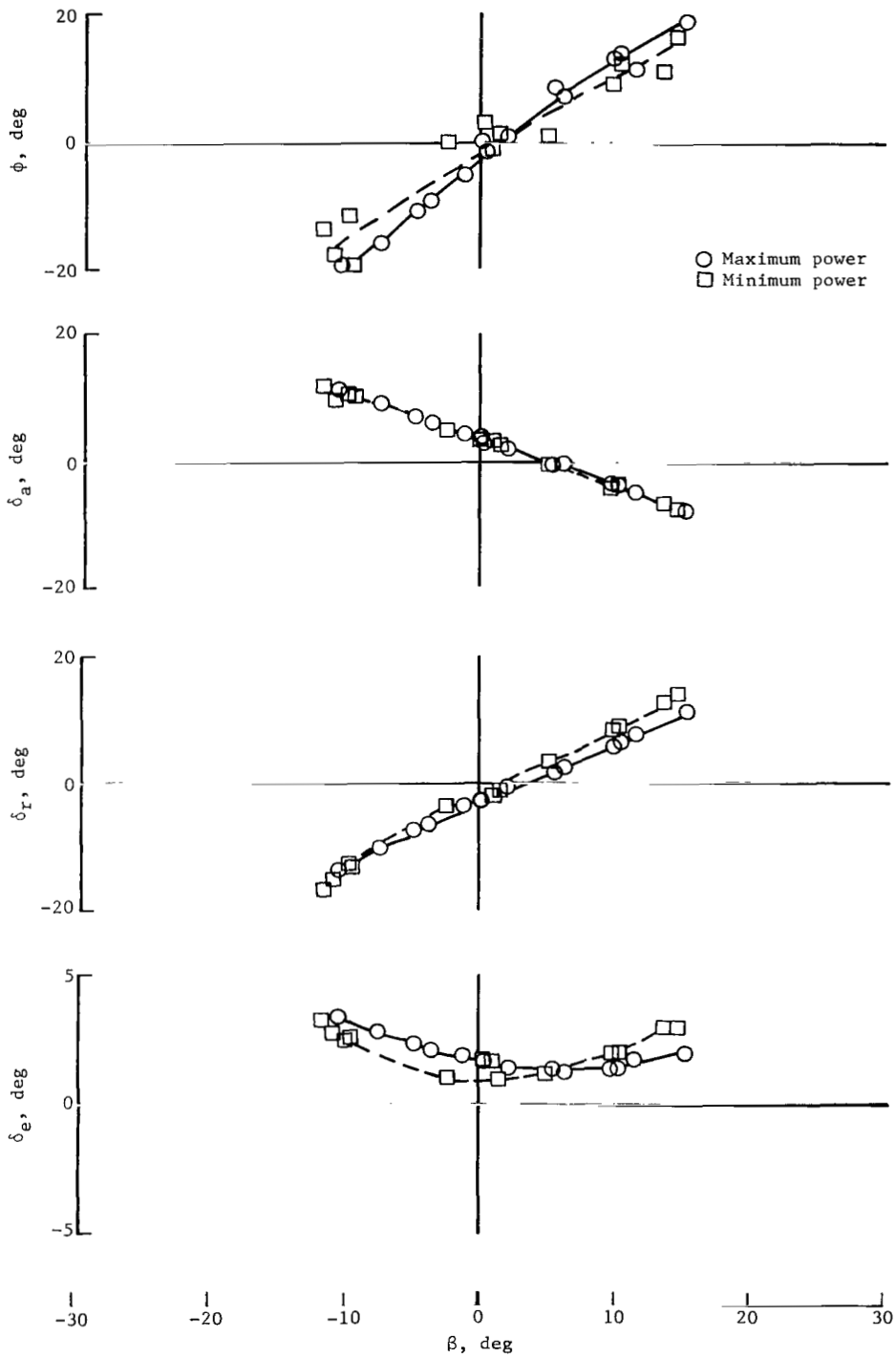

(d) Effect of power with flaps up at V_c = 99 knots.

Figure 18.- Continued.

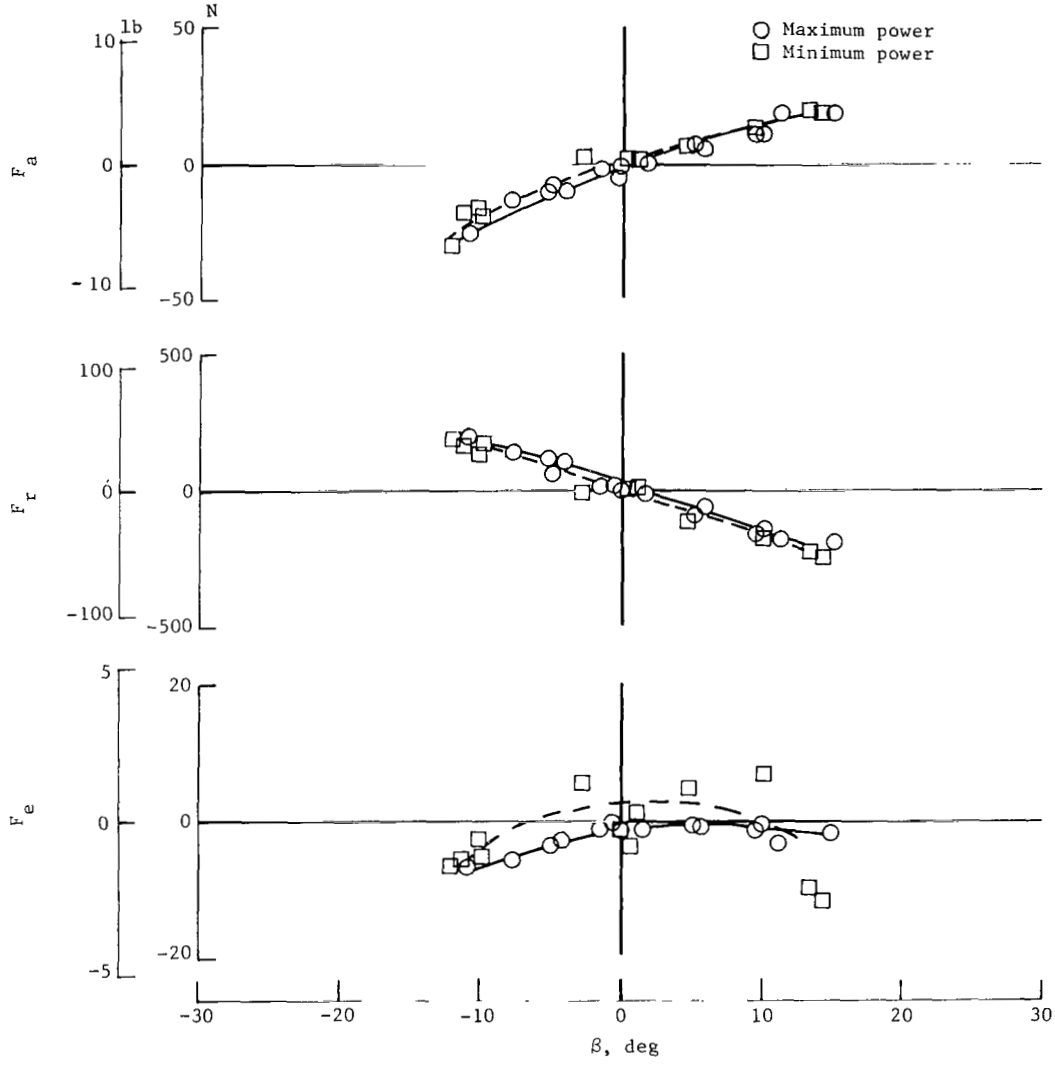

(d) Concluded.

Figure 18.- Concluded.

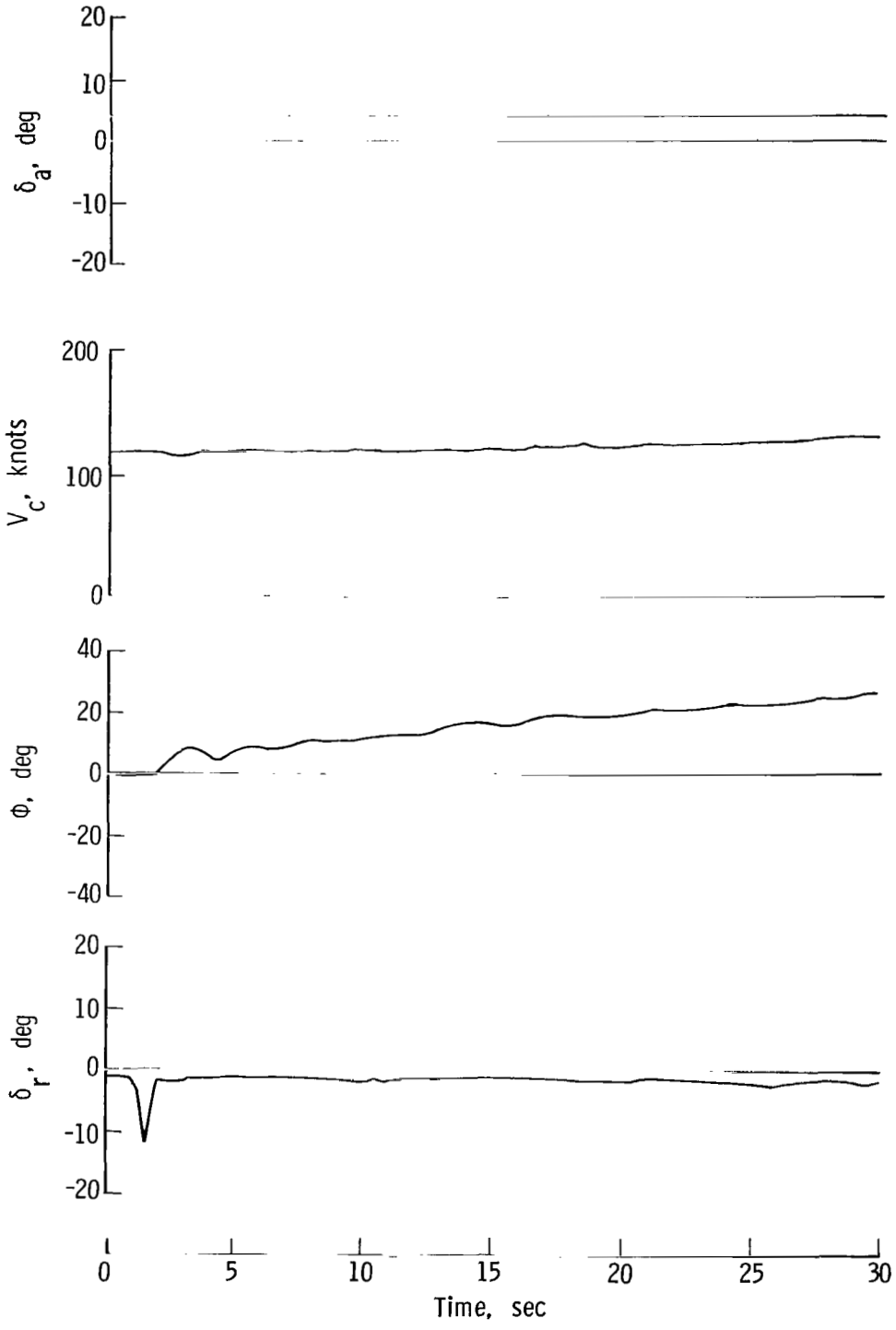

Figure 19.- Time history of spiral mode for low-wing airplane. Controls free with PLF (V_c = 100 knots) and flaps up.

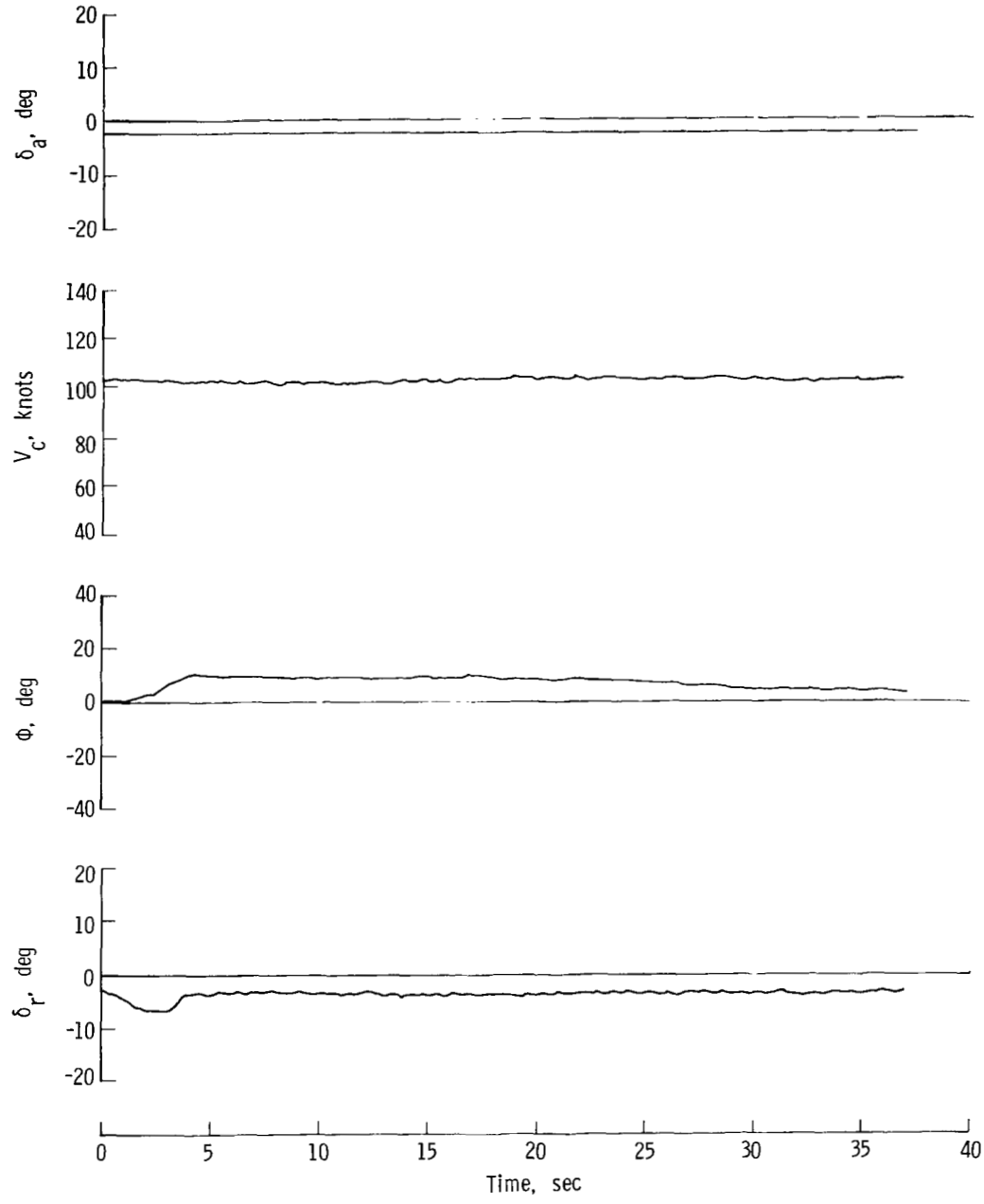

(a) Flaps up; controls fixed; PLF (V_c = 104 knots).

Figure 20.- Time histories of spiral mode for high-wing airplane.

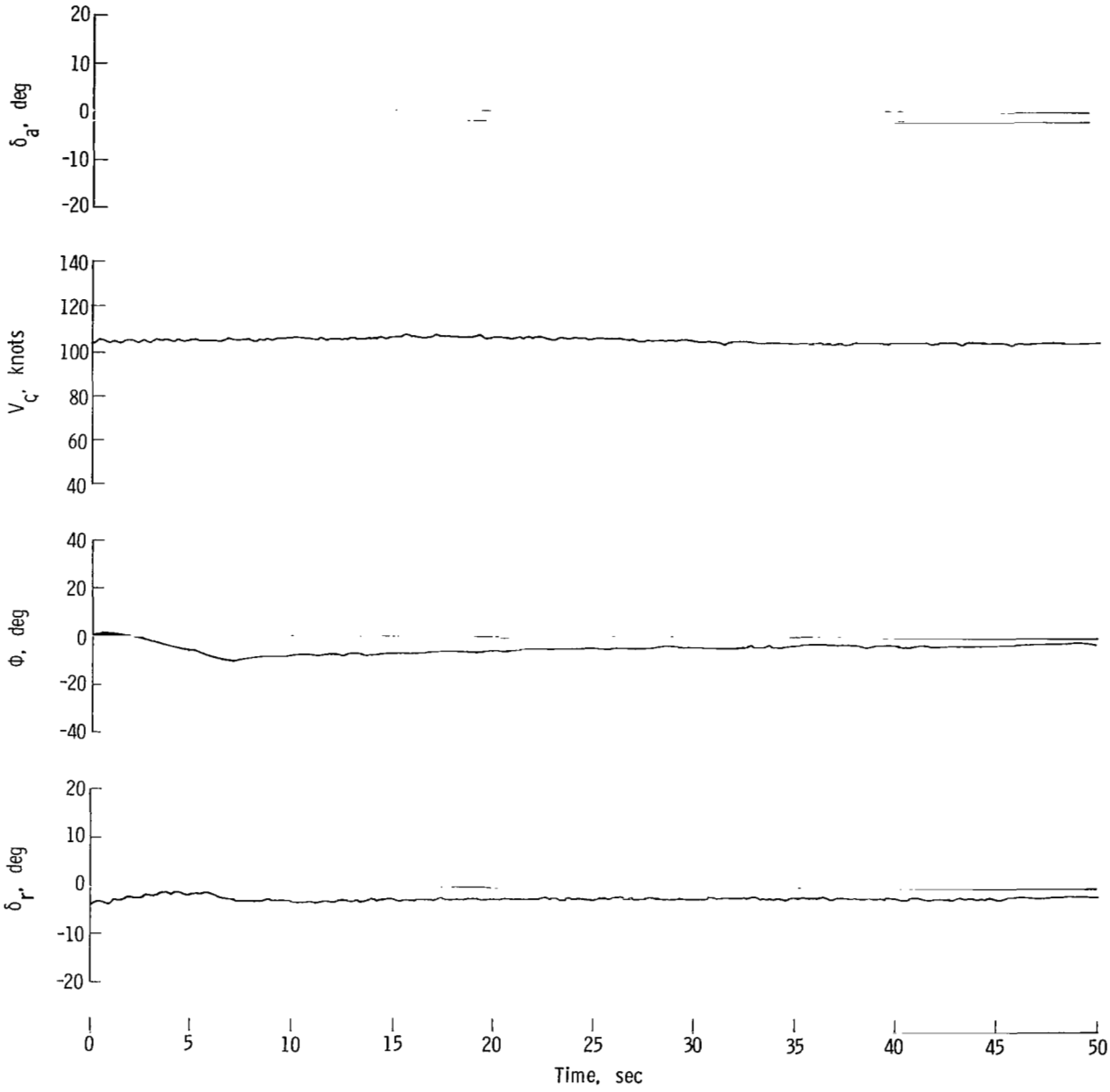

(b) Flaps up; controls free; PLF (V_C = 104 knots).

Figure 20.- Continued.

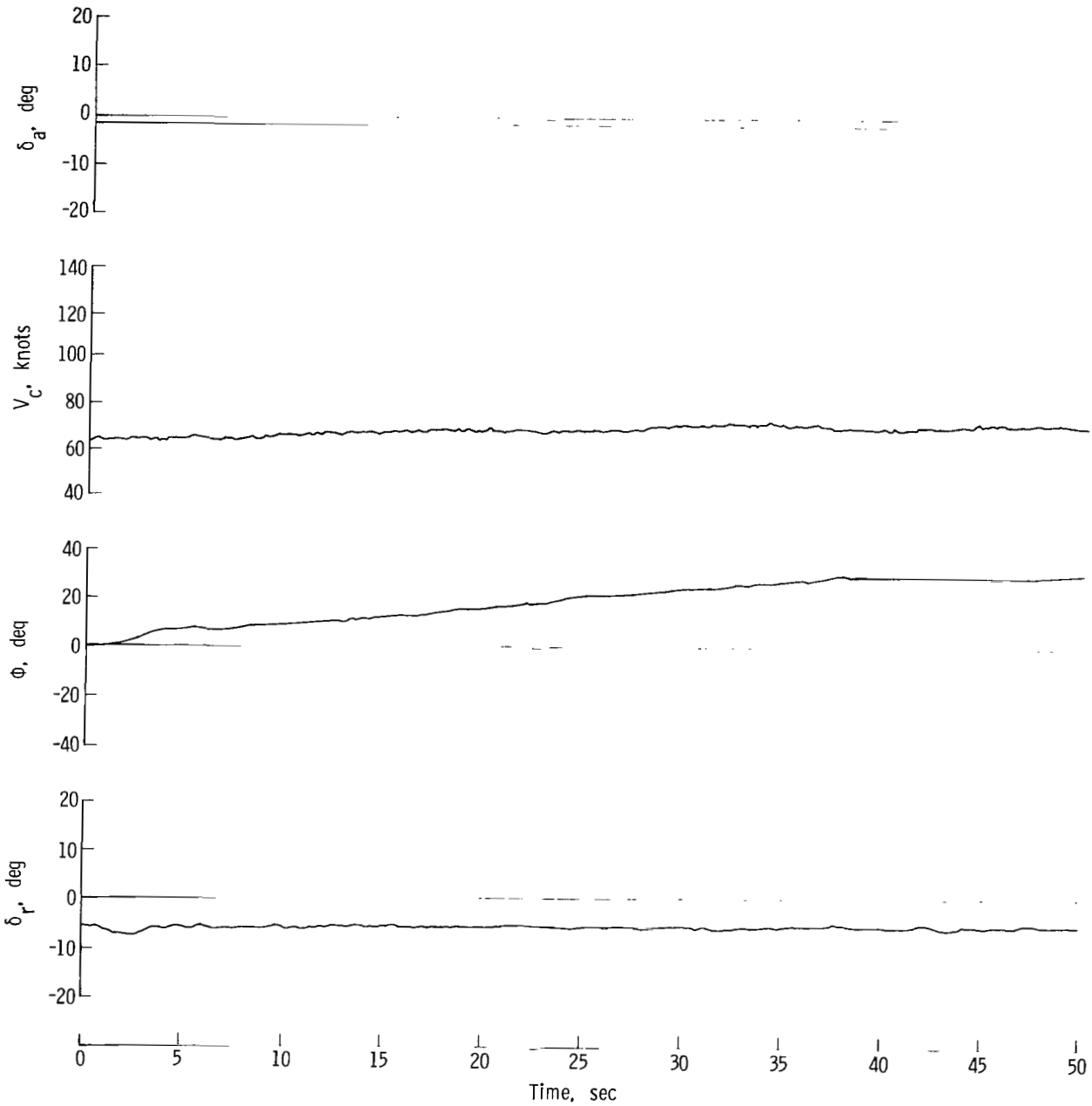

(c) Flaps up; controls fixed; PLF (V_c = 69 knots).

Figure 20.- Continued.

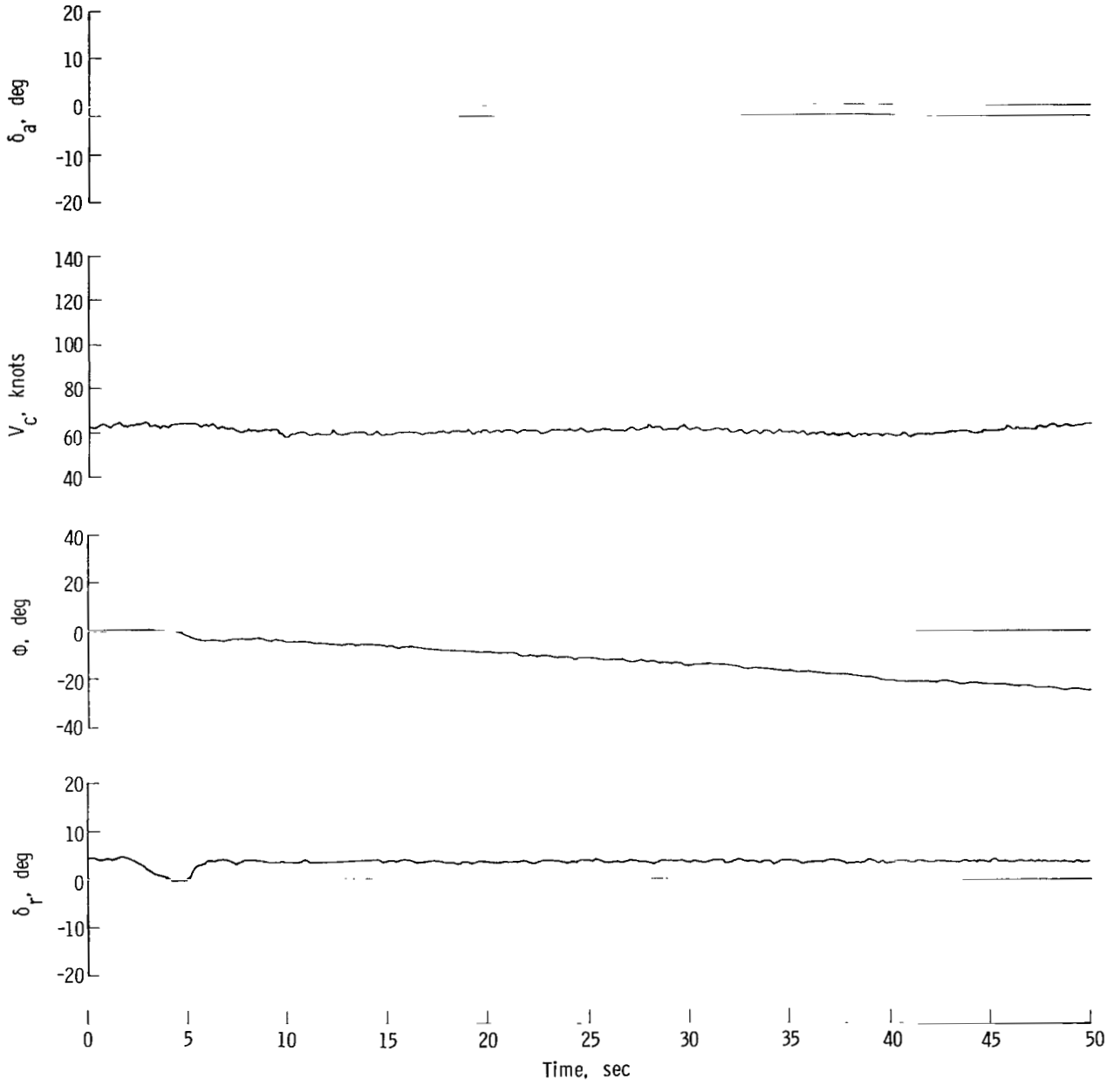

(d) Flaps down; controls fixed; PLF (V_c = 63 knots).

Figure 20.- Concluded.

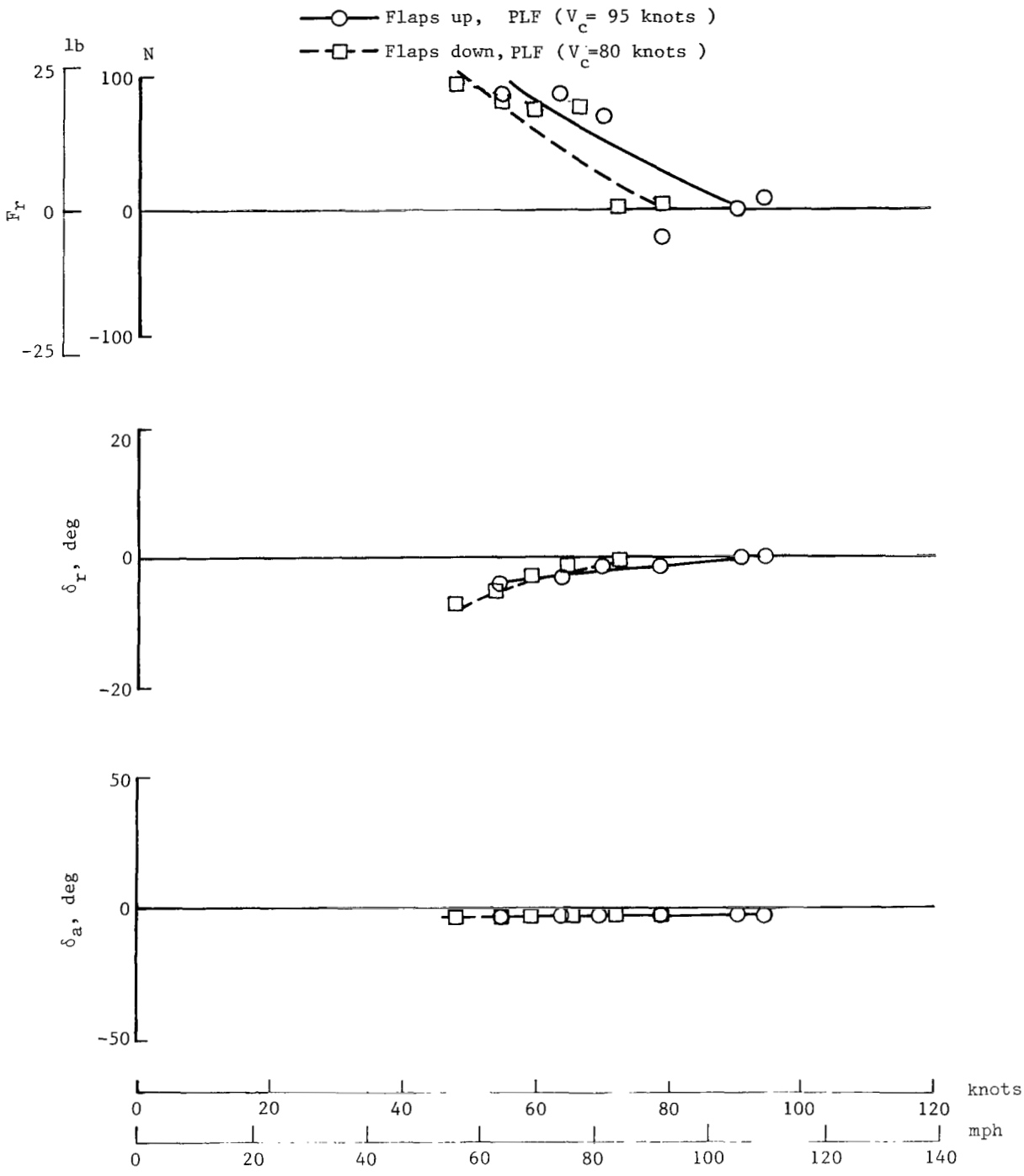

(a) Low-wing airplane.

Figure 21.- Aileron and rudder characteristics required to trim out rolling and yawing moments.

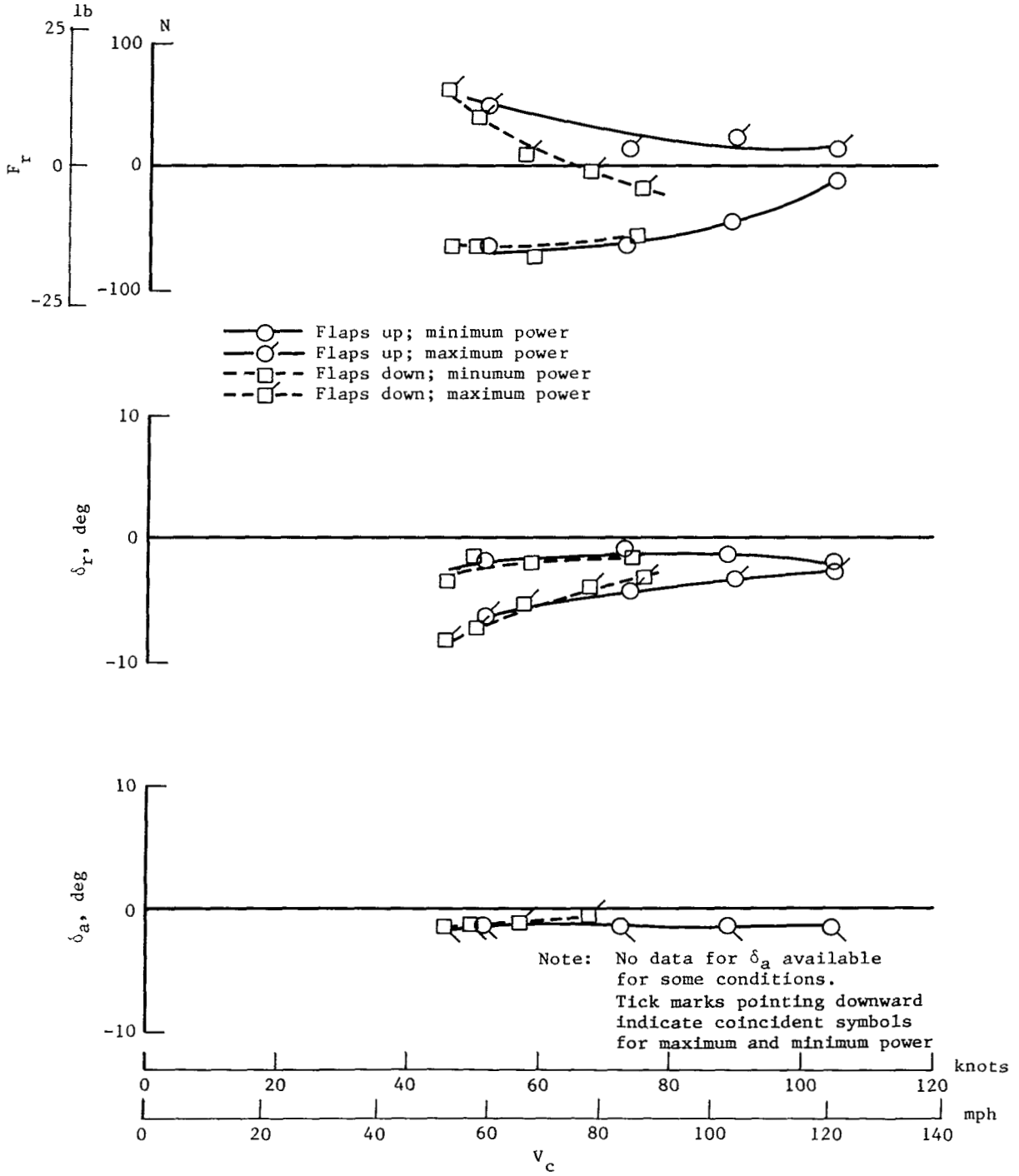

(b) High-wing airplane.

Figure 21.- Concluded.

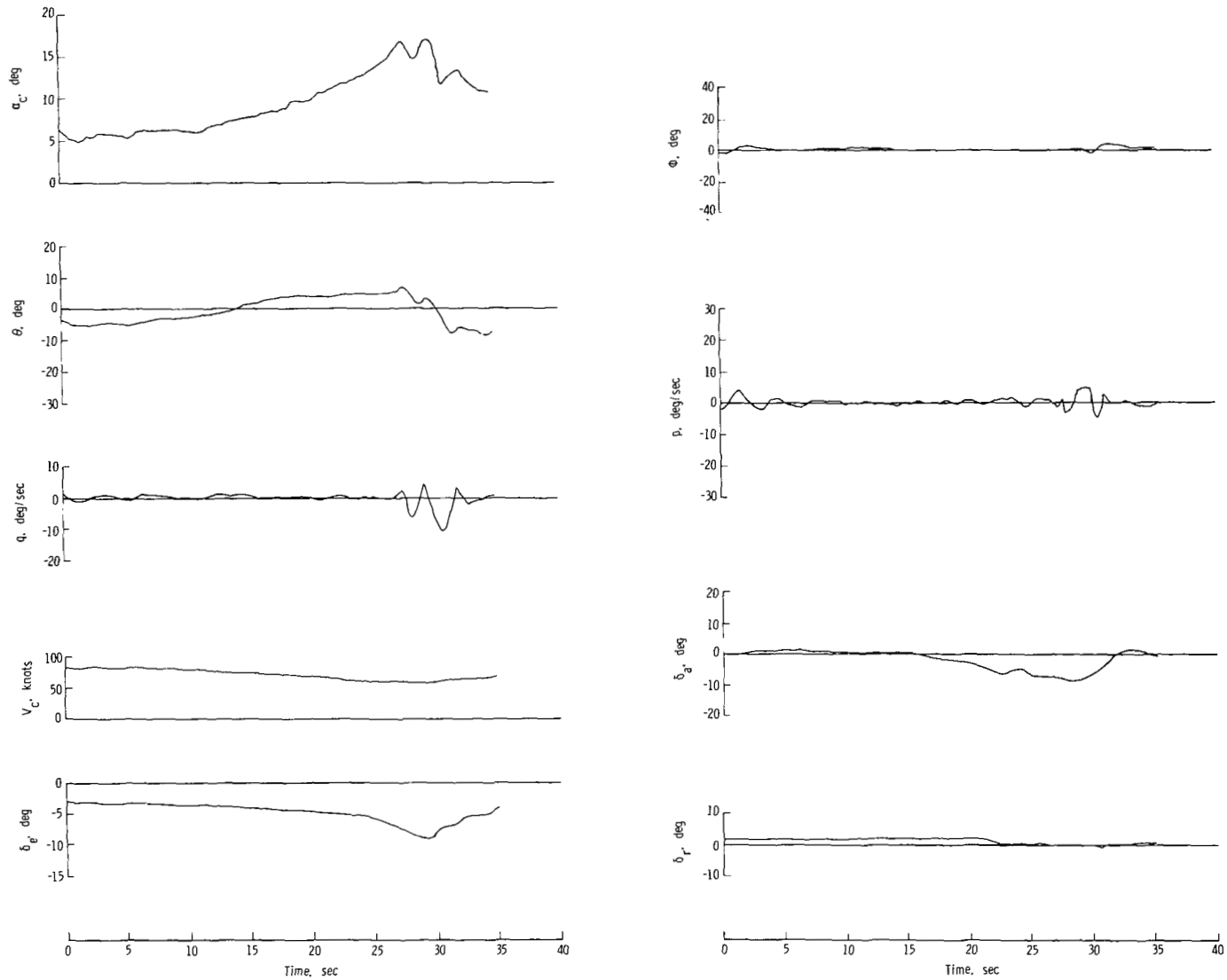

(a) Flaps up; minimum power; c.g. at $0.255\bar{c}$.

Figure 22.- Time histories of unaccelerated stalls for low-wing airplane for various flight conditions.

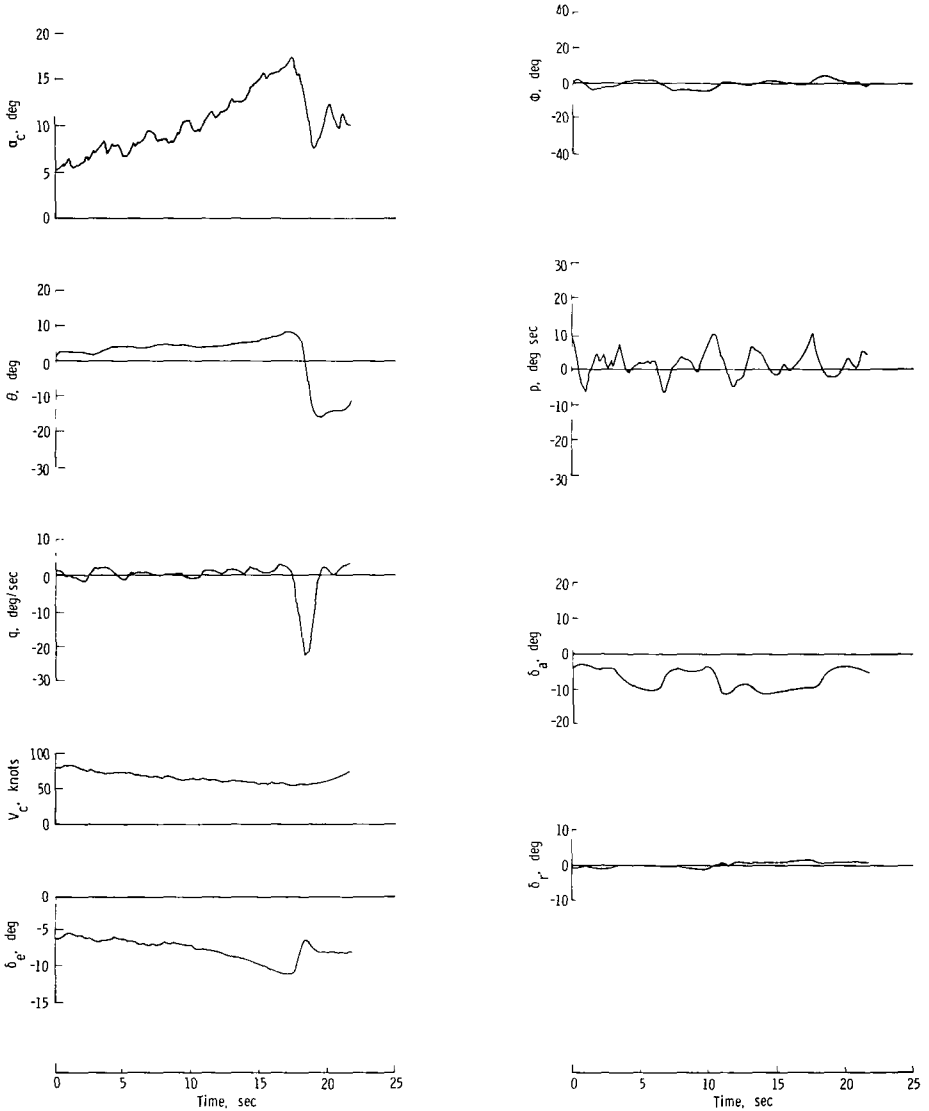

(b) Flaps up; minimum power; c.g. at 0.198$\bar{c}$.

Figure 22.- Continued.

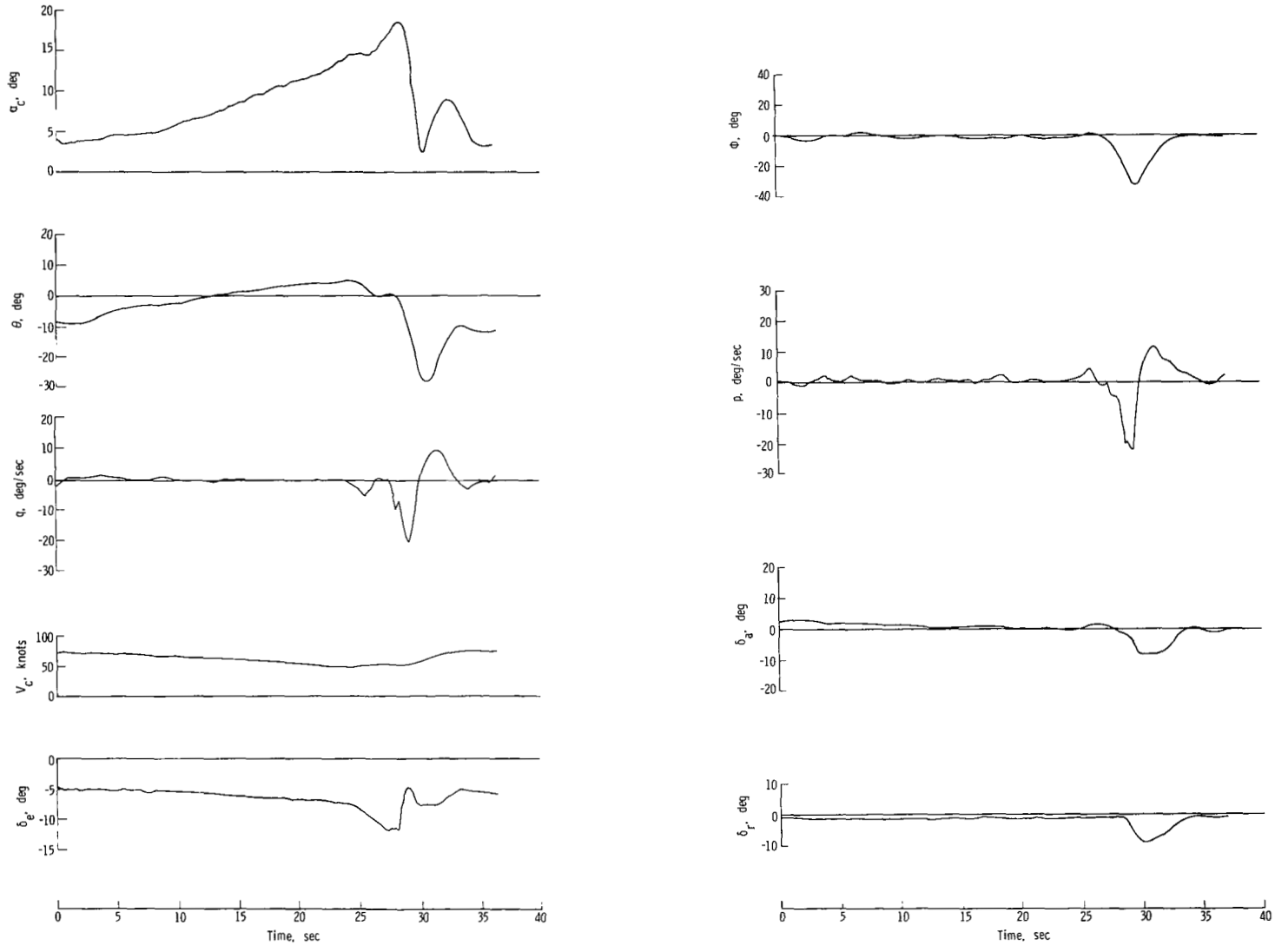

(c) Flaps down; minimum power; c.g. at $0.255\bar{c}$.

Figure 22.- Continued.

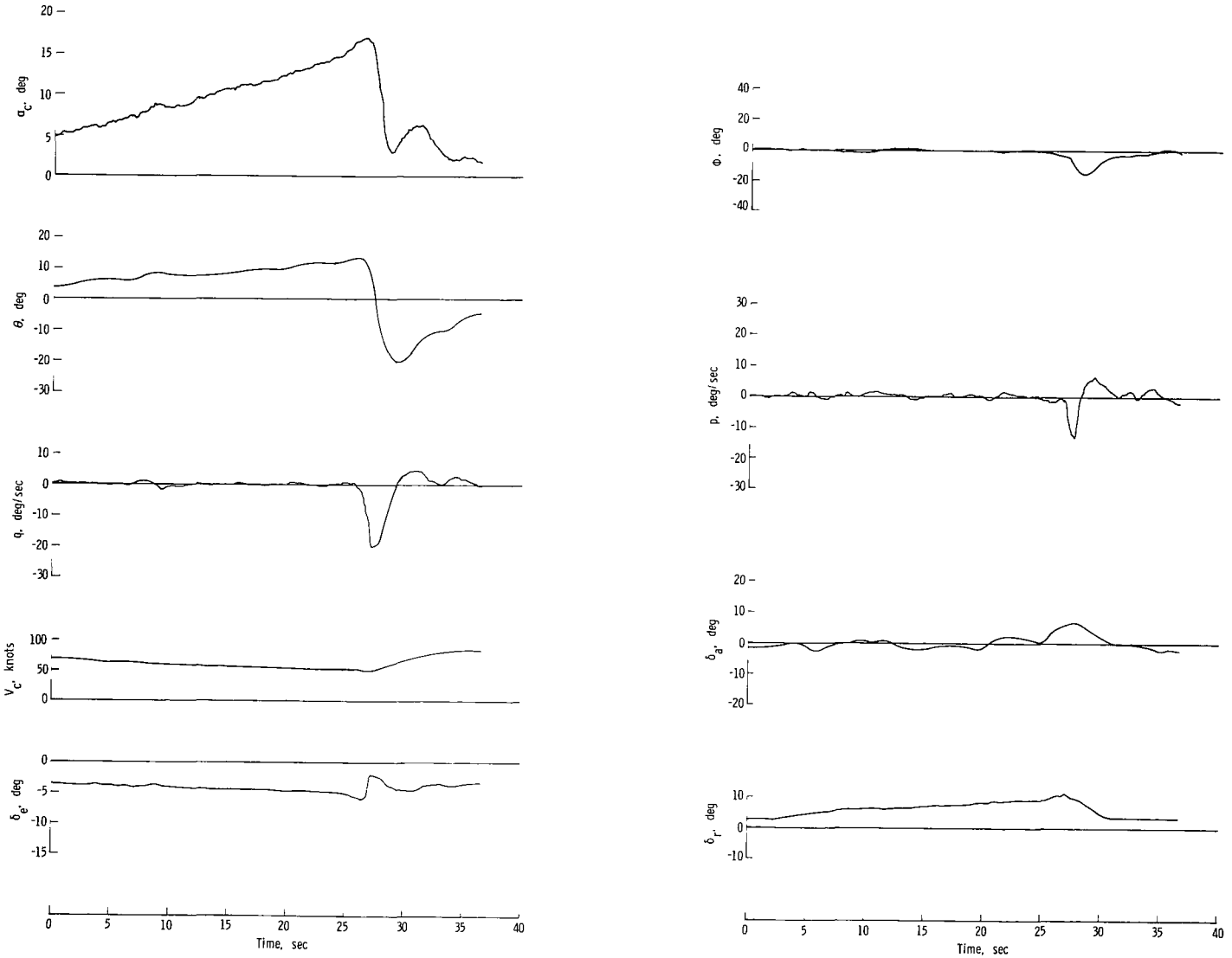

(d) Flaps down; PLF (V_c = 60 knots); c.g. at 0.255$\bar{c}$.

Figure 22.- Continued.

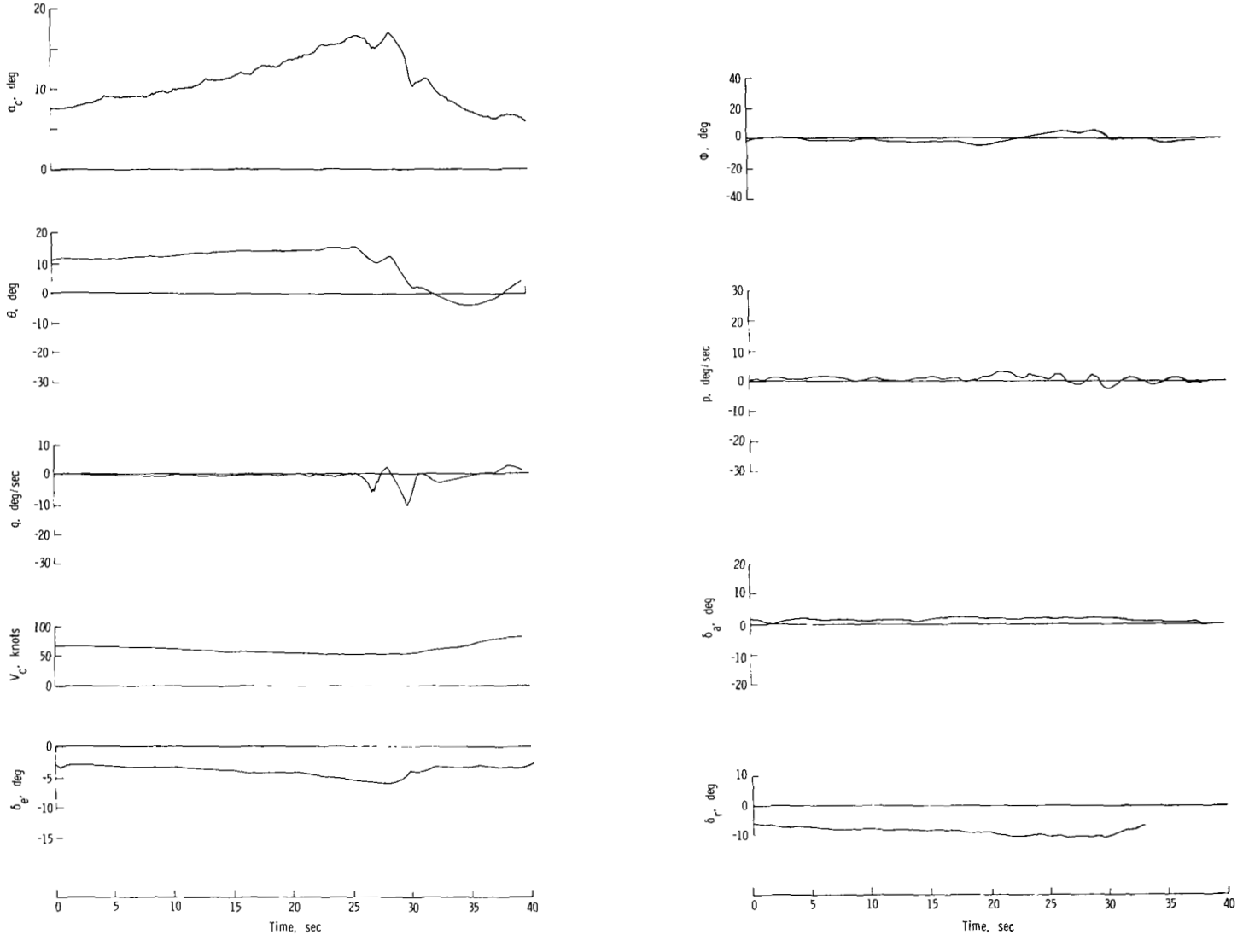

(e) Flaps up; maximum power; c.g. at $0.255\bar{c}$.

Figure 22.- Concluded.

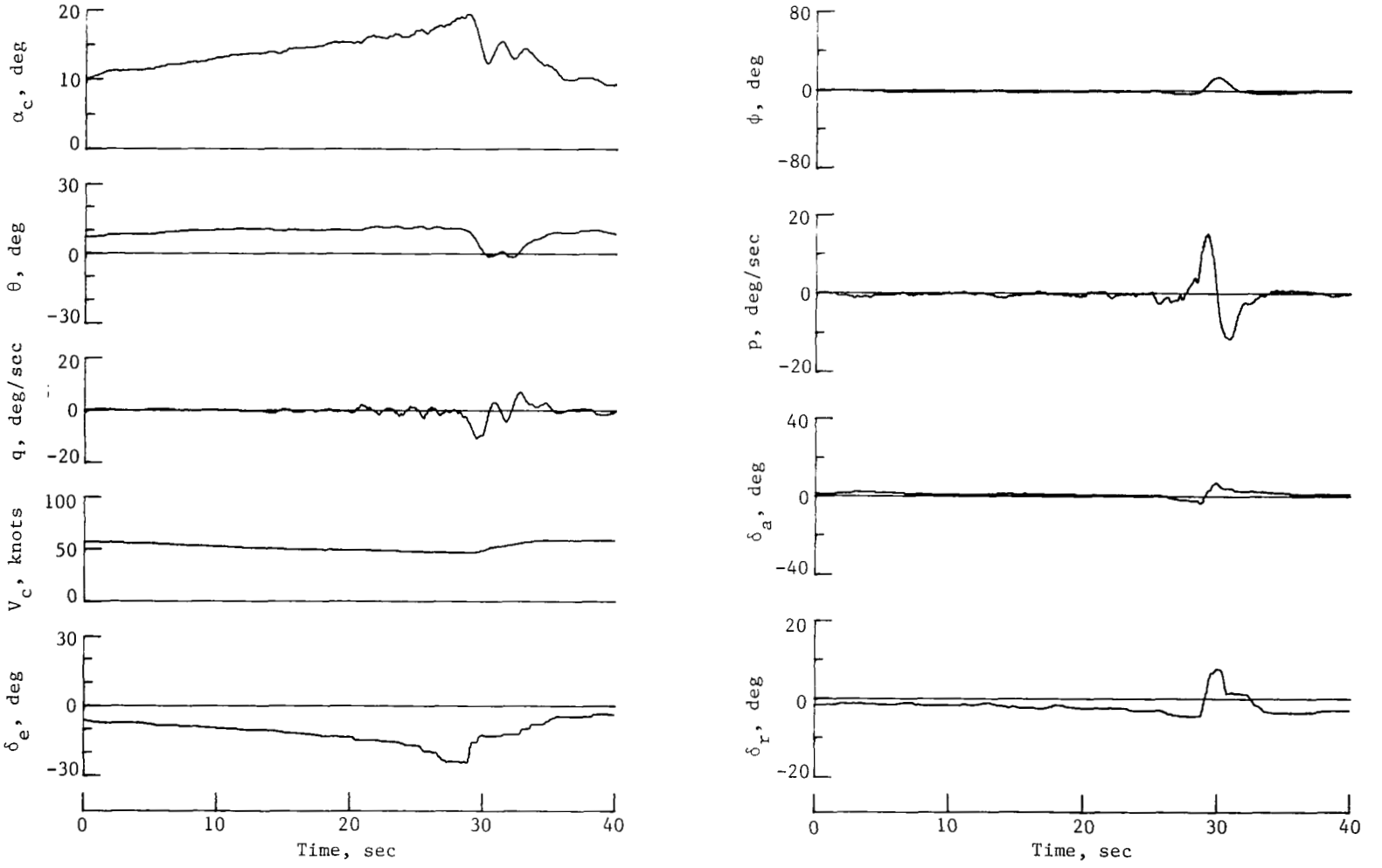

(a) Flaps up; minimum power; immediate recovery by pilot.

Figure 23.- Time histories of unaccelerated stalls for high-wing airplane with c.g. at 0.325$\bar{c}$.

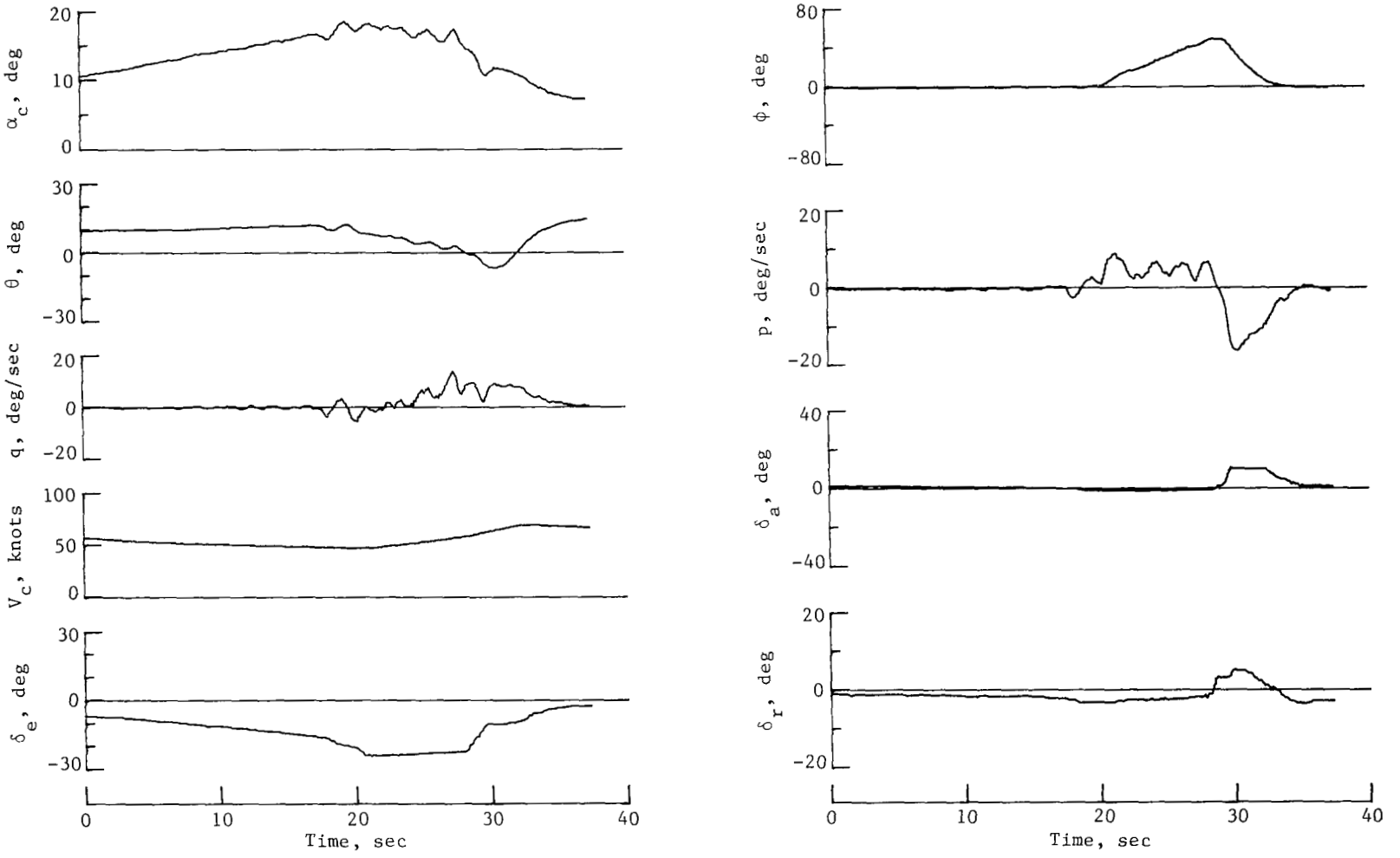

(b) Flaps up; minimum power; delayed recovery by pilot.

Figure 23.- Continued.

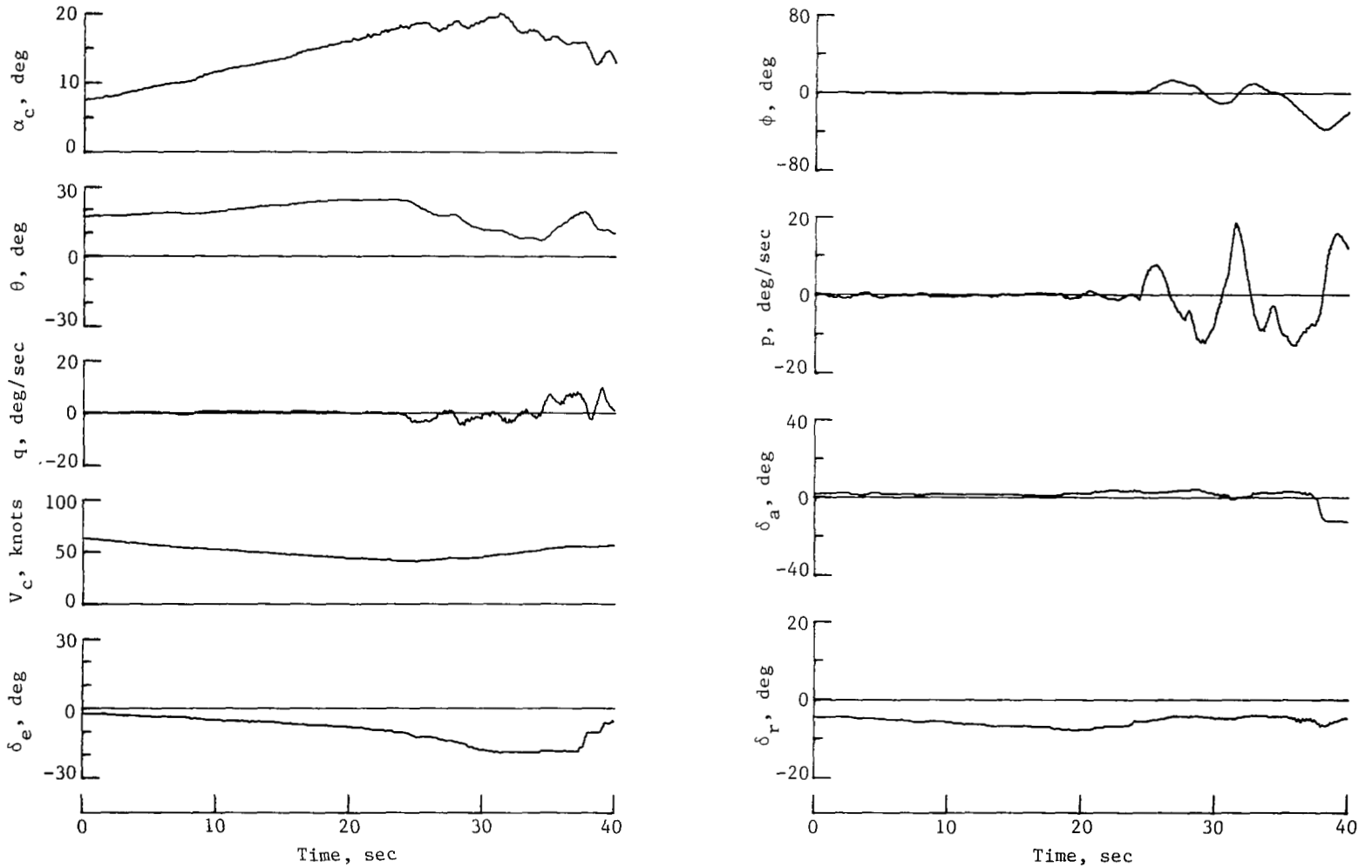

(c) Flaps up; maximum power; delayed recovery by pilot.

Figure 23.- Continued.

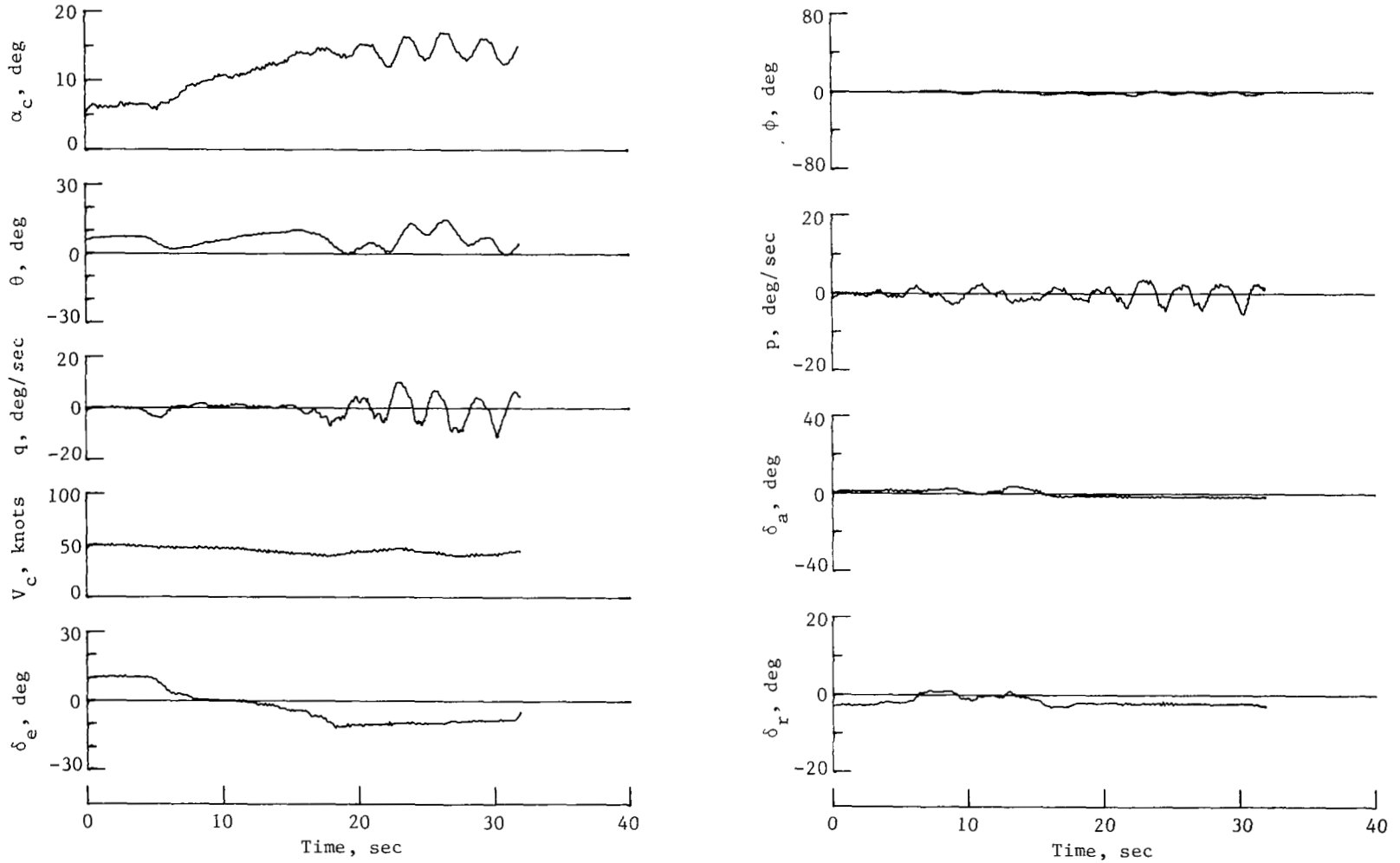

(d) Flaps down; minimum power; delayed recovery by pilot.

Figure 23.- Continued.

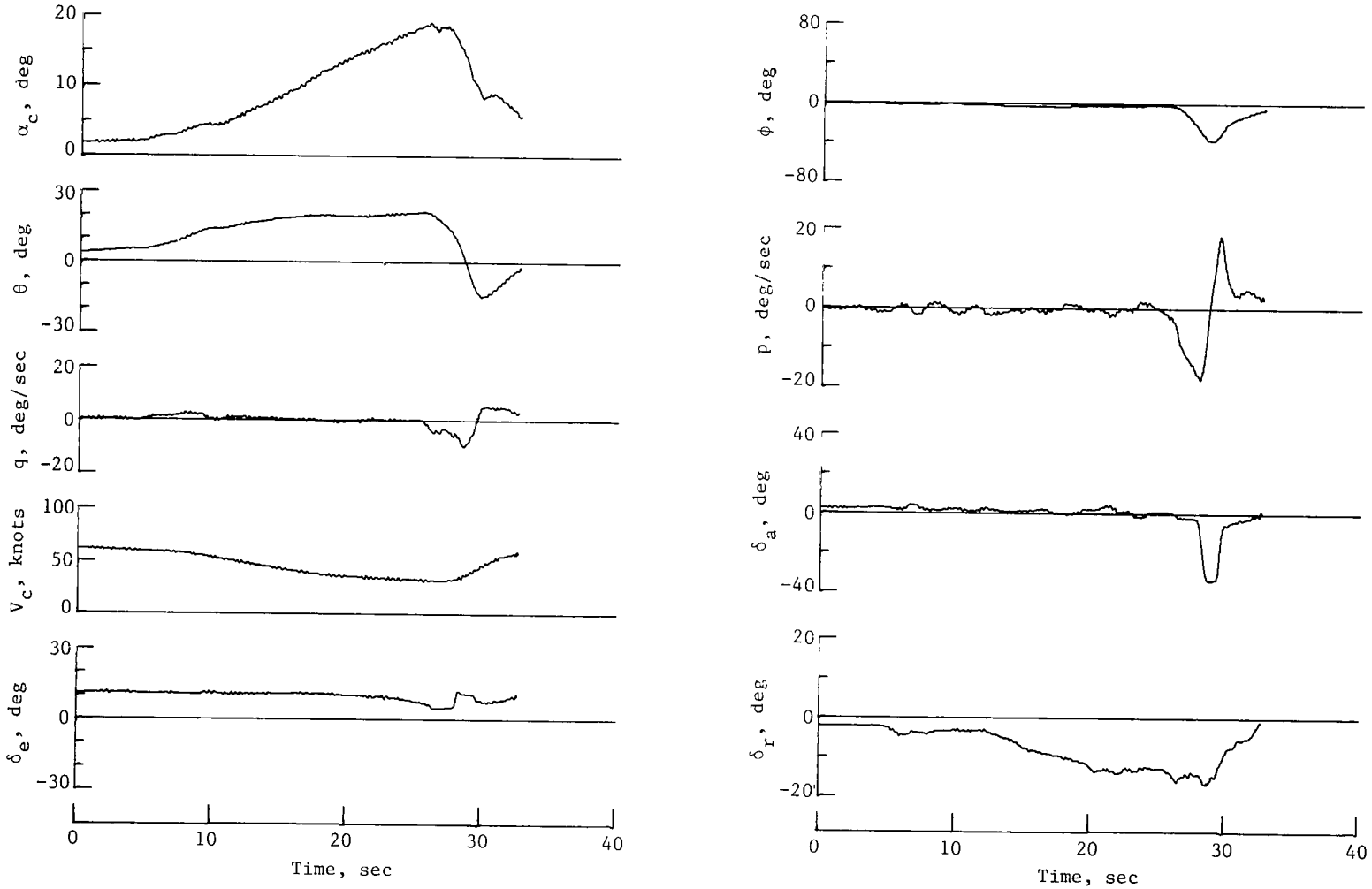

(e) Flaps down; maximum power; immediate recovery by pilot.

Figure 23.- Concluded.

1. Report No.	2. Government Accession No.	3. Recipient's Catalog No.
NASA TP-1636		

4. Title and Subtitle	5. Report Date
MEASUREMENT OF THE HANDLING CHARACTERISTICS OF TWO LIGHT AIRPLANES	June 1980
	6. Performing Organization Code
7. Author(s)	8. Performing Organization Report No.
Staff of the Flight Dynamics Branch	L-13054
	10. Work Unit No.
9. Performing Organization Name and Address	505-41-13-03
NASA Langley Research Center Hampton, VA 23665	11. Contract or Grant No.
	13. Type of Report and Period Covered
12. Sponsoring Agency Name and Address	Technical Paper
National Aeronautics and Space Administration Washington, DC 20546	14. Sponsoring Agency Code

15. Supplementary Notes

16. Abstract

A flight investigation of the handling characteristics of two single-engine general aviation airplanes, one a high-wing and the other a low-wing, included a variety of measurements of different characteristics of the airplanes. The characteristics included those of the control systems, performance, longitudinal and lateral responses, and stall motions.

17. Key Words (Suggested by Author(s))

General aviation
Flight test
Handling characteristics

18. Distribution Statement

Unclassified - Unlimited

Subject Category 08

19. Security Classif. (of this report)	20. Security Classif. (of this page)	21. No. of Pages	22. Price*
Unclassified	Unclassified	77	$6.00

* For sale by the National Technical Information Service, Springfield, Virginia 22161

NASA-Langley, 1980

National Aeronautics and Space Administration

Washington, D.C.
20546

Official Business
Penalty for Private Use, $300

THIRD-CLASS BULK RATE

Postage and Fees Paid
National Aeronautics and Space Administration
NASA-451

U.S.MAIL

2 1 1U,A, 051080 S00903DS
DEPT OF THE AIR FORCE
AF WEAPONS LABORATORY
ATTN: TECHNICAL LIBRARY (SUL)
KIRTLAND AFB NM 87117

NASA

POSTMASTER: If Undeliverable (Section 158 Postal Manual) Do Not Return